

X-500-67-228

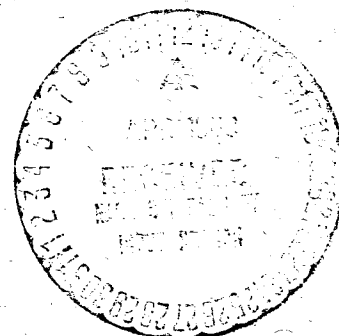
PREPRINT

NASA FILE 63149

# A MISSION, TRACKING, COMMUNICATION AND FLIGHT OPERATION STUDY FOR THE GALACTIC JUPITER PROBE

**N 68-20036**  
(ACCESSION NUMBER)  
143  
(PAGES)  
TMX-63149  
(NASA CR OR TMX OR AD NUMBER)

(THRU)  
1  
(CODE)  
07  
(CATEGORY)



SEPTEMBER 1967

GPO PRICE \$ \_\_\_\_\_  
CSFTI PRICE(S) \$ \_\_\_\_\_  
Hard copy (HC) 300  
Microfiche (MF) 65

ff 653 July 65

**GODDARD SPACE FLIGHT CENTER**  
**GREENBELT, MARYLAND**

TRACKING AND DATA SYSTEMS DIRECTORATE

A MISSION, TRACKING, COMMUNICATION, AND  
FLIGHT OPERATION STUDY FOR THE  
GALACTIC JUPITER PROBE

September 1967

Tracking and Data Systems Directorate

Goddard Space Flight Center  
Greenbelt, Maryland

A MISSION, TRACKING, COMMUNICATION, AND  
FLIGHT OPERATION STUDY FOR THE  
GALACTIC JUPITER PROBE

FOREWORD

This document represents the contribution of the Tracking and Data Systems Directorate to Phase A of the Galactic Jupiter Probe study conducted at Goddard Space Flight Center. In this report the results of an appropriate mission analysis and an associated study of tracking, communication, and flight operation are presented.

The investigations were carried out by a study cadre consisting of the following personnel of the Tracking and Data Systems Directorate:

Cadre Leader: Richard Lehnert, Mission and Trajectory Analysis Division

Chapter Chairman of Mission Analysis: Robert T. Groves, Mission and  
Systems Analysis Branch

Associates: Robert E. Coady, Mission and Systems Analysis Branch  
Charles R. Newman, Mission and Systems Analysis Branch  
Bernard Kaufman, Mission and Systems Analysis Branch

Chapter Chairman of Ground Network Support: Victor R. Simas, RF Sys-  
tems Branch

Associates: C. Curtis Johnson, RF Systems Branch  
Wayne Hughes, RF Systems Branch  
T. E. McGunigal, RF Systems Branch  
John W. Bryan, RF Systems Branch

Chapter Chairman of Communication and Data Handling: Ronald M. Muller,  
Space Electronics  
Branch

Associates: Willis S. Campbell, Space Electronics Branch  
John J. Yagelowich, Space Electronics Branch

Chapter Chairman of Flight Operations: Ralph R. Stroble, Project Opera-  
tions Support Division

# CONTENTS

	<u>Page</u>
I. INTRODUCTION . . . . .	1
Philosophy and Assumptions . . . . .	1
II. SUMMARY . . . . .	3
III. MISSION ANALYSIS . . . . .	7
A. <u>Trajectory Analysis</u> . . . . .	7
1. Earth Escape Phase . . . . .	8
a. Injection Requirements and Launch Period . . . . .	8
b. Launch Vehicle Payload Estimates . . . . .	8
2. Cruise Phase . . . . .	12
3. Jupiter Approach Phase . . . . .	13
a. Approach Asymptote, Sun, Earth Relationship . . . . .	21
b. Hyperbolic Excess Speed ( $V_{hp}$ ) . . . . .	23
4. Post-Encounter Phase . . . . .	23
a. Encounter Geometry . . . . .	25
b. Flybys for Post-Encounter Missions . . . . .	29
B. <u>Guidance and Navigation Analysis</u> . . . . .	34
1. Midcourse Guidance and Attitude Laws . . . . .	35
2. Midcourse Velocity and Fuel Requirements . . . . .	37
3. Navigation Accuracy from Tracking Data . . . . .	41
IV. GROUND NETWORK SUPPORT . . . . .	48
A. <u>Ground Network</u> . . . . .	48

	<u>Page</u>
1. Function . . . . .	48
2. NASA Facility Availability . . . . .	48
B. <u>Station Description</u> . . . . .	49
1. STADAN Data Acquisition Stations, Rosman and Orroral . . . .	49
2. Deep Space Network 85-foot and 210-foot - Data Acquisition Stations - Goldstone, Canberra, Madrid . . . . .	51
3. MSFN 85-foot - USBS Stations - Goldstone, Canberra, Madrid	52
C. <u>Station Selection</u> . . . . .	55
1. Program Requirements . . . . .	56
2. DSN Advantages . . . . .	56
3. Coverage Restrictions . . . . .	56
4. STADAN Use . . . . .	57
D. <u>Coverage</u> . . . . .	57
1. Station Use vs. Mission Phases . . . . .	57
2. Trajectory . . . . .	58
3. Launch and Near-Earth Operations . . . . .	60
4. Visibility by Stations during Cruise . . . . .	61
E. <u>Improvements to the Rosman Station</u> . . . . .	62
1. Frequency and Noise-Temperature . . . . .	62
2. Receiving System Improvements . . . . .	63
3. Command Transmitter Installation . . . . .	63

	<u>Page</u>
F. <u>Down-Link Performance (Telemetry)</u> . . . . .	64
1. Received Signal Levels . . . . .	64
2. Phase and Frequency Stability Performance . . . . .	68
G. <u>Command Systems Performance</u> . . . . .	73
1. Power and Antenna Gain . . . . .	76
2. Exciter Characteristics . . . . .	78
3. Up-Link Margin Calculations . . . . .	79
H. <u>Tracking System Performance</u> . . . . .	79
1. Instrumentation Accuracy Requirements . . . . .	81
2. Galactic Jupiter Probe Range-Rate System . . . . .	82
V. THE GALACTIC JUPITER PROBE COMMUNICATION AND DATA HANDLING SYSTEM . . . . .	86
A. <u>Introduction</u> . . . . .	86
B. <u>Communication System</u> . . . . .	87
1. Command or Up-Link . . . . .	87
a. Encoding . . . . .	89
b. Modulation Subcarrier . . . . .	89
c. Modulation Carrier . . . . .	90
d. Transmitter . . . . .	90
e. Spacecraft Receivers . . . . .	90
f. Subcarrier Detectors . . . . .	91
g. Command Coding Check . . . . .	91
h. Decoding . . . . .	91
i. Command Operation . . . . .	92
2. Data or Down-Link . . . . .	93

	<u>Page</u>
a. Link Performance . . . . .	93
b. Spacecraft Transmitter - Power Amplifier . . . . .	93
c. Antenna Switching . . . . .	95
d. Transmitter Modulation . . . . .	96
e. Transmitter Oscillator . . . . .	97
f. Ground RF System . . . . .	98
g. Down-Link Data Coding and Decoding . . . . .	100
h. Ground Communications . . . . .	100
C. <u>Tracking Function</u> . . . . .	100
D. <u>Data Handling System</u> . . . . .	101
1. Introduction and Functional Description . . . . .	101
a. Examples of Processing Gain . . . . .	102
(1) Logarithmic Compression . . . . .	102
(2) Spin-related Data . . . . .	102
(3) Pulse Height Spectrum . . . . .	102
2. Spacecraft Services . . . . .	103
a. Spacecraft Time . . . . .	103
b. Spin Angle Determination . . . . .	103
c. Programmable Processor . . . . .	104
d. Data Manipulation . . . . .	105
e. Memory . . . . .	105
f. Command Processing . . . . .	106
3. SRT for the C&DH Subsystem . . . . .	107
a. Spacecraft Oscillator . . . . .	107
b. Transmitter . . . . .	107
c. S to X Band Multiplier . . . . .	107
VI. SPACECRAFT FLIGHT OPERATIONS . . . . .	108
A. <u>Assumptions</u> . . . . .	108
B. <u>General Considerations</u> . . . . .	108

	<u>Page</u>
C. <u>Tracking and Operational Scheduling</u> . . . . .	109
1. Projected Loading . . . . .	109
2. Galactic Jupiter Probe Support . . . . .	110
3. Attitude Determination and Control . . . . .	111
4. Orbit Determination . . . . .	111
5. Command . . . . .	111
6. Scheduling . . . . .	111
D. <u>Communications</u> . . . . .	112
E. <u>Control Center</u> . . . . .	112
F. <u>Personnel</u> . . . . .	113
G. <u>Training</u> . . . . .	113
H. <u>Analysis</u> . . . . .	113
VII. APPENDICES . . . . .	115
A. <u>Spin Axis Direction Determination for the Galactic Jupiter Probe</u> . . . . .	115
B. <u>The Modulation/Detection Method</u> . . . . .	121

## LIST OF FIGURES

<u>Figure No.</u>	<u>Title</u>	<u>Page</u>
III-1	Geocentric Injection Speed Versus Launch Date . . . . .	9
III-2	Geocentric Injection Energy Versus Launch Date . . . . .	10
III-3	Arrival Date Versus Launch Date . . . . .	11
III-4	Launch Vehicle Capabilities . . . . .	12
III-5	Communications Distance at Jupiter Arrival Versus Launch Date . . . . .	13
III-6	Ecliptic Projection of an Earth-to-Jupiter Trajectory Flight Time to Jupiter = 500 Days . . . . .	14

<u>Figure No.</u>	<u>Title</u>	<u>Page</u>
III-7	Ecliptic Projection of an Earth-to-Jupiter Trajectory Flight Time to Jupiter = 600 Days . . . . .	15
III-8	Communications Distance Versus Time from Injection . . . . .	16
III-9	Geocentric Radial Acceleration Versus Time from Injection . . . . .	17
III-10	Geocentric Range Rate Versus Time from Injection . . . . .	18
III-11	Earth-Sun-Vehicle Angle Versus Time from Injection . . . . .	19
III-12	Earth-Vehicle-Sun Angle Versus Time from Injection . . . . .	20
III-13	Planetary Encounter Hyperbolic Trajectory . . . . .	21
III-14	Angle Between Approach Asymptote and the Jupiter-Sun Vector Versus Launch Date . . . . .	22
III-15	Angle Between Approach Asymptote and the Jupiter-Earth Vector Versus Launch Date . . . . .	24
III-16	Approach Hyperbolic Excess Speed Versus Launch Date . . . . .	25
III-17	Variation of the Jupiter Centered Speed with Radial Distance from Jupiter . . . . .	26
III-18	Hyperbolic Flyby Geometry . . . . .	28
III-19	Planetary Approach Coordinate Systems and Impact Plane . . . . .	30
III-20	Time to 10 AU, Transfer Time 500 Days . . . . .	31
III-21	Solar Ecliptic Latitude After 500 Days, Transfer Time 500 Days . . . . .	32
III-22	Inclination to the Ecliptic, Transfer Time 500 Days . . . . .	33
III-23	Earth-Jupiter Transfer Trajectory . . . . .	36
III-24	Miss Parameters to a Velocity Impulse Along the Restricted Axis . . . . .	38
III-25	Injection and Trajectory Correction Ellipses, Impact Plane Projection . . . . .	39
III-26	99% Midcourse Fuel Requirements Using the TE-364 (TRW Injection Errors) . . . . .	40
III-27	Midcourse Correction Time (Days from Injection) . . . . .	42
III-28	Midcourse Fuel-Weight - $\Delta V$ Tradeoff . . . . .	43
III-29	Early Trajectory Correction Feasibility . . . . .	46
IV-1	85-Foot Data Acquisition Antennas Rosman, North Carolina. . . . .	50
IV-2	Rosman Data Acquisition Facility, Functional Block Diagram. . . . .	53
IV-3	Tracking Coverage . . . . .	58
IV-4	Sub-Orbital Trajectory - Galactic Jupiter Probe . . . . .	59
IV-5	Probe Visibility 0 to 2 Days After Injection, March 1972 Launch . . . . .	60
IV-6	Probe Visibility 300 to 301 Days After Injection, March 1972 Launch . . . . .	61
IV-7	Noise Temperature Characteristics of Cassegrain Antenna with Maser Preamplifier . . . . .	62

<u>Figure No.</u>	<u>Title</u>	<u>Page</u>
IV-8	Received Signal to Noise Ratio ST/No (db) . . . . .	66
IV-9	Received Signal Level . . . . .	68
IV-10	Allowable Bit Rate Versus Range . . . . .	69
IV-11	Ground Receiver Coherent Detector Loop Noise - 85' Antenna	71
IV-12	Ground Receiver Coherent Detector Loop Noise - 210' Antenna	72
IV-13	Communication System Block Diagram . . . . .	74
IV-14	Spacecraft Transponder Loop Phase Noise . . . . .	75
IV-15	Command System . . . . .	77
IV-16	Command Link Performance from Various Antenna and Power Combinations . . . . .	80
V-1	Block Diagram of the Spacecraft - Ground Communication and Data Handling System . . . . .	88
V-2	Telemetry Link Performance with Various Antenna Combina- tions . . . . .	94
V-3	Block Diagram of Spacecraft Transmitter . . . . .	94
V-4	Telemetry Link Performance at Jupiter Mean Distance (5 AU)	99

#### LIST OF TABLES

<u>Table No.</u>	<u>Title</u>	<u>Page</u>
III-1	One-Sigma Miss Vector Uncertainties due to Injection Errors for a 500-day Flight to Jupiter . . . . .	35
III-2	Miss-Vector Uncertainties (1 Sigma) due to Navigation Errors	45
IV-1	NASA Big Dish Stations - 1972 . . . . .	49
IV-2	Deep Space Network Parameters . . . . .	55
IV-3	Rosman II Station Parameters After Modification for the Galactic Jupiter Probe . . . . .	64

# A MISSION, TRACKING, COMMUNICATION, AND FLIGHT OPERATION STUDY FOR THE GALACTIC JUPITER PROBE

## I. INTRODUCTION

### Philosophy and Assumptions

Upon the establishment of scientific objectives to measure certain quantities in prescribed areas of interest in deep space a thorough analysis must be made for planning the most reliable and most economical mission of carrying pertinent sensors and associated equipment to the defined loci of measurements. Furthermore, provision must be made to have acquired data transmitted from the instrumented spacecraft to the earth in correlation with time of measurement and spacecraft position at the time of measurement.

In order to fulfill the general requirements mentioned above, detailed analyses have to be performed for the generation of appropriate trajectories; the development of a suitable guidance and navigation logic; the selection of a launch vehicle capable of propelling a minimum-permissible instrumented payload into a prescribed trajectory at a required injection velocity; the provision of real-time trajectory determination from tracking data, the possibility of trajectory correction by midcourse maneuvers, and trajectory verification throughout the mission by continued tracking; the establishment of a command link to control from the ground spacecraft maneuvers and spacecraft attitude as well as the sequence and duration of scientific experiments; and the transmission of scientific data and their proper handling.

The numerous problems which have to be solved simultaneously by the various analyses make it often necessary to agree to certain compromises between the different, interrelated territories of interest and, in case of preliminary unknowns, to rely on plausible assumptions in order to plan within a prescribed time frame for the development of an integrated spacecraft system completely compatible with an existing or augmented ground network system and capable of performing scheduled scientific space explorations with a reasonable probability of success.

With the philosophy of approach indicated above the area of Mission Analysis and Spacecraft Flight Operations for the Galactic Jupiter Probe (GJP) has been studied. This study in its details was comprised of trajectory analysis, guidance and navigation analysis, ground network support analysis, communication and data handling systems analysis, and spacecraft flight operations analysis.

Based on the scientific objectives, the following three types of missions are considered feasible:

1. Jupiter fly-by with closest planetary approach of 10 to 15 Jupiter radii and subsequent deep space post-encounter flight in the plane of ecliptic
2. Jupiter fly-by with post-encounter flight out of the plane of ecliptic
3. Jupiter fly-by with post-encounter solar orbit

Main emphasis at this time was given to the first type of mission while the other types of missions will be further pursued in the continuing study.

Certain assumptions had to be made which pertain to the correlation of periodic launch opportunities (every 13 months) with the availability of a suitable launch vehicle and the readiness of a properly augmented ground network; to the minimum permissible payload to carry a worthwhile number of scientific instrumentation and necessary equipment for attitude determination, attitude control, rf transmitters and receivers, power supply, etc., as compared to the launch vehicle capability; to the choice of an achievable upper and lower limit of a sufficiently flexible region of mission duration to Jupiter encounter in order to be able to compensate by travel time variation for uncertainties in launch vehicle capability and payload implementation; to the minimum ultimate heliocentric distance of the spacecraft satisfactory to scientific mission objectives and communications and data handling requirements; to the mode of spacecraft orientation as an adequate compromise to fulfill the multitude of requirements connected with scientific experiments, communications, data handling, attitude control, midcourse maneuvers, thermal considerations, payload, etc; to the selection of a most suitable rf carrier frequency and needed transmitted power on-board spacecraft and on the ground; to the choice of a high-gain spacecraft antenna fulfilling communication requirements as well as dimensional restrictions dictated by launch vehicle shroud and at highly reliable operational conditions; and to the commitment of ground support networks.

A list of assumptions used for this study is given below:

First Launch Opportunity: March 1972

Minimum Payload Requirement: 500 lbs

Minimum Launch Vehicle Requirement: Atlas-Centaur-TE364 with permissible improvement and development time up to 4 years

Mission Duration to Jupiter Encounter: Max: 600 Days  
Min: 500 Days

Minimum Achievable Heliocentric Distance: 10 A.U.

Spacecraft Orientation: Spin-Stabilized - Earth Oriented

8-foot Non-Deployable Spacecraft Antenna (minimum requirement)

S-Band Transmitter (10 watts)

Minimum Bit Rate. 10 Bits/Sec at Jupiter Encounter

Ground Support: 85-foot STADAN  
210-foot DSN  
85-foot MSFN

## II. SUMMARY

### A. Mission Analysis

The Mission Analysis chapter of this report deals with the trajectory, guidance and navigation analyses of a fly-by mission to Jupiter and beyond. Each subject was studied as an individual but not independent factor in the overall Mission Analysis effort. Some of the salient results of the studies that are reported in this chapter are summarized in the following paragraphs.

Trajectory analysis was primarily slanted toward determining launch opportunities and correlation of injection energy requirements with launch vehicle capabilities. The ultimate goal is the selection of a launch vehicle, payload and flight time combination. Energy requirements for a 1972 launch are such that a launch window of 20 days (February 25 through March 15) will allow a 500 pound spacecraft to be launched by an SLVHIX/Centaur-70/Burner II (027A) on a flight to Jupiter of 515 to 550 days. It was determined also, that a flight time of nearly 500 days provided nearly minimum communications distance at Jupiter arrival when the launch occurs on the date that requires minimum injection velocity. The text of this report shows the effect of the gravitational field of Jupiter on the heliocentric trajectory of the spacecraft. The effect of aim point at Jupiter on the resulting post encounter trajectory is discussed along with a development of the mathematical model that was used to arrive at the results.

Guidance analysis, as applied to the Galactic Jupiter Probe mission, means the determination of the velocity requirements for a midcourse correction under

the restriction of a specific spacecraft attitude. The following attitude constraints were studied for the Galactic Jupiter Probe subject to the assumption that the velocity increment is applied along the spin axis of the spacecraft; (1) spin axis oriented along the Earth-probe line, (2) spin axis oriented along the Sun-probe line, and (3) spin axis fixed in the injection condition (i.e., parallel to the injection velocity vector). The results of the studies show that a total midcourse correction capability of 100 meters/sec should be sufficient for any of the attitude restrictions if the midcourse correction can be executed within 20 days from injection. A single midcourse correction should be adequate for the achievement of a deep space probe mission objective. If the desired post encounter mission is to fly out of the ecliptic, however, an optimum arbitrary pointing midcourse correction or multiple corrections – or both – may be necessary.

The navigation studies are intended to relate to the problem of orbit determination from ground tracking and make recommendations for the proper use and necessary modifications of the tracking networks. In this report, a preliminary error analysis of the trajectory determination process using range, range rate, and angular data has been performed. It was done primarily to answer questions related to the midcourse corrections. The effects of tracking system and speed of light uncertainties as well as uncertainties due to the AU-to-kilometer conversion, astronomical ephemerides, and solar radiation pressure were considered in this study.

The results of the study show that for tracking considerations very little difference exists between tracking 2.5 and 10.0 days after spacecraft injection. The addition of range measurements, along with range rate, decreases a projection of the miss-vector uncertainty at Jupiter by a factor of two. When the uncertainties due to the AU-to-kilometer conversion, ephemerides, and solar radiation pressure are combined with the tracking uncertainties, the total one-sigma trajectory prediction uncertainties (in terms of the miss-vector at Jupiter) range from 10,000 to 10,600 kilometers. This includes all the tracking situations considered.

Midcourse execution errors have been assumed to be represented by a proportional error (1 percent of  $\Delta V$ ), a resolution error ( $\sigma_{\Delta V} = 0.1$  m/sec) and a pointing error ( $\sigma_{\theta} = \sigma_x = 1^\circ$ ). If a 500 day, spin axis, earth-oriented mission has a single midcourse correction in which the in-plane miss ( $\vec{B} \cdot \vec{T}^\circ$ ) alone is corrected, then the resulting miss-vector uncertainty due to midcourse execution errors is approximately 22,000 kilometers (1 sigma). This uncertainty is for midcourse corrections performed at both 2.5 and 10 days from injection.

## B. Ground Network

The Ground Network Support chapter of this report deals with the investigation of the proper coverage of all phases of the Galactic Jupiter Probe mission by earth-based tracking stations.

From a spacecraft surveillance and facility availability study the following conclusions have been drawn:

The launch and near earth phases can be adequately covered by the ETR and MSFN C-Band radars at Patrick AFB, Grand Bahama, Grand Turk, Antigua, Bermuda, Canary Island, Ascension, Pretoria and Tananarive; and by DSN and MSFN USB instrumentation at Cape Kennedy, MILA, Grand Bahama, Antigua, Ascension, Bermuda and Madrid. The STADAN station at Tananarive can supply extended S-Band coverage during the early hours.

For the cruise phase to and beyond Jupiter encounter, the ROSMAN II STADAN station in North Carolina has been selected as an appropriate facility to perform the routine tracking, telemetry, and command operations. This station will be refurbished with a 100 KW transmitter and a very sensitive antenna and receiving system designed specifically for this program.

The NASA Deep Space Network will be tasked to support this project at times, not only to supply the additional coverage that Madrid, Spain supplies but to provide, as required, the higher sensitivity of 210 foot dishes. Additional back-up will come from the Manned Space Flight Network.

Using very efficient coding and modulation techniques, a transmitter power level of 10 watts and the gain of the 8 foot spacecraft dish at 2.3 GHz, substantial information, in the order of tens of bits per sec, can be conveyed from the spacecraft to ground even at ranges of 10 AU, twice the nominal distance to Jupiter at encounter.

Utilizing 100 KW ground transmitters and the omnidirectional spacecraft antenna, the required 1 bit/sec command up-link will operate properly out to 3.5 AU with the 85 foot ground antenna and 9 AU with the 210 foot dish. Higher spacecraft antenna gain, normally usable, assuming proper spin axis orientation, will provide substantial margin.

The trajectory of the spacecraft will be determined by two-way range rate tracking systems, this information obtained through accurate measurements of the Doppler shift on signals transmitted to the spacecraft and returned to the ground stations. An uncertainty, due to ground instrumentation only, of less than 0.03 cm/sec appears realizable.

A number of improvements can be made to the ground tracking and telemetry instrumentation, the most significant being the addition of a hydrogen maser frequency standard. Exploiting both the long and short term stability of this device, which is now being developed for field use, tracking bandwidths of coherent demodulators can be made much narrower with a resulting increase in sensitivity of the radio links. In addition, transmitter frequency drift during signal transit time, the predominate instrumentation uncertainty in deep space range rate systems, can be made negligible from today's standards.

#### C. The Galactic-Jupiter Probe Communication and Data Handling System

The proposed Galactic-Jupiter Probe Communications and Data Handling System (C&DHS) is designed to perform at ranges beyond ten (10) Astronomical Units (AU) with reliability commensurate with the minimum mission time of 5 years. The performance characteristics are summarized as follows: For a 210-foot ground antenna, a worst case communication capability from the Galactic Jupiter Probe to earth will provide 480 bits per second at Jupiter encounter and 120 bits per second at 10 AU. Seventy-six (76) bits per second are available through an 85 foot ground antenna at Jupiter encounter. Command through the spacecraft omnidirectional antenna, at the rate of one bit per second, is possible at ranges up to 9 AU if a 100 KW ground transmitter with a 210-foot dish is utilized. A high degree of onboard data processing is employed to achieve as much information per bit as possible.

A primary concern of the long mission times is reliability. The C&DHS design contains enough options and redundancy so that a "few" failures may occur and still allow the data to get through. This approach to reliability also will contribute to the mission survival of such uncharted environments as the Jupiter radiation belts and the asteroid hazard. The ability to reprogram the data handling system also can minimize the effect of other failures. One can optimally reassign communication capacity to all communications users to minimize the effects of such degradations.

Two related functions that use the communication links are also covered. These are the tracking function and a RF spacecraft spin axis determination and reorientation function.

#### D. Spacecraft Flight Operations

Consideration of spacecraft flight operations has been based upon several broad assumptions. One is that all operations will be accomplished under the control of an Operations Control Center at the Goddard Space Flight Center. A second is that all facilities will be adequate and in a state of technical readiness for support of the mission. Another is that suitable operational priority will be

given the project to permit schedule feasibility, especially for unique operations.

Operational support of the Galactic Jupiter Probe will require support from the Space Tracking and Data Acquisition Network (STADAN), the Deep Space Network (DSN), the Manned Space Flight Network (MSFN), the Eastern Test Range (ETR), the NASA Communications System (NASCOM) and the Goddard Space Flight Center (GSFC). Presently planned facilities; augmented for the Galactic Jupiter mission; appear adequate.

Operational scheduling under conditions of projected loading of facilities appears completely feasible. Operational activities will be inclusive of the following:

- Tracking Data and Telemetry Acquisition
- Attitude Determination and Control
- Orbit or Trajectory Determination
- Command Generation and Transmission
- Ground Communications
- Control Center Functions
- Operational Orientation and Training

There are no known insurmountable problems in operational support at this time.

Detailed planning, programming, budgeting and scheduling of equipment, software and personnel requirements will begin in Phase B of the project.

### III. MISSION ANALYSIS

#### A. Trajectory Analysis

The Galactic Jupiter Probe mission is separated into the following major phases:

- a. Earth escape phase
- b. Cruise phase
- c. Jupiter-approach phase
- d. Post-encounter phase

The powered ascent phase is not included because the launch vehicle has not as yet been specified. The trajectory computations were made using the patched-conics method (Reference 1). The following basic assumptions apply to the trajectory data:

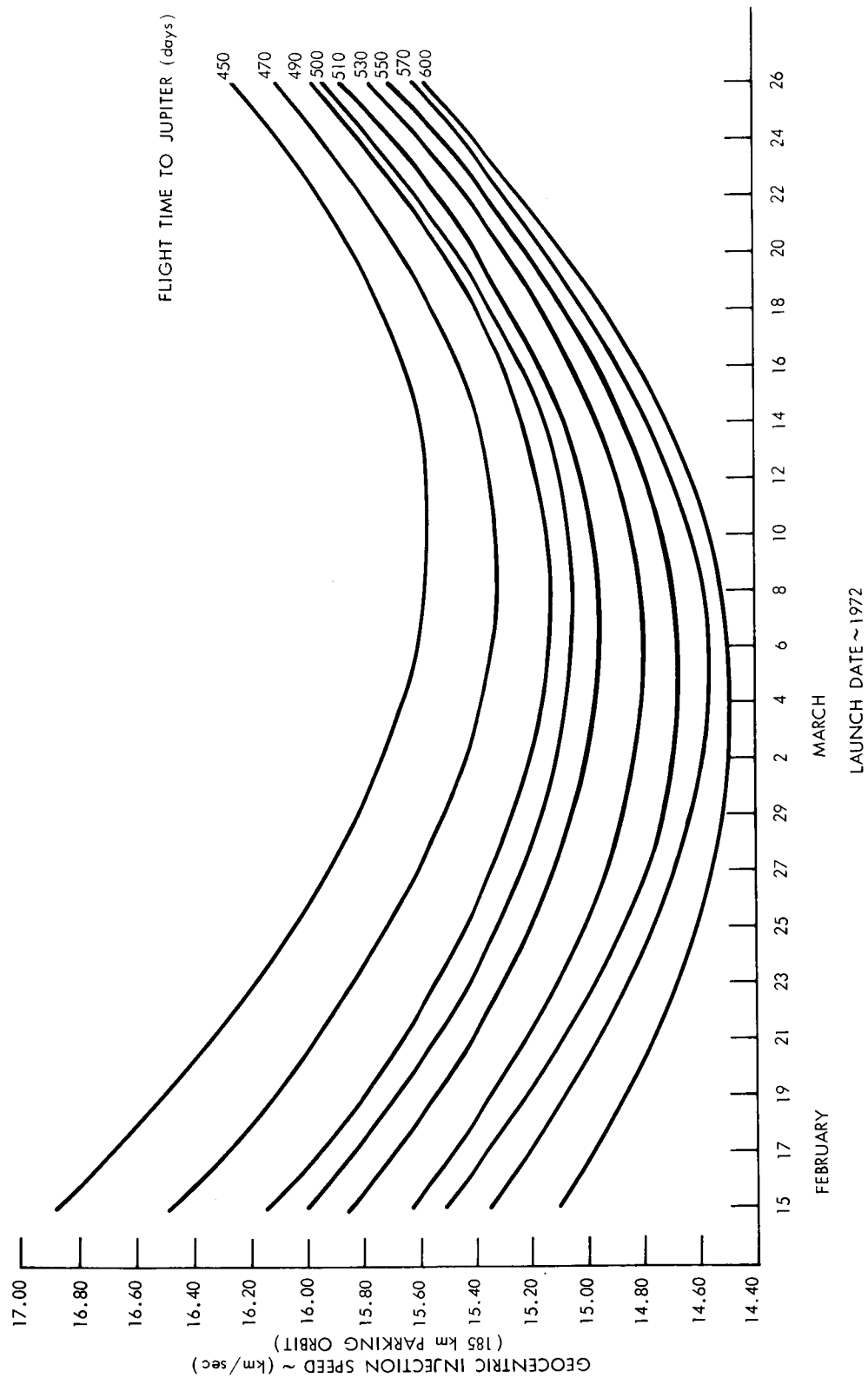
- a. The probe is acted on only by the gravitational force of the earth during the geocentric phase.
- b. The probe is acted on only by the gravitational force of Jupiter during the Jupiter-centered phase.
- c. The oblateness effects of the planets are neglected.
- d. During the heliocentric phase, the launch and target planets are massless; therefore, the only force acting on the probe is the gravitational field of the sun.

#### 1. Earth Escape Phase

a. Injection Requirements and Launch Period. The required injection speed and energy as functions of flight time and launch date, are shown in Figures III-1 and III-2. Injection energy ( $C_3$ ) is defined as  $C_3 = V^2 - 2\mu/r$ , where  $V$  is injection speed,  $\mu$  is the earth's gravitational constant, and  $r$  is the radial distance between the center of the earth and the injection point. The data assume a variable arrival date for each launch date and flight time. If a constant arrival date is desired, as the launch date is stepped through an arbitrary launch period, a corresponding increment in flight time is required. Arrival dates are shown in Figure III-3 for the launch dates and flight times being considered.

The 1972 launch period will be specified when the payload weight has been determined and a launch vehicle has been selected. The launch period (Reference 2) is the separation between the earliest and latest launch dates at which the mission can be performed. The launch period then becomes apparent by neglecting all injection speeds in Figure III-1 that are in excess of the launch vehicle capabilities. For example, if the maximum injection speed that can be attained for a given payload is 15 kilometers per second, the corresponding launch period for a 530-day flight to Jupiter is 20 days, centered about March 6, 1972. The launch period will vary for different flight times to Jupiter and will increase for longer flight times because of the decrease in required injection speed for a given launch date.

b. Launch Vehicle Payload Estimates. The launch vehicle performance data shown in Figure III-4 represent the Lewis Research Center estimate of launch vehicle capabilities in 1972 (Reference 3). The characteristic speed shown in Figure III-4 is the speed of a payload at an altitude of 100 nautical miles, after a due east launch from Cape Kennedy. Payload injection requirements for a given launch vehicle are determined by matching the characteristic speed shown in Figure III-4 with the injection speed shown in Figure III-1. A penalty from 30 to 100 meters per second for launch azimuths between 45



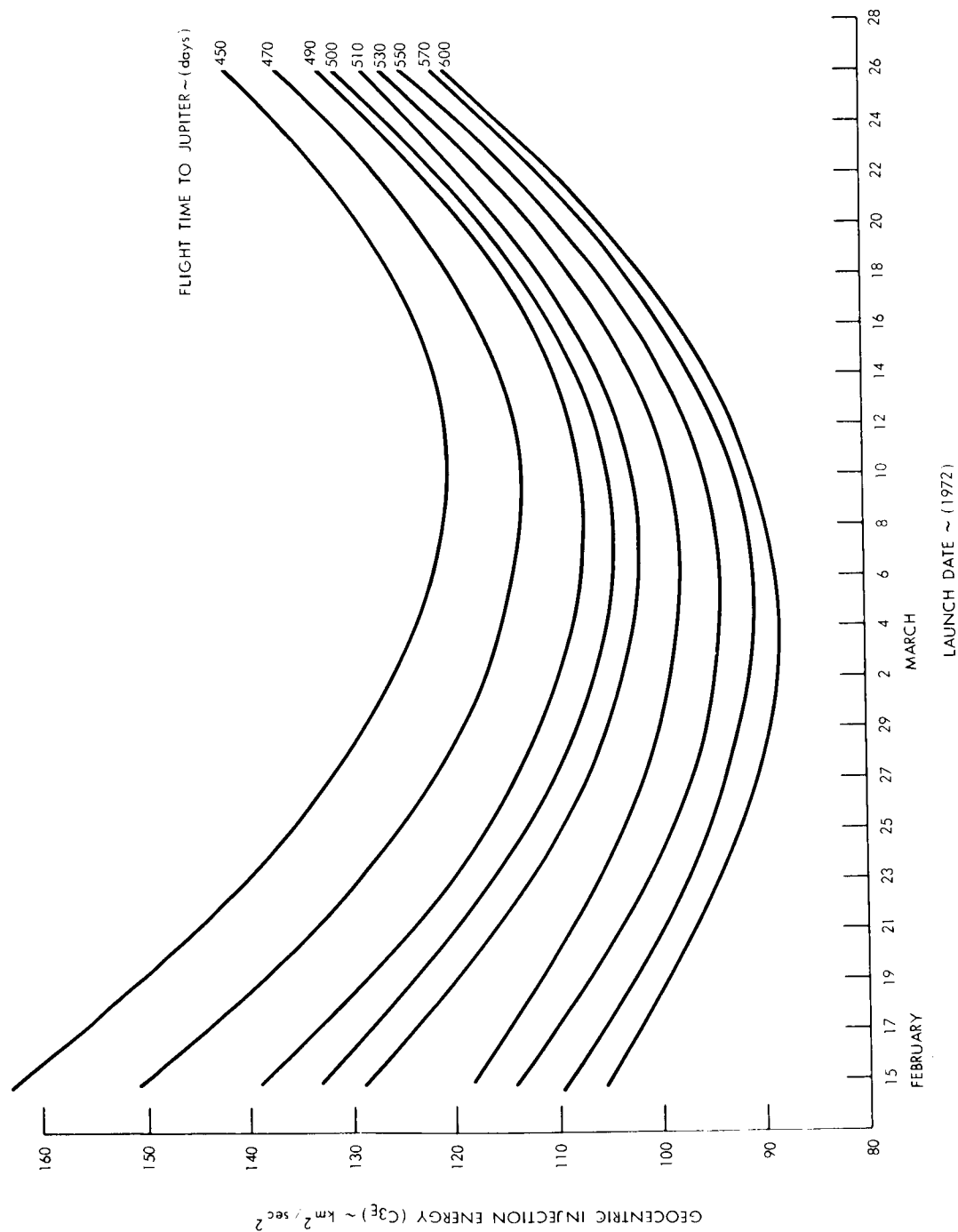


Figure III-2. Geocentric Injection Energy Versus Launch Date

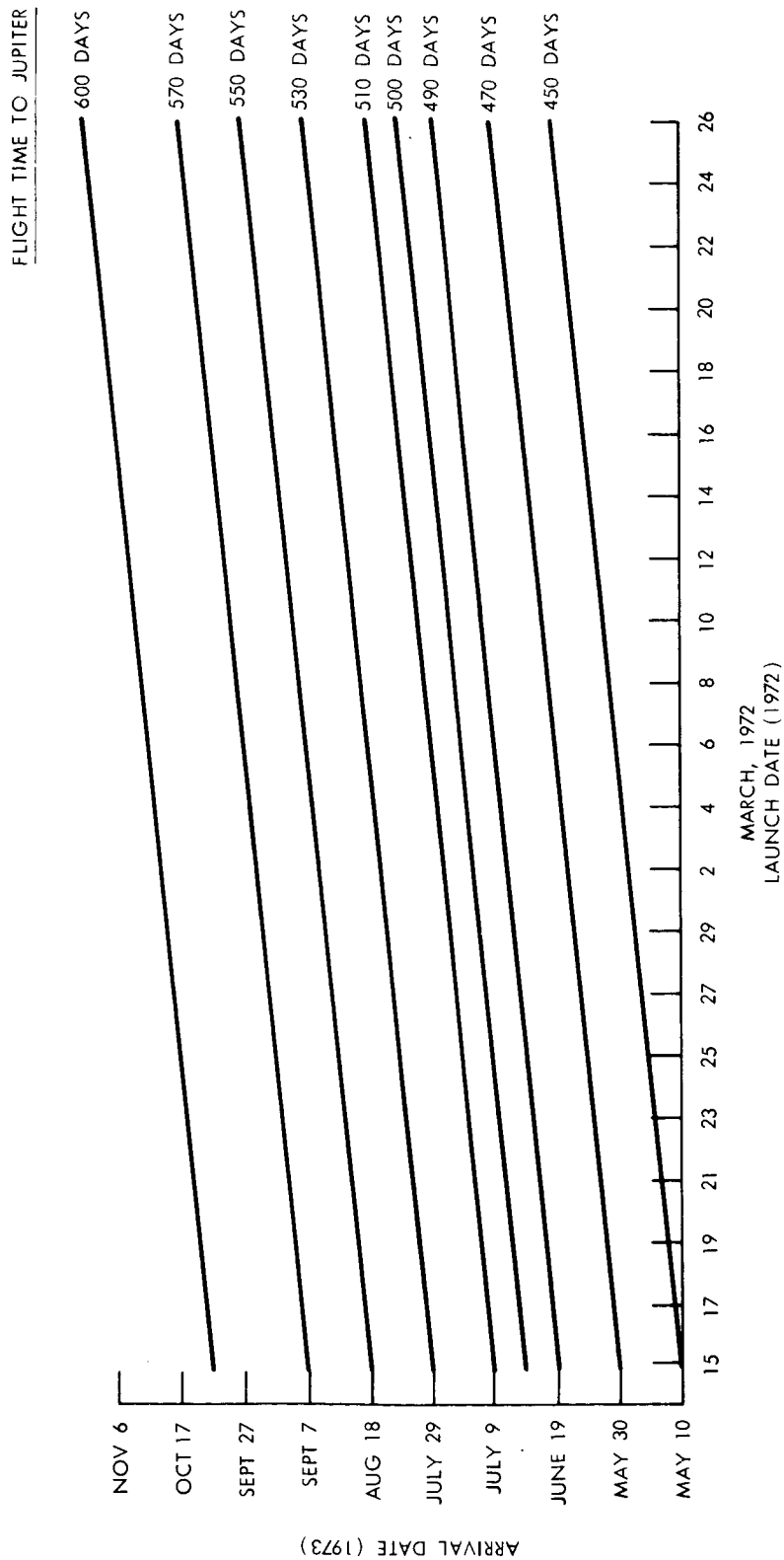


Figure III-3. Arrival Date Versus Launch Date

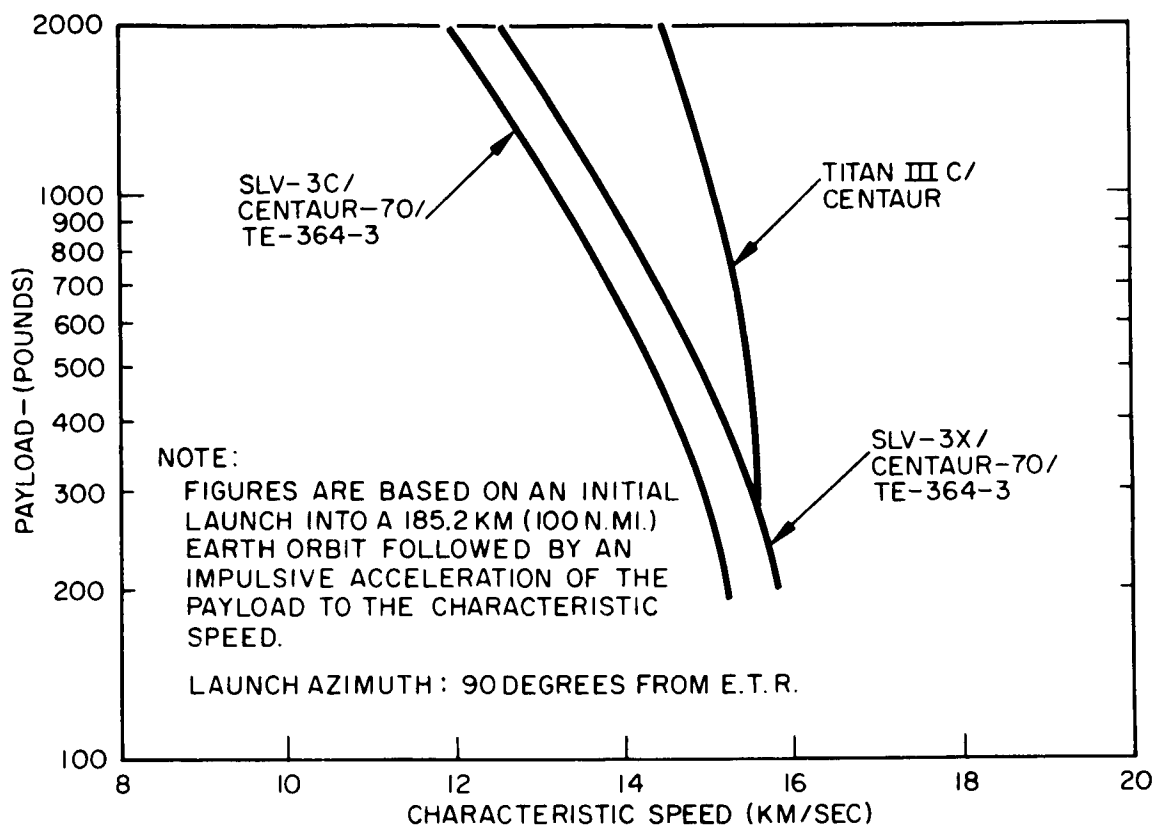


Figure III-4. Launch Vehicle Capabilities

and 110 degrees must be subtracted from the characteristic speed for a launch azimuth other than 90 degrees.

An increased payload capability may be possible by using a direct ascent (one Centaur burn) as opposed to an ascent from a parking orbit (two Centaur burns). To use a direct ascent, the geometric constraint of achieving a necessary outgoing asymptote must be satisfied with a single Centaur burn. The required geometry for a flight of this type appears favorable in 1972; however, factors such as launch-window duration, length of time the window opens daily, and the relative complexity of using the direct ascent must be weighed against the increased payload capability.

## 2. Cruise Phase

The cruise phase begins when the payload is injected into ballistic flight after a powered ascent and terminates when the probe enters the gravitational influence of Jupiter.

The earth-sun-probe geometry during the mission dictates the communications capabilities and instances of possible communications blackout due to occultation by the sun. It is assumed that the arrival at Jupiter will be a period of high data transmission activity from the probe; therefore, it would be desirable if encounter should occur when the earth-probe distance is at a minimum. In this respect, a flight time of approximately 500 days is attractive because launching on the date requiring the minimum injection speed also provides a minimum communications distance at Jupiter arrival. No other flight times have this feature. Figures III-6 and III-7 illustrate the transfer trajectory projected into the ecliptic plane during the cruise phase. These plots depict typical 500- and 600-day flight times to Jupiter. Figures III-6 and III-7 also illustrate the earth-sun-probe geometry during the transfer trajectory. Communications distance, range rate, and radial acceleration, each versus time from injection, are plotted in Figures III-8, III-9, and III-10. These parameters are used to calculate tracking and communications power requirements.

### 3. Jupiter Approach Phase

The approach geometry at Jupiter (Figure III-13) is governed primarily by the Jupiter-centered hyperbolic excess velocity vector ( $\vec{V}_{hp}$ ). This vector

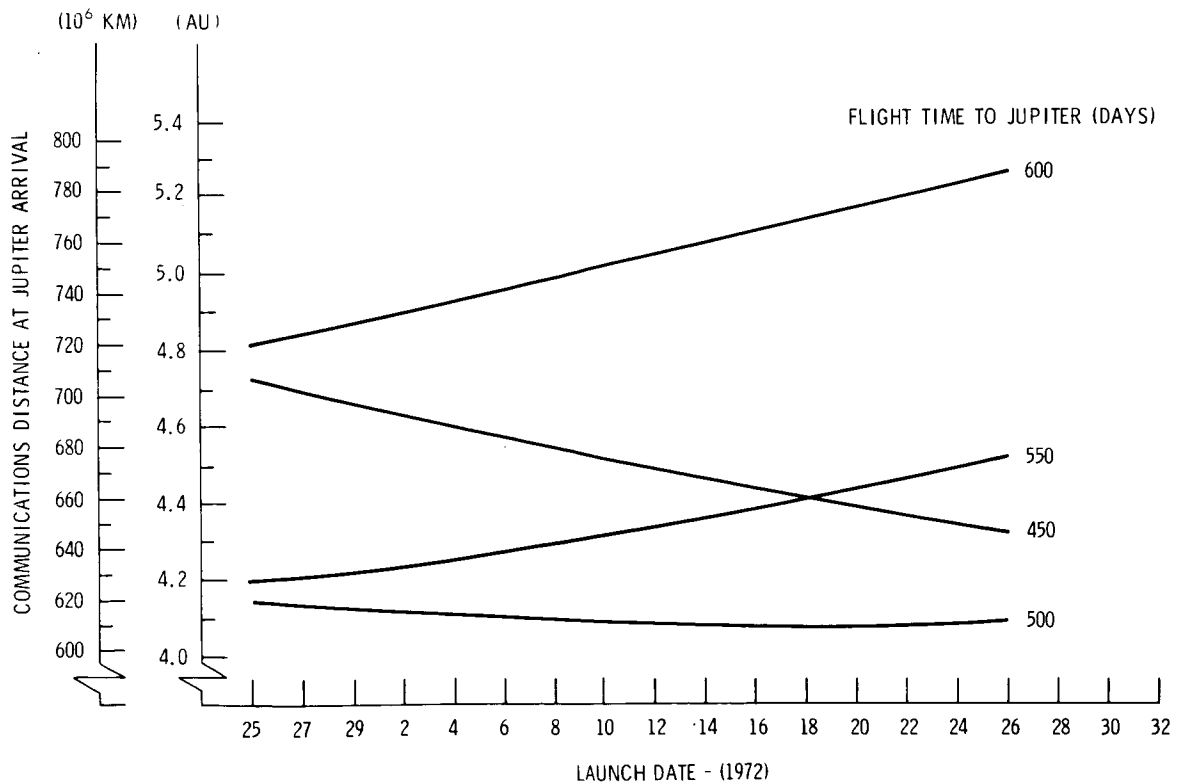


Figure III-5. Communications Distance at Jupiter Arrival Versus Launch Date

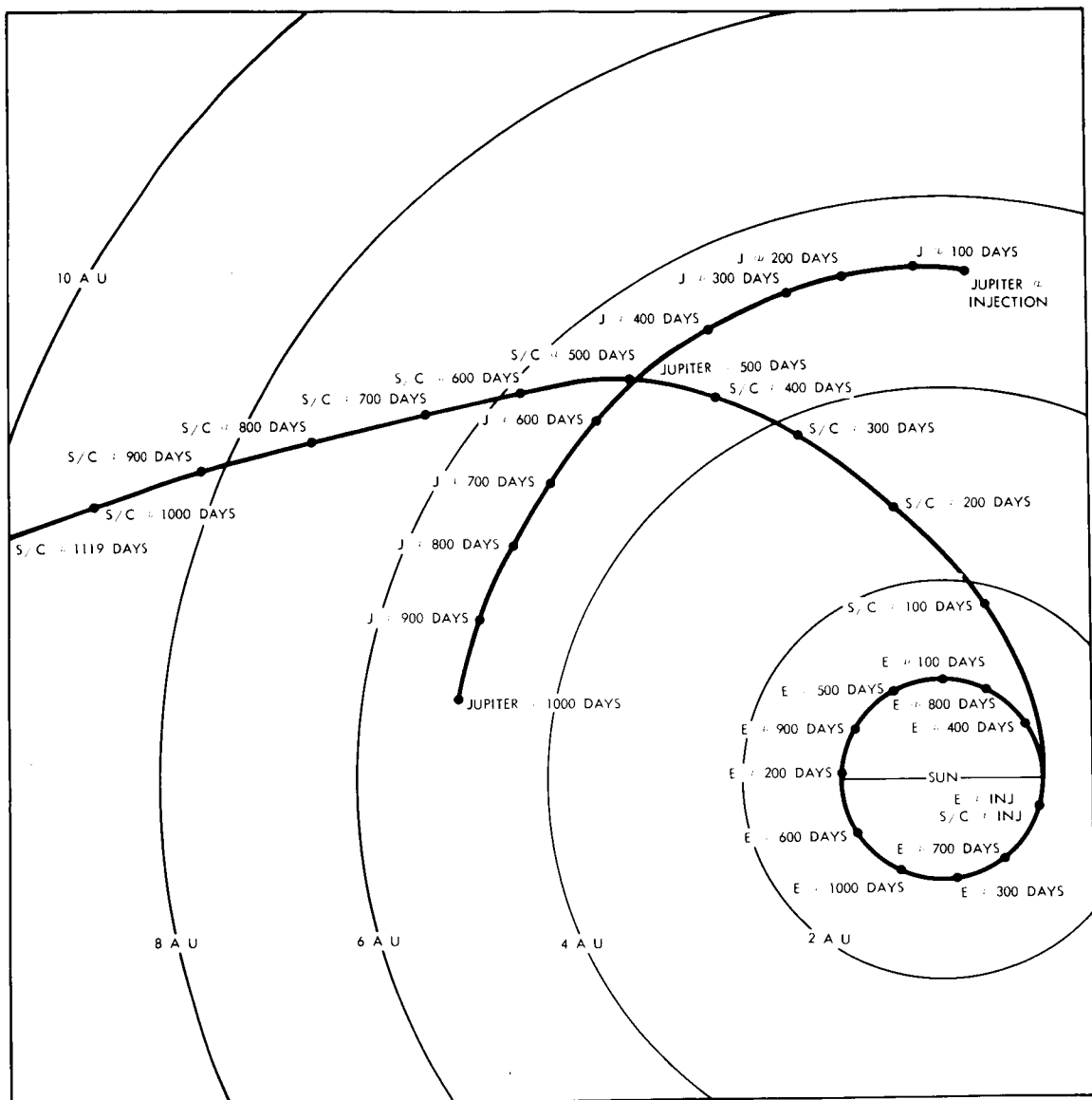


Figure III-6. Ecciptic Projection of an Earth-to-Jupiter Trajectory  
Flight Time of 500 Days to Jupiter

(magnitude and direction) forms the basis for the post-encounter mission of the Galactic Jupiter Probe.  $\vec{V}_{hp}$  is approximated as the vector difference between the heliocentric velocity of Jupiter and the heliocentric velocity of the spacecraft entering the gravitational influence of Jupiter, i.e.,

$$\vec{V}_{hp} = \vec{V}_{p/\odot} - \vec{V}_{J_1}$$

where:

$\vec{V}_{hp}$  = hyperbolic excess velocity vector,

$\vec{V}_{p/\odot}$  = heliocentric velocity vector of probe at Jupiter's sphere of influence, and

$\vec{V}_J$  = heliocentric velocity vector of planet Jupiter.

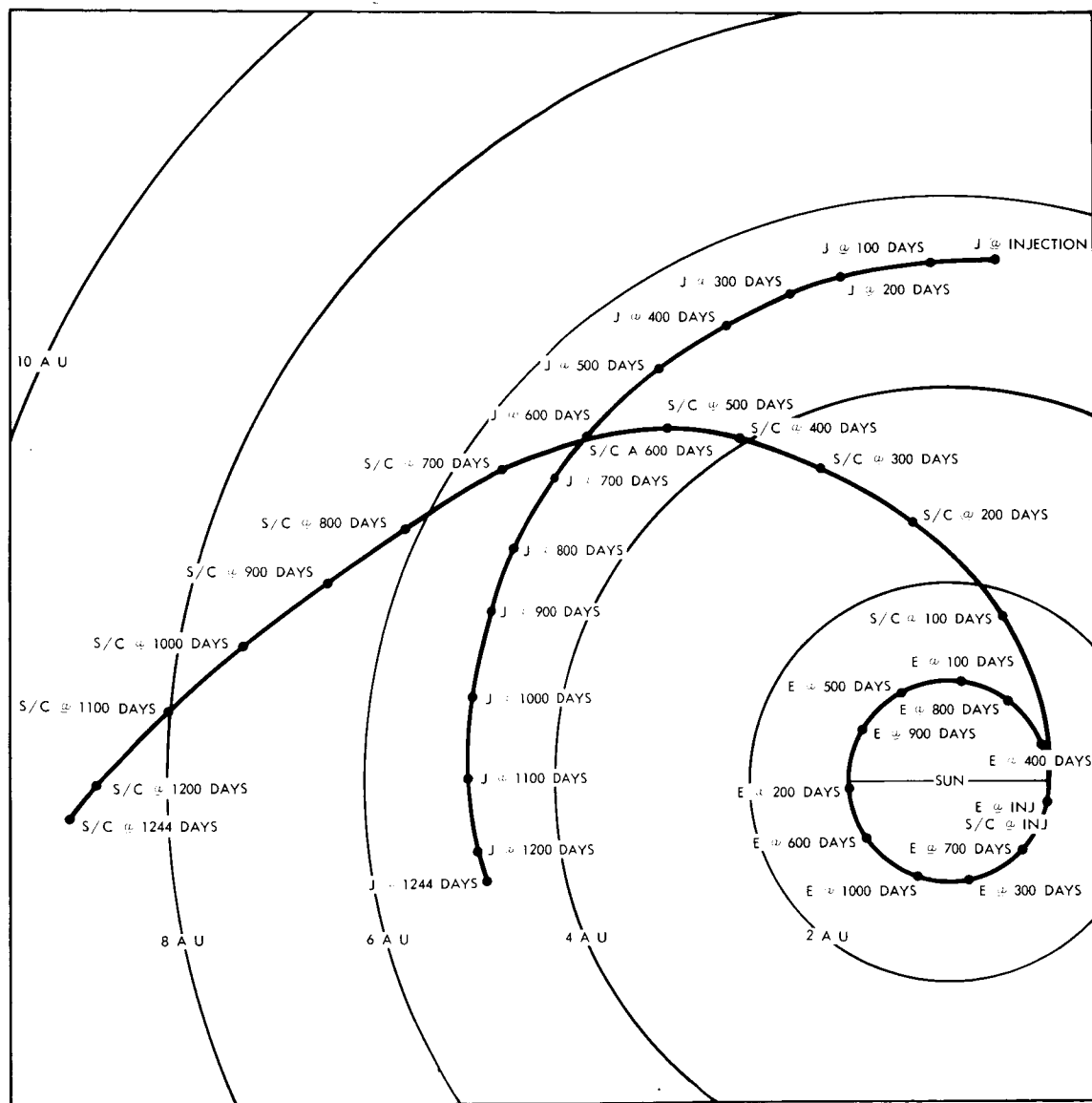


Figure III-7. Ecliptic Projection of an Earth-to-Jupiter Trajectory  
Flight Time of 600 Days to Jupiter

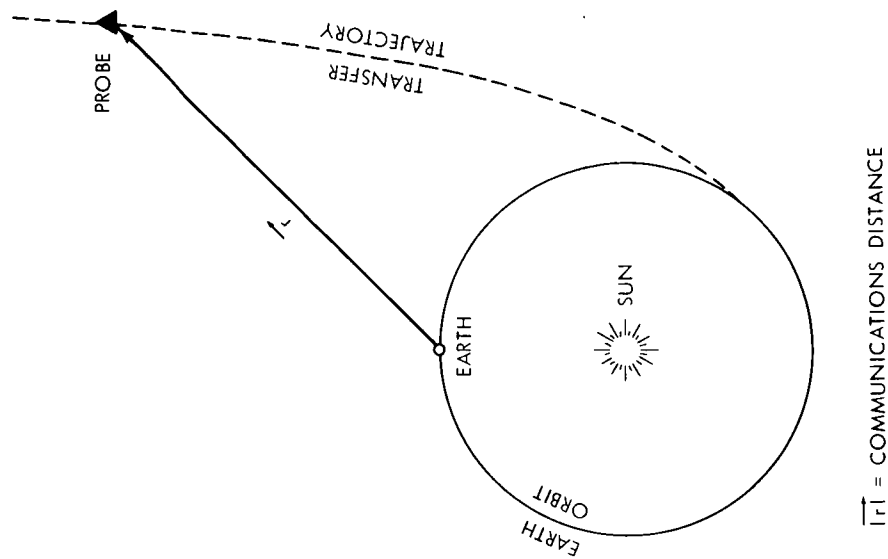
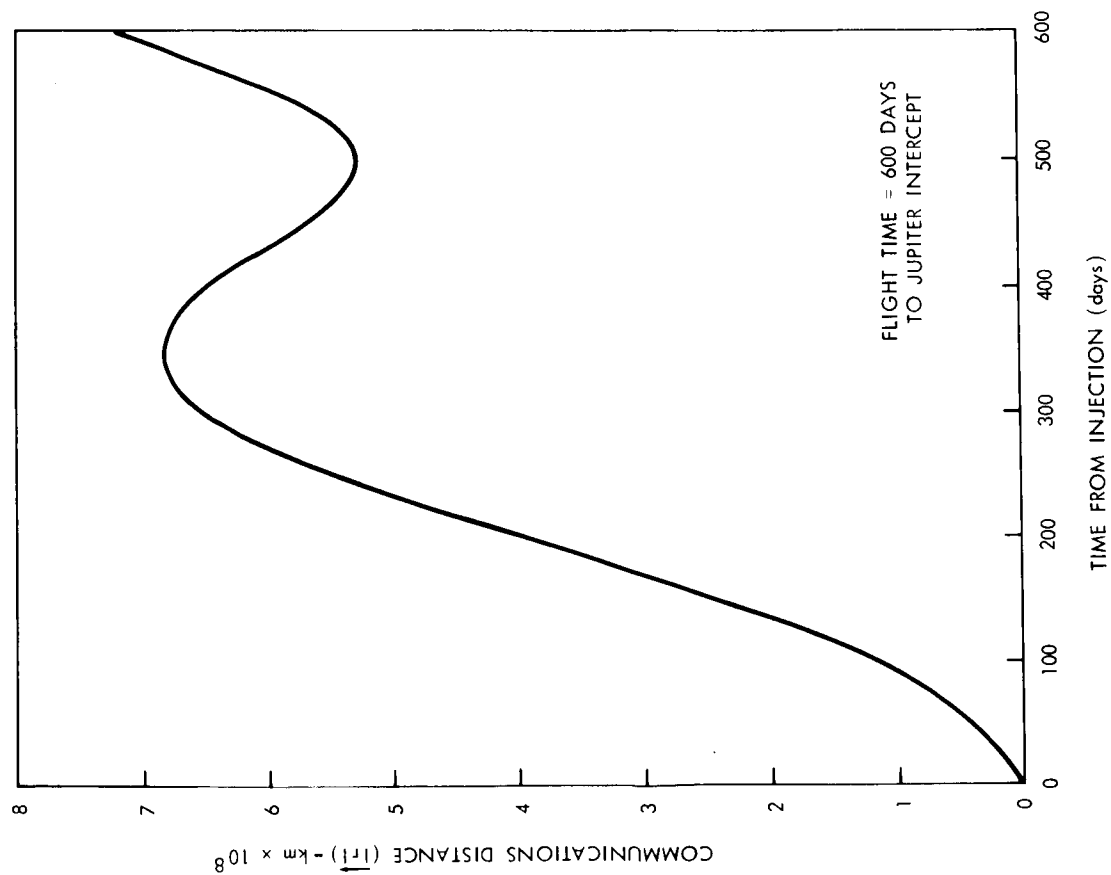


Figure III-8. Communications Distance Versus Time from Injection

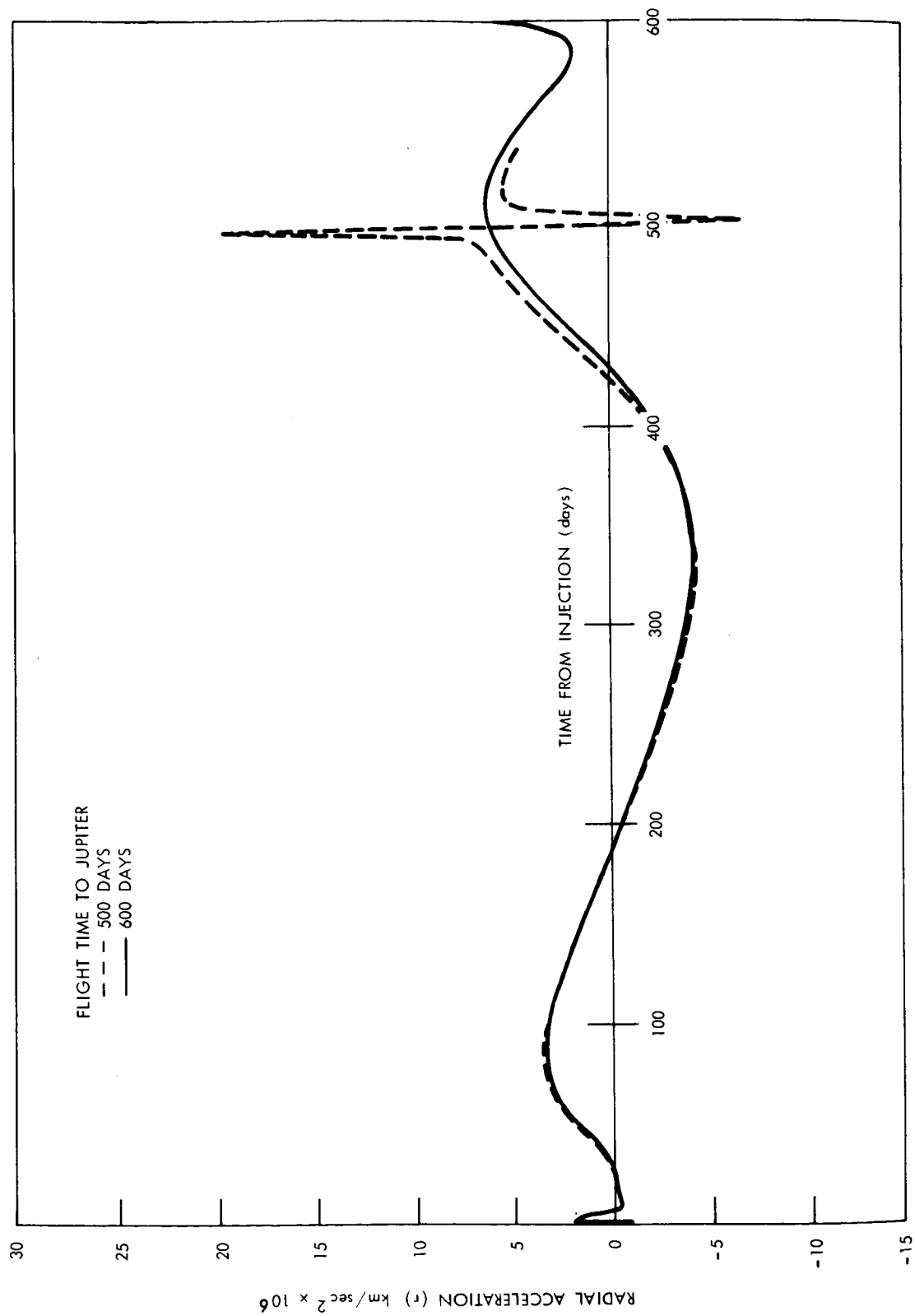


Figure III-9. Geocentric Radial Acceleration Versus Time from Injection

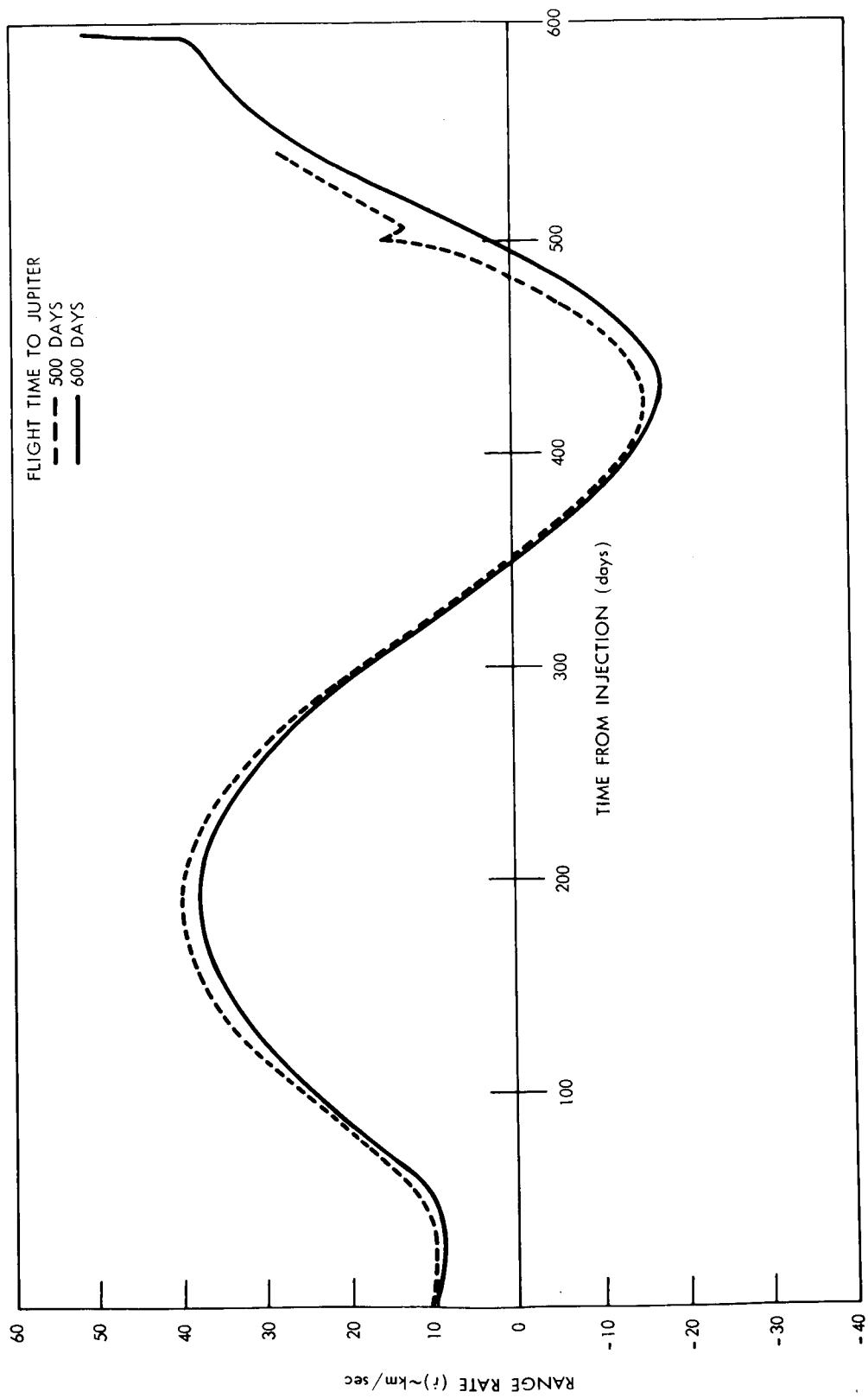


Figure III-10. Geocentric Range Rate Versus Time from Injection

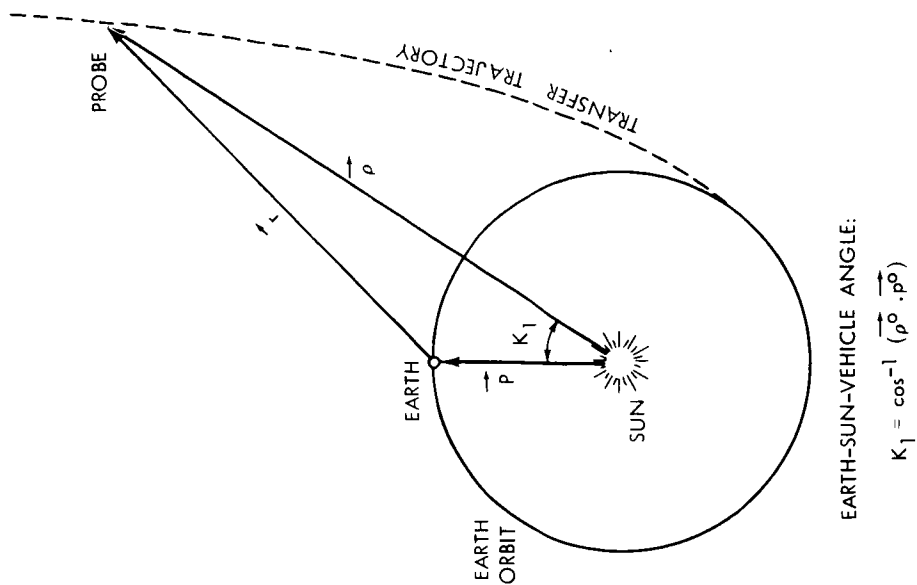
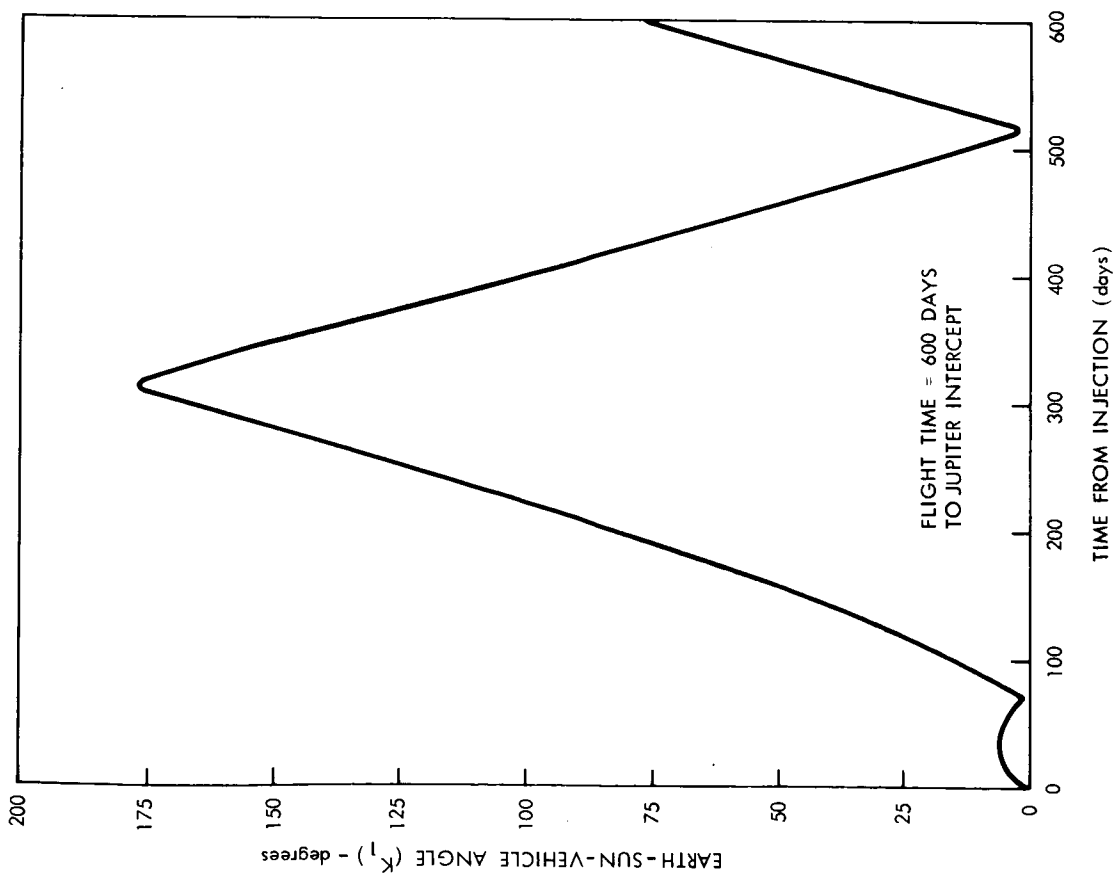


Figure III-11. Earth-Sun-Vehicle Angle Versus Time from Injection

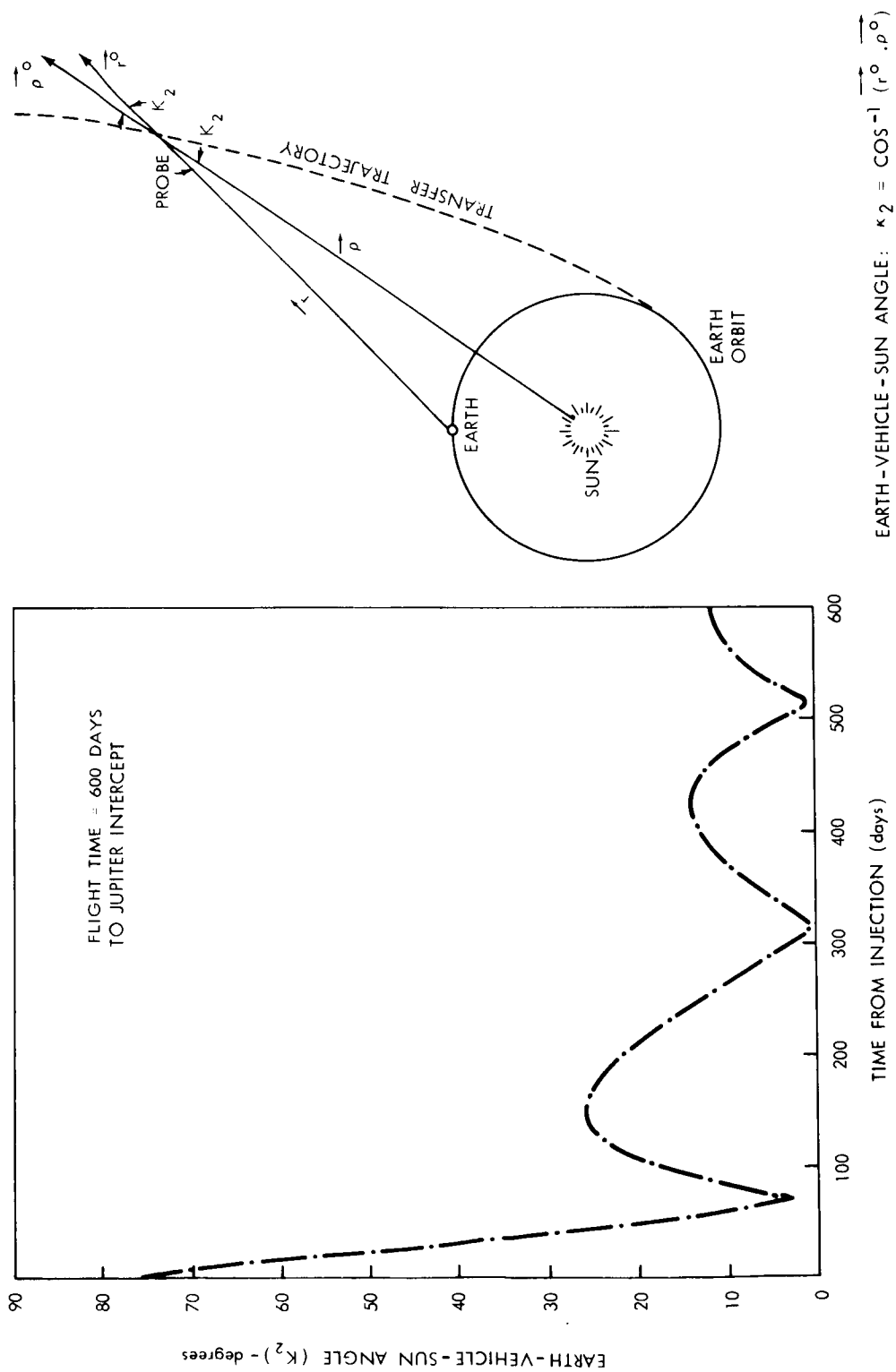
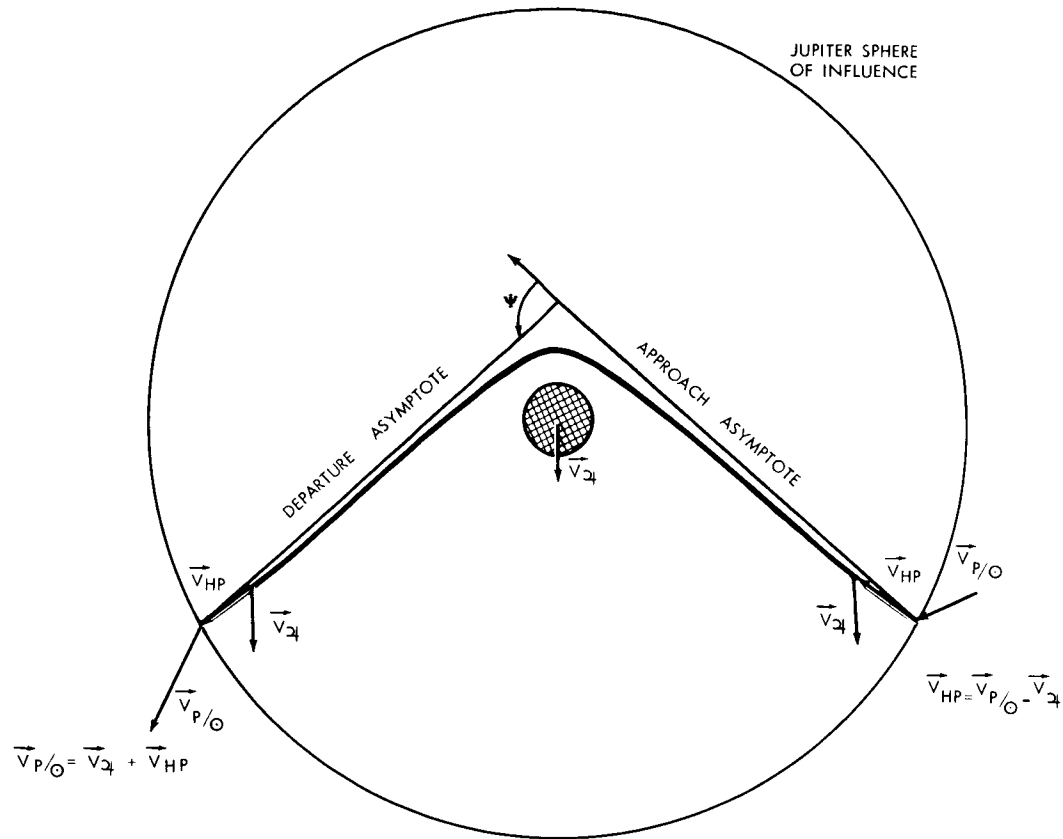


Figure III-12. Earth-Vehicle-Sun Angle Versus Time from Injection



DEFINITIONS:

$\vec{V}_{P/O}$  = HELIOCENTRIC VELOCITY VECTOR OF THE PROBE

$\vec{V}_{HP}$  = HYPERBOLIC EXCESS VELOCITY VECTOR OF THE PROBE

$\vec{V}_J$  = HELIOCENTRIC VELOCITY OF JUPITER (NOTE:  $\vec{V}_J$  IS ASSUMED TO BE INVARIANT DURING THE PERIOD OF ENCOUNTER)

$\psi$  = DEFLECTION OF THE ASYMPTOTES BY THE GRAVITATIONAL INFLUENCE OF JUPITER.

Figure III-13. Planetary Encounter Hyperbolic Trajectory

a. Approach Asymptote, Sun, Earth Relationship. The angular relationship between the approach asymptote and the Jupiter-sun vector at Jupiter encounter is defined by the angle ZAS (Reference 2). The variation of this angle with launch date and flight time to Jupiter is shown in Figure III-14, and is due to the heliocentric motion of Jupiter ( $\approx 0.1$  deg/day) in an orbital path. This angle will determine the illumination of the planetary disk during the approach phase as seen from the spacecraft. The magnitudes of the angle through the 1972 launch period (trip time of 450 to 600 days show that the spacecraft approaches Jupiter from the sunlit side and views an almost "full" planet during the approach.

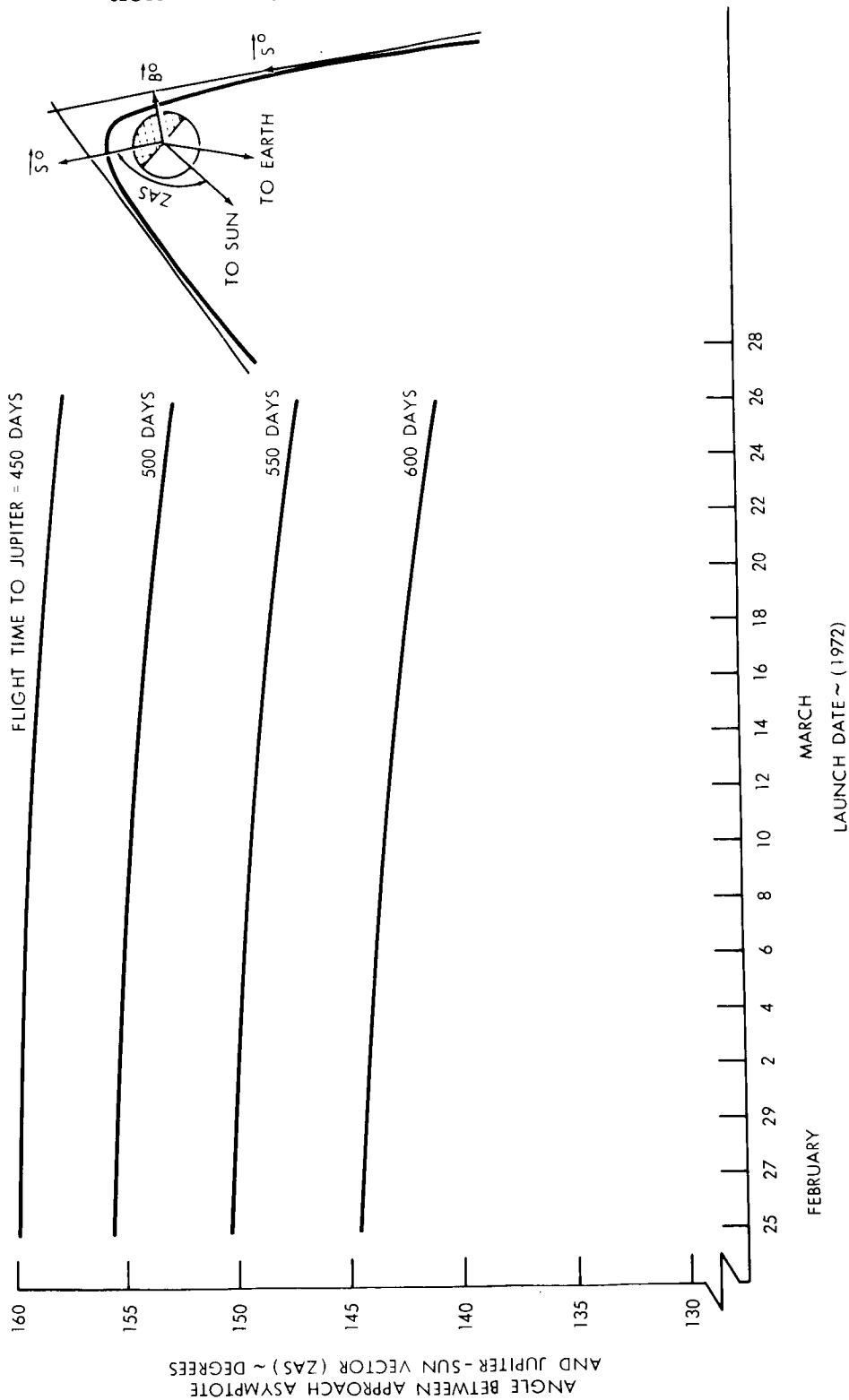


Figure III-14. Angle Between Approach Asymptote and the Jupiter-Sun Vector Versus Launch Date

The angular relationship between the approach asymptote and the Jupiter-earth vector at encounter is defined by the angle ZAE, with launch date and flight time to Jupiter as shown in Figure III-15. The conjugate angle ZAE is equal to the cone angle of a spacecraft instrument which can view Jupiter while pointing the spacecraft spin-axis toward the earth. The variation of angle ZAE with launch date and flight time is more pronounced and is the effect of the alignment of earth and Jupiter at Jupiter encounter. This same variation can be seen in the plot of communications distance (Figure III-5) for the 1972 launch opportunity.

b. Hyperbolic Excess Speed ( $V_{hp}$ ). The hyperbolic excess speed ( $V_{hp}$ ) is a measure of the spacecraft energy in the hyperbolic orbit relative to Jupiter.  $V_{hp}$  is the magnitude of the hyperbolic excess velocity vector and is approximated as the speed of the spacecraft at an infinite distance from the planet. The variation of  $V_{hp}$  with the 1972 launch date is shown in Figure III-16. The speed of the spacecraft along the approach hyperbola can be calculated using the following equation:

$$V_{p/24}^2 = V_{HP}^2 + \frac{2\mu_{24}}{r},$$

where

$\mu_{24}$  = gravitational parameter of Jupiter,

$r$  = radial distance of spacecraft from the center of Jupiter

$V_{HP}$  = approach hyperbolic excess speed.

The quantity  $V_{p/24}$  versus radial distance from Jupiter is plotted in Figure III-17. This range of values for hyperbolic excess speed is expected during the 1972 launch opportunity. The accelerating effect of the gravitational field of Jupiter on the probe can be seen from this figure. This figure also points out the problems that would be encountered in the design of an atmospheric probe. The atmospheric entry speeds would be greater than 50 kilometers per second (> 150,000 feet per second). By comparison, the earth entry speed of the Apollo command module after a lunar return is approximately 11 kilometers per second (36,000 feet per second).

#### 4. Post-Encounter Phase

When a probe is launched in a free-fall trajectory to the vicinity of a planet, the gravitational field of the planet may alter the probe's orbit about the sun. The post-encounter heliocentric trajectory, therefore, depends on the pre-encounter geometry.

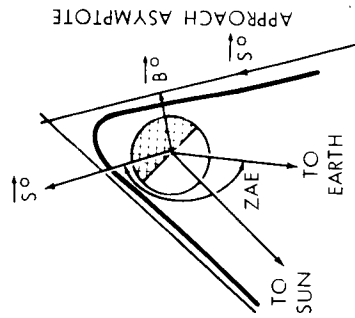
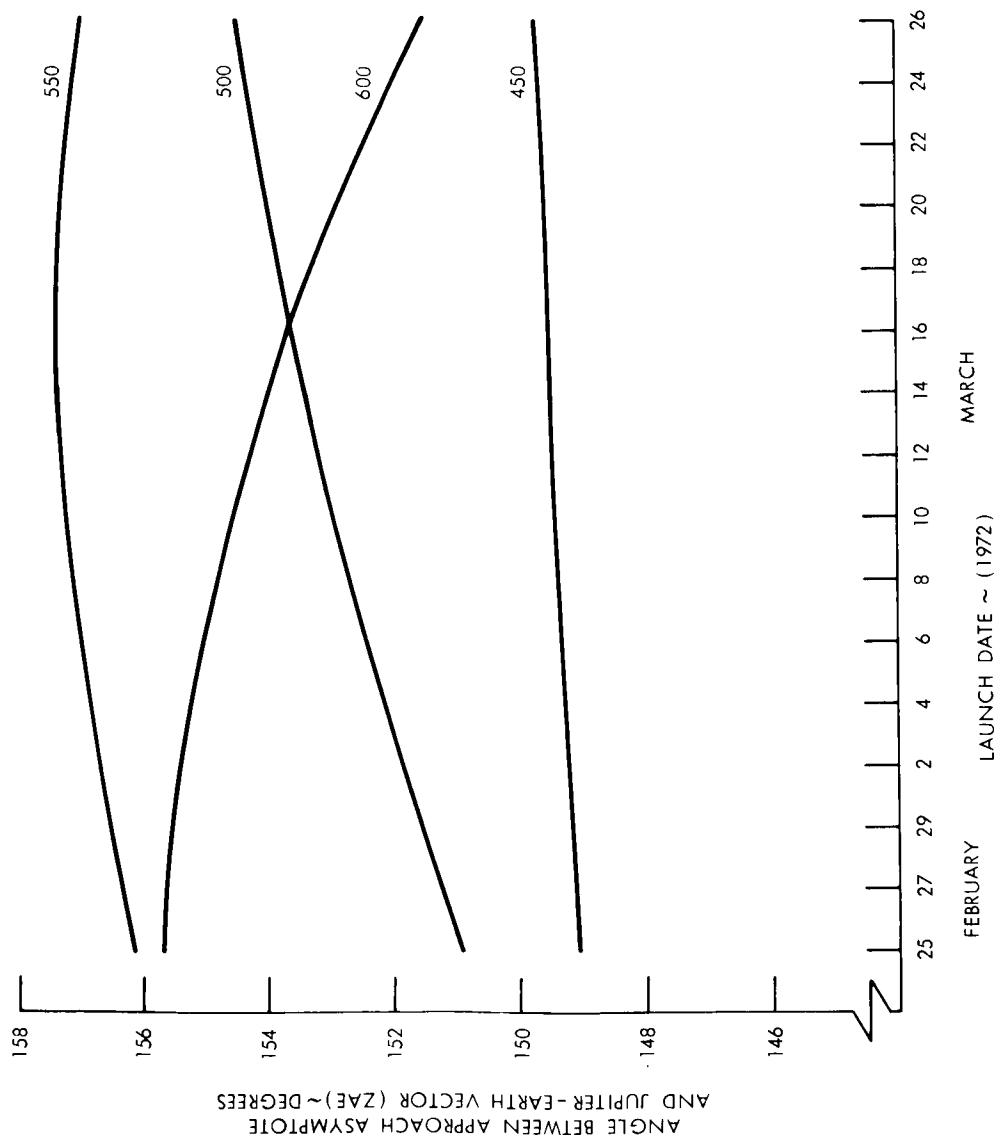


Figure III-15. Angle Between Approach Asymptote and the Jupiter-Earth Vector Versus Launch Date

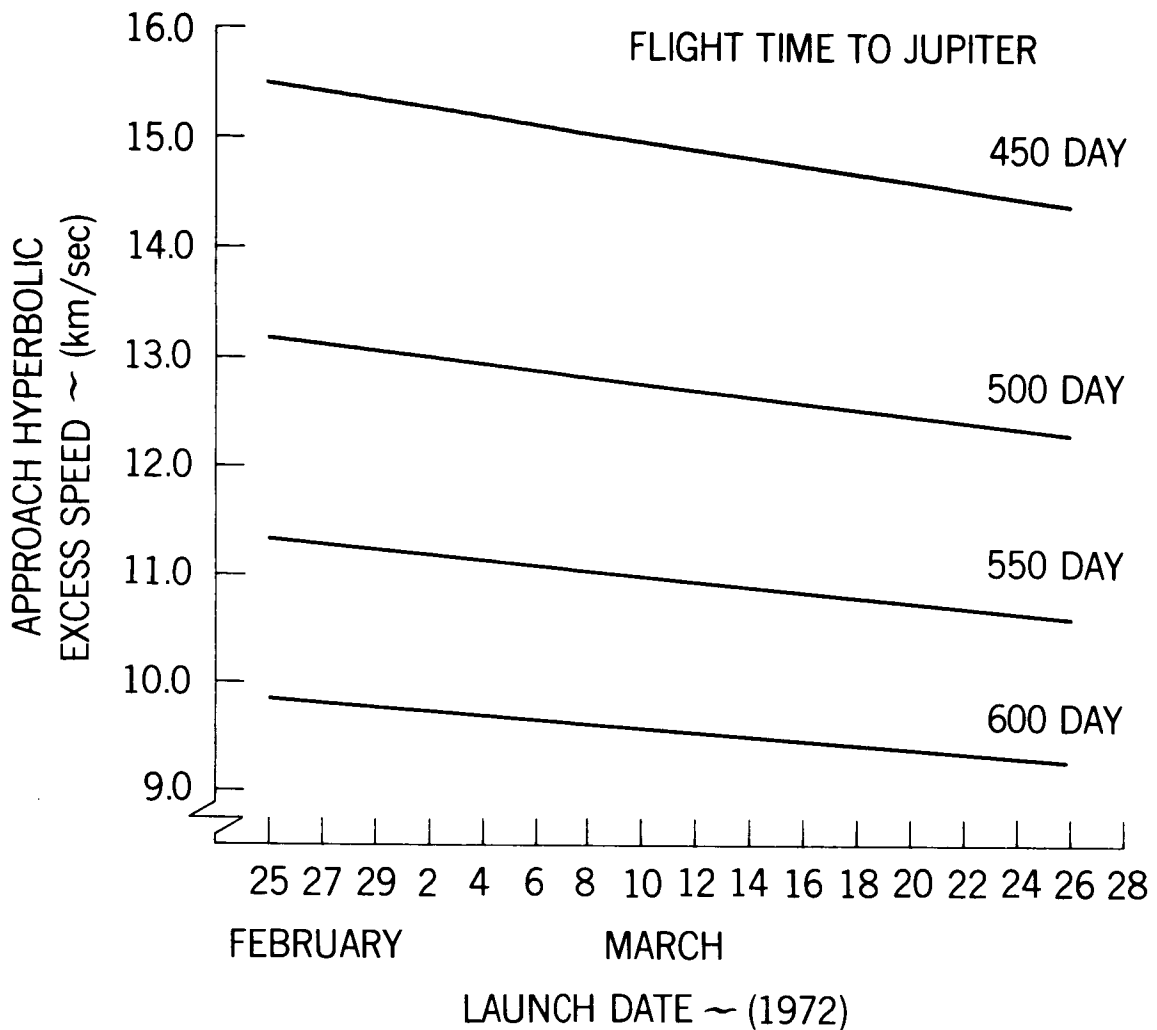


Figure III-16. Approach Hyperbolic Excess Speed Versus Launch Date

a. Encounter Geometry. Assuming a fixed transfer time from a parking orbit about the earth, an approximate transfer trajectory to the target (Reference 1) may be obtained. This trajectory assumes that the earth and the target planet are massless points. As a result, the velocity vector ( $\vec{V}_{1/\odot}$ ) of the probe with respect to the sun at entrance to the sphere of influence of Jupiter is obtained.

We then consider the gravitational field of the planet using the patched-conic assumption that states that at any given time the probe is under the influence of only one body. If  $m$  and  $M$  are the masses of the planet and sun, respectively, the radius of the sphere of influence ( $R_s$ ) can be shown by (Reference 4):

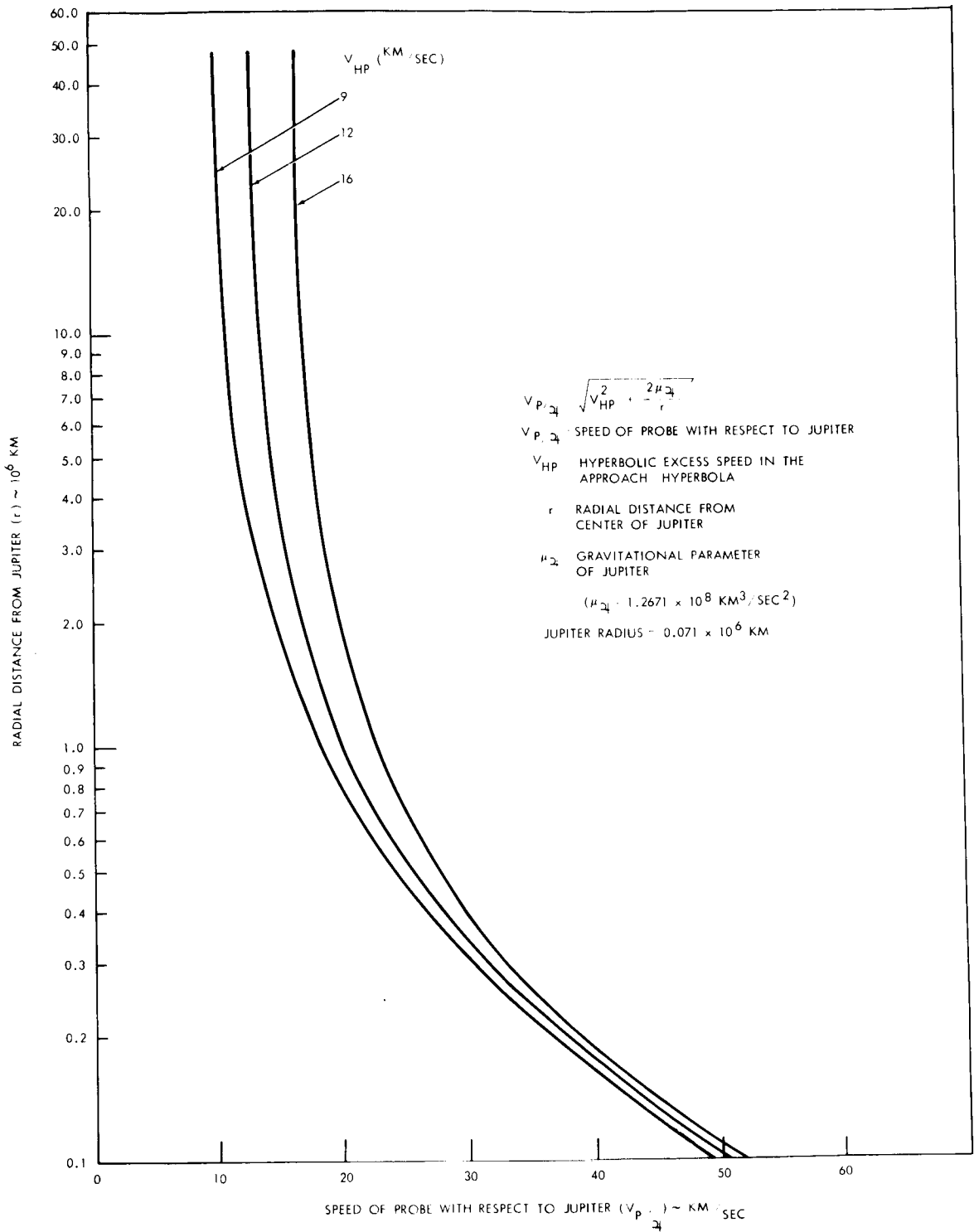


Figure III-17. Variation of the Jupiter Centered Speed with Radial Distance from Jupiter

$$R_s = \left(\frac{m}{M}\right)^{2/5} R_p,$$

where  $R_p$  is the planet's distance from the sun. Having  $V_{1/\odot}$ , the injection date of the probe, and the transfer time, the heliocentric velocity of the target planet from ephemeris data ( $V_1^{24}$ ) can be found. The velocity of the probe with respect to the planet at entrance to the sphere of influence is then given by:

$$\vec{V}_{1/24} = \vec{V}_{1/\odot} - \vec{V}_1^{24},$$

where

$\vec{V}_{1/24}$  is the asymptotic approach velocity vector of the probe with respect to Jupiter as it enters the sphere of influence,

$\vec{V}_{1/\odot}$  is the heliocentric velocity vector of the probe at entrance to the sphere of influence, and

$\vec{V}_1^{24}$  is the heliocentric velocity vector of Jupiter when the probe enters the sphere of influence.

#### NOTE

The symbols used in this section have been altered from those of previous sections. This was necessary in order to differentiate between conditions at entrance and exit of the sphere of influence.

Within the sphere of influence, we assume that the probe's trajectory will be hyperbolic with respect to the planet (Reference 4). We may also choose the radius of closest approach ( $r_p$ ) of the probe without significantly altering the direction or magnitude of the asymptotic approach velocity ( $\vec{V}_{1/24}$ ). Assuming that the direction and magnitude of  $\vec{V}_{1/24}$  are fixed at the calculated value, we can choose the point at which the vehicle pierces the surface of influence (point A in Figure III-18). The validity of this assumption is discussed in Reference 5.

For a given asymptote and energy level at entrance to the sphere of influence, the entire trajectory, including radius of closest approach, is determined by the location of the point at which the probe pierces the sphere of influence. There is a convenient method for specifying the location of this point and the radius of closest approach. It is in terms of the magnitude of the miss vector ( $|\vec{B}| = \text{BMAG}$ ) and an angle  $\phi$  measured between the miss vector  $\vec{B}$  and another vector

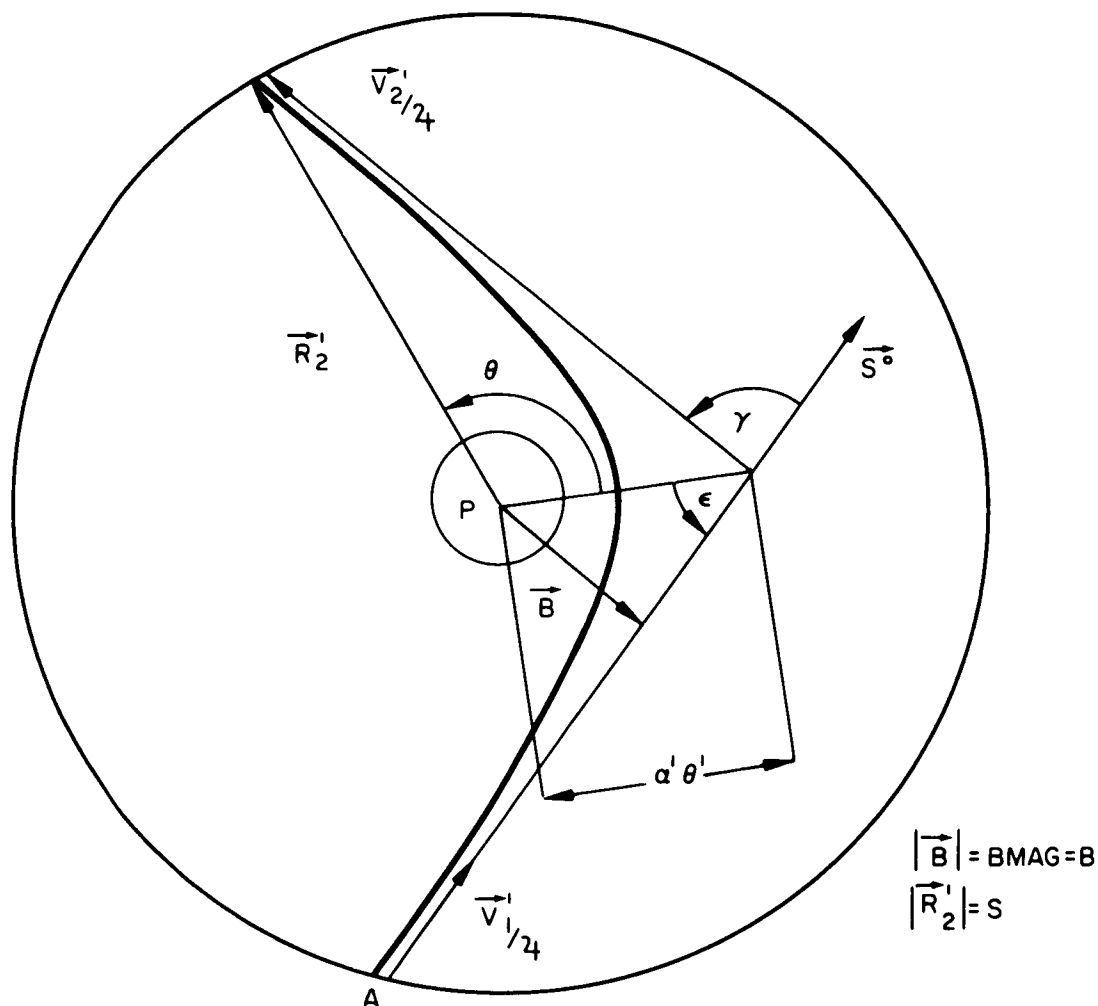


Figure III-18. Hyperbolic Fly-by Geometry

( $\vec{T}^\circ$ ) which is fixed in the orbital plane of Jupiter. The vector  $\vec{T}^\circ$  is one component of the Cartesian system used for approach geometry to a planet. These parameters are developed by W. Kizner of the Jet Propulsion Laboratory (Reference 8) and are based on a technique used in the atomic physics scattering theory.

To derive the planetary impact parameters properly it is first necessary to describe the concept of patched-conic trajectory. Precision trajectories for spacecraft are normally computed by direct integration of equations of motion, such as Cowell's method; or by a variational scheme, such as Encke's method. A precision trajectory can also be approximated by a patched-conic trajectory. The term "conic" arises from the fact that the solution to a two-body problem in celestial mechanics is a conic section, i.e., a circle, ellipse, parabola, or

hyperbola. The type of conic produced is dependent on the energy in the system, relative to a central body. A conic-trajectory is always referenced to a central force field the way an orbit about the earth is referenced to the earth's central force field. A conic approximation to the actual trajectory is initially referenced to the central force field of body 1. Approaching the central force field sphere of influence of body 2, the conic trajectory then is referenced to the central force field of body 2. The immediate effect is the alteration of the conic section characteristics. In this case, the trajectory is an ellipse with respect to the central force field of the sun. Upon entering the Jupiter central force field sphere of influence, the trajectory becomes referenced to Jupiter. The result is a conic section characterized by a hyperbola. The process of combining the two conics in order to approximate an integrated trajectory is known as patching of conics, from which the term patched-conic is derived.

From the concept of patched-conic trajectories, it is possible to develop a set of parameters which describe the miss geometry at a target planet (i.e. Jupiter). Figure III-19 describes the geometry as a spacecraft approaches the planet. The target plane, given by the unit vectors,  $\vec{R}^\circ$  and  $\vec{T}^\circ$ , contains the miss vector  $\vec{B}$ . This plane is perpendicular to the asymptote of the approach hyperbola. The approach hyperbola is the conic that results from switching to Jupiter's force field from that of the sun. A unit vector  $\vec{S}^\circ$  is therefore defined as that vector directed along the incoming asymptote which is normal to the impact plane. The vector  $\vec{T}^\circ$  represents an arbitrary vector normal to  $\vec{S}^\circ$ , which in this case is assumed to be in the orbital plane of Jupiter; the vector  $\vec{R}^\circ$  is the normal to both  $\vec{S}^\circ$  and  $\vec{T}^\circ$  (i.e.,  $\vec{R}^\circ = \vec{S}^\circ \times \vec{T}^\circ$ ). The miss vector  $\vec{B}$ , is that vector perpendicular to the asymptote of the approach hyperbola and originating at the center of the target body.

b. Flybys for Post-Encounter Missions. The effects of Jupiter's gravitational influence on the post-encounter heliocenter orbit of the spacecraft are shown in Figures III-20 through III-22. The following information can be obtained from these graphs and can be related to approach conditions at the target planet:

- a. The time to reach 10 AU from the sun after encounter (i.e., exit from the sphere of influence)
- b. The maximum solar ecliptic latitude that can be attained by the probe within 500 days after encounter
- c. The ecliptic inclination of the probe's orbital plane after encounter.

These data are shown for an earth-to-Jupiter trip time of 500 days. A more complete parametric study can be found in Reference 10. The abscissas and

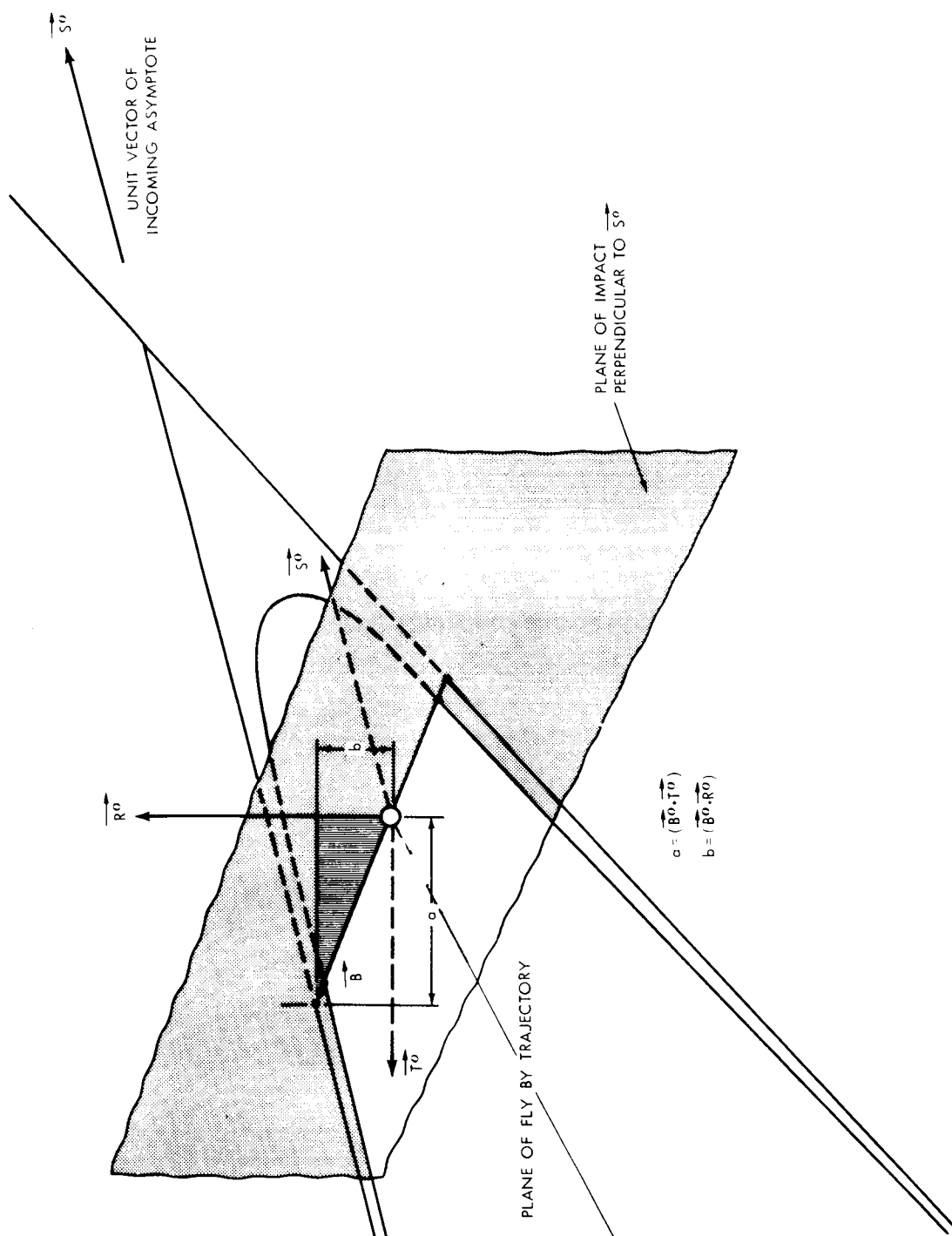


Figure III-19. Planetary Approach Coordinate System and Impact Plane

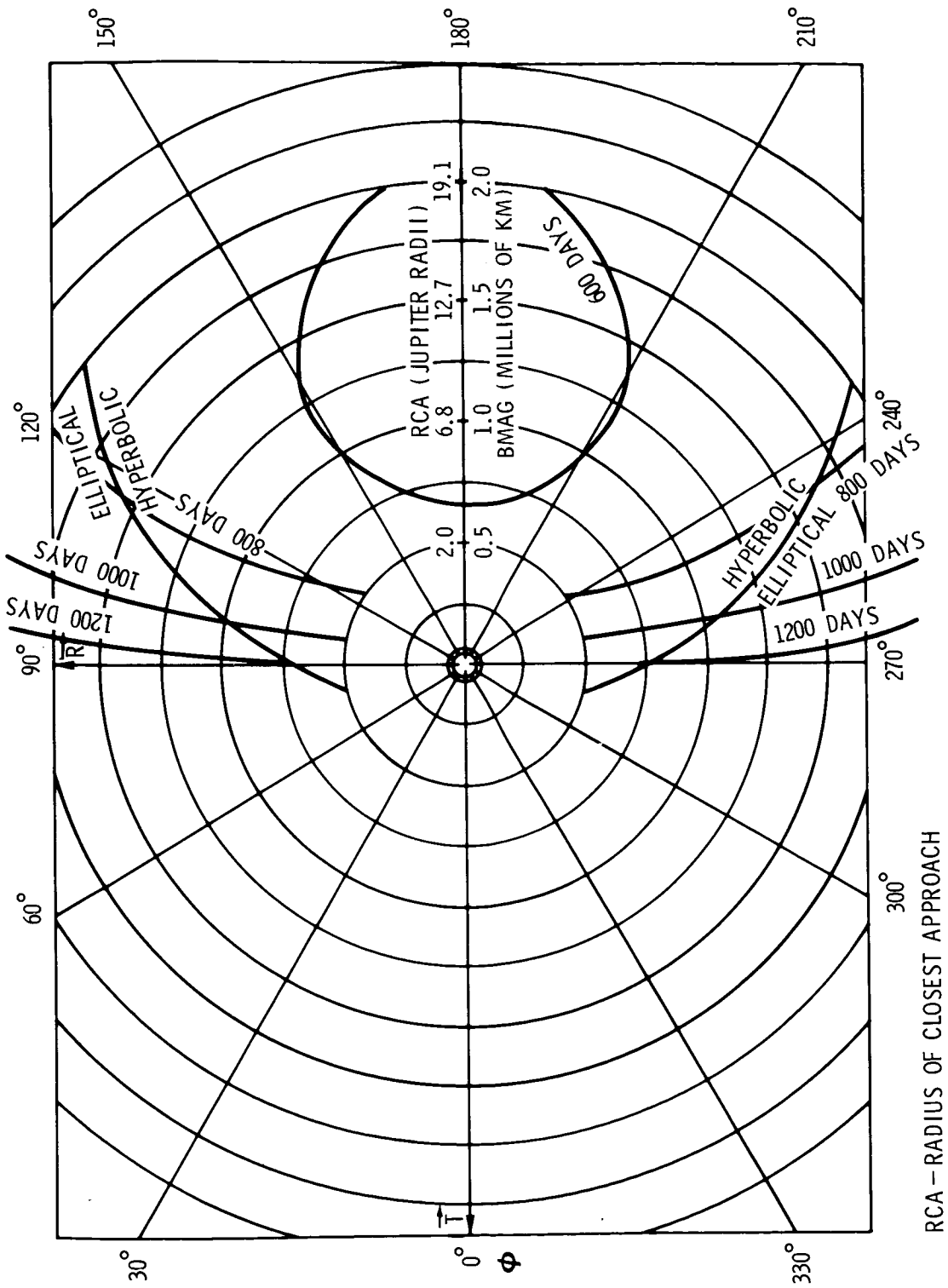


Figure III-20. Time to 10 AU, Transfer Time 500 Days

RCA - RADIUS OF CLOSEST APPROACH

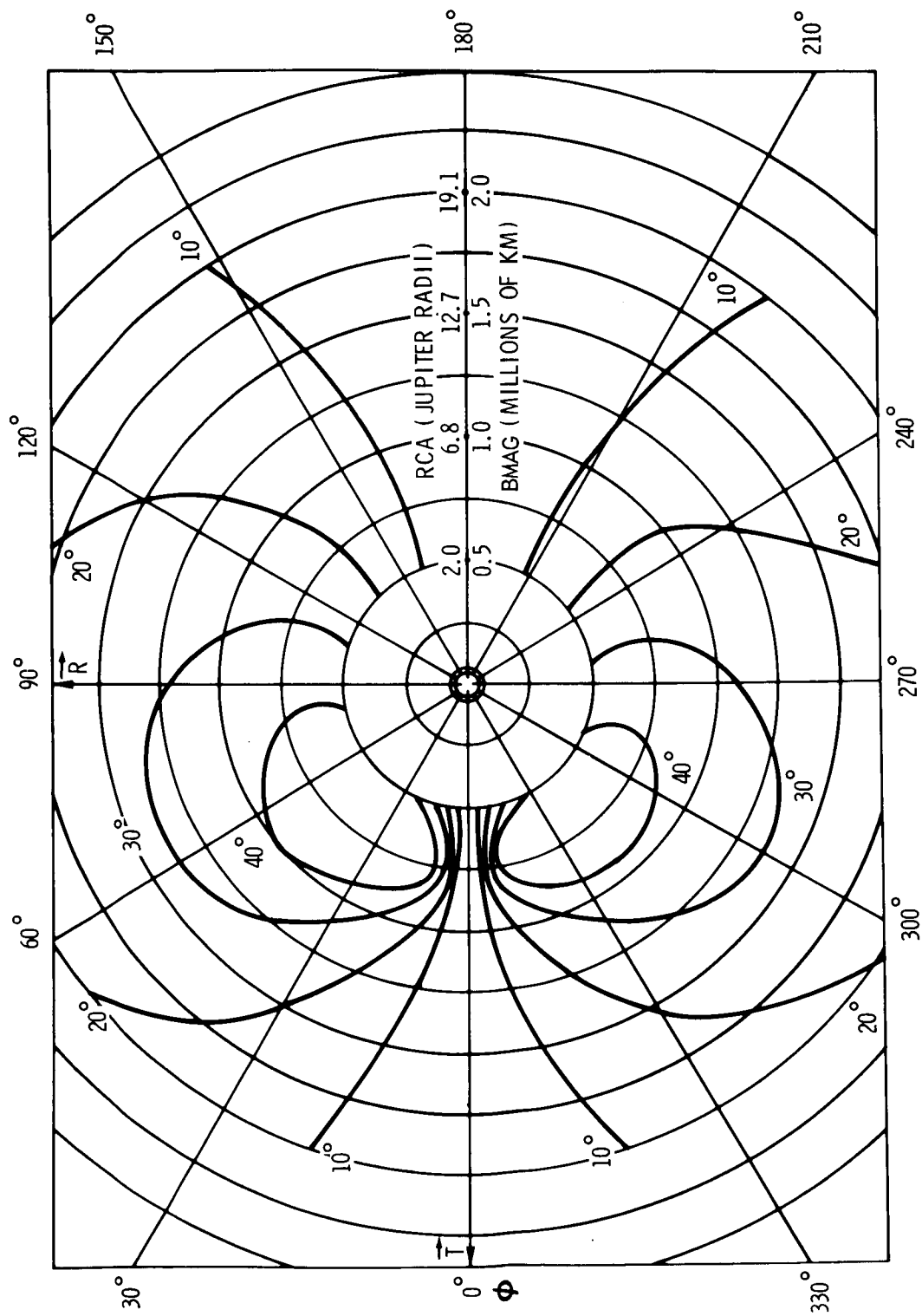


Figure III-21. Solar Ecliptic Latitude After 500 Days, Transfer Time 500 Days

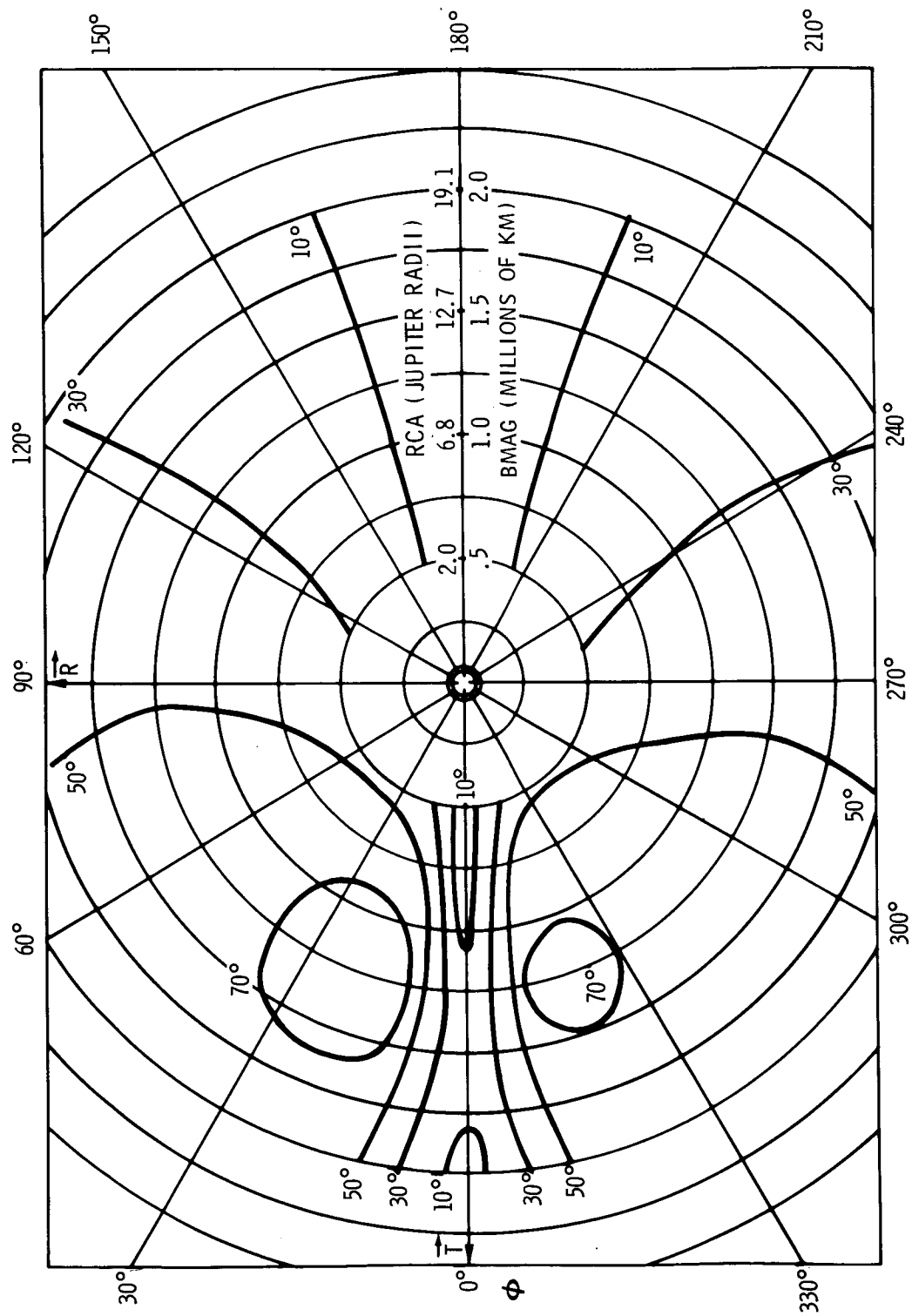


Figure III-22. Inclination to the Ecliptic, Transfer Time 500 Days

ordinates of the graphs are components ( $\vec{T}^\circ$  and  $\vec{R}^\circ$ ) of the impact planet at Jupiter. The angle  $\Phi$ , which is measured positive clockwise from the  $\vec{T}^\circ$  axis, is superimposed on the figures with the miss vector magnitude. The miss vector magnitude  $|\vec{B}|$  (i.e.,  $\text{BMAG} = |\vec{B}|$ ) is denoted by concentric circles. These quantities are common to the figures discussed in the following paragraphs. It should be noted that information on these graphs can be used in either of two ways: (1) the miss distances in terms of the miss vector ( $\vec{B}$ ) can be determined for a mission requirement specified by time to 10 AU, maximum solar ecliptic latitude and inclination, or (2) the post-encounter mission, which will be determined by the miss distance at Jupiter.

Time contours required for the probe to reach 10 AU from the sun after leaving Jupiter's sphere of influence are shown in Figure III-20. The combination of miss vector magnitude (BMAG) and direction ( $\Phi$ ) can be used to determine the Jupiter impact plane aim point that will allow a specified transit time to 10 AU after encounter. A contour of zero vis-viva energy is also shown which indicates whether the resultant post-encounter orbit is hyperbolic or elliptic.

Figures III-21 and III-22 are used in similar fashion. They deal exclusively with missions out of the ecliptic, and can be used in conjunction with flight time curves since solar distance in figure III-21 is not restricted to the ecliptic plane.

#### B. Guidance and Navigation Analysis

In order to accomplish a desired Galactic Jupiter Probe mission, particularly the flyby and post-encounter objectives, a midcourse correction, or corrections, may be necessary. An estimate of the injection accuracy of the Atlas-Centaur-TE-364 vehicle has been published by TRW (Reference 2), and estimates of injection errors using the Atlas-Centaur-Burner II vehicle have been supplied by Boeing (Reference 11). These estimates consider three versions of the Burner II:

- a. three-axis stabilized with vernier velocity capability,
- b. three-axis stabilized without vernier capability, and
- c. a spin-stabilized version (which should correspond to the TE-364 alone). Table III-1 summarizes the resulting 1-sigma miss vector uncertainties ( $\vec{B} \cdot \vec{T}^\circ$  and  $\vec{B} \cdot \vec{R}^\circ$ ) based on injection errors for the different vehicle configurations.

Table III-1  
One-Sigma Miss-Vector Uncertainties Due to Injection  
Errors for a 500-Day Flight to Jupiter

Vehicle Configuration (Atlas-Centaur x—)	One Sigma Errors	
	$\vec{B}_6 \cdot \vec{T}^\circ$ (10 KM)	$\vec{B}_6 \cdot \vec{R}^\circ$ (10 KM)
TE-364 (TRW injection errors)	±1.25	±0.28
Burner II (Boeing injection errors) 3-axis stabilized with vernier capability	0.42	0.05
Burner II (Boeing injection errors) 3-axis stabilized without vernier capability	0.64	0.07
Burner II (Boeing injection errors) spin-stabilized	0.93	0.14

#### 1. Midcourse Guidance and Attitude Laws

A spin-stabilized spacecraft at injection will essentially maintain an inertially-fixed spin-axis orientation until a disturbing torque is applied. The propagation axis of the large antenna is parallel to the spin axis, and the midcourse propulsion system nozzles (thrust axes) are parallel and antiparallel to the spin axis. Consequently, there arises a potential interface between communications, midcourse requirements, and possibly thermal control of the spacecraft. It may be desirable, for example, to continually orient the spin axis along the earth-probe line in order to use the high-gain antenna for communications; or along the earth-sun line for thermal control purposes. An initial re-orientation of the spin axis must therefore take place before the low-gain (omnidirectional) antenna approaches its threshold.

Based on the foregoing reasoning, three restricted attitude-control laws are postulated for the midcourse correction problem, namely:

- a. spin axis continually oriented along the earth-probe line,
- b. spin axis continually oriented along the sun-probe line, and
- c. spin axis unchanged from the original injection spin-axis (assumed to be parallel to the injection velocity vector).

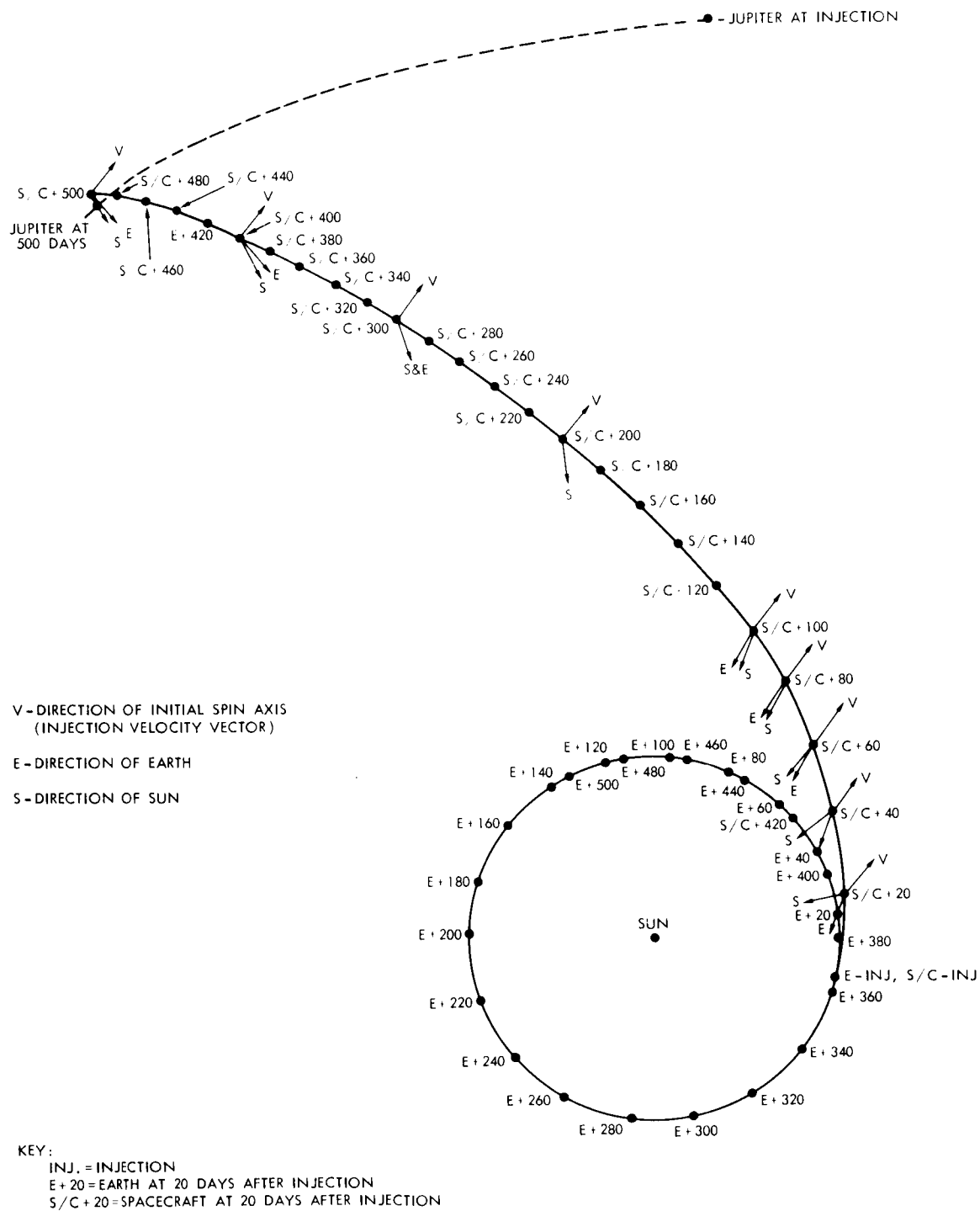


Figure III-23. Earth-Jupiter Transfer Trajectory

Figure III-23 shows a time history of the ecliptic projection of attitude vectors throughout the transfer trajectory to Jupiter. Optimum attitude midcourse corrections were also studied since the spacecraft has an attitude control system that permits a precession of the spin axis to any arbitrary orientation (which could be measured by sun-Canopus sensors, or in the case of earth-pointing, by an RF interferometer system; an RF interferometer system is described in Appendix A. This involves completely arbitrary optimum attitudes, and those restricted to the ecliptic plane.

With respect to restricted spin-axis orientations, the partial derivatives of miss parameters to a velocity impulse along the restricted axis are presented in Figure III-24. This shows that in the 10 to 50 days from the injection time frame studied, sensitivities of the in-plane miss ( $\vec{B} \cdot \vec{T}^\circ$ ) are generally an order of magnitude higher than those of the out-of-plane miss ( $\vec{B} \cdot \vec{R}^\circ$ ). This fact, coupled with the relatively loose targeting requirements for a deep-space, post-encounter mission, shown in Figure III-25, leads to the conclusion that only the in-plane miss need be corrected. The alternatives to this are:

- a. waiting until the required correction vector is aligned, or nearly aligned, with spin-axis orientation dictated by that particular attitude control law, and
- b. making corrections at two different times so that the total miss vector deviation can be nulled.

The disadvantage of these alternatives are:

- a. a significant increase in required midcourse fuel,
- b. the reliability penalty incurred if two corrections are required, and
- c. the potentially long waiting period for the execution of the correction(s).

For optimum arbitrary spin-axis orientation, obviously the in-plane and out-of-plane miss vector components would be corrected. For the case of optimum orientation restricted to the ecliptic plane, however, only the in-plane miss vector component can be corrected with a reasonable fuel expenditure, since the interplanetary trajectory, for practical purposes, is in the ecliptic plane.

## 2. Midcourse Velocity and Fuel Requirements

The midcourse  $\Delta V$  and resulting fuel requirements have been determined using the guidance and attitude control laws from the previous section. The

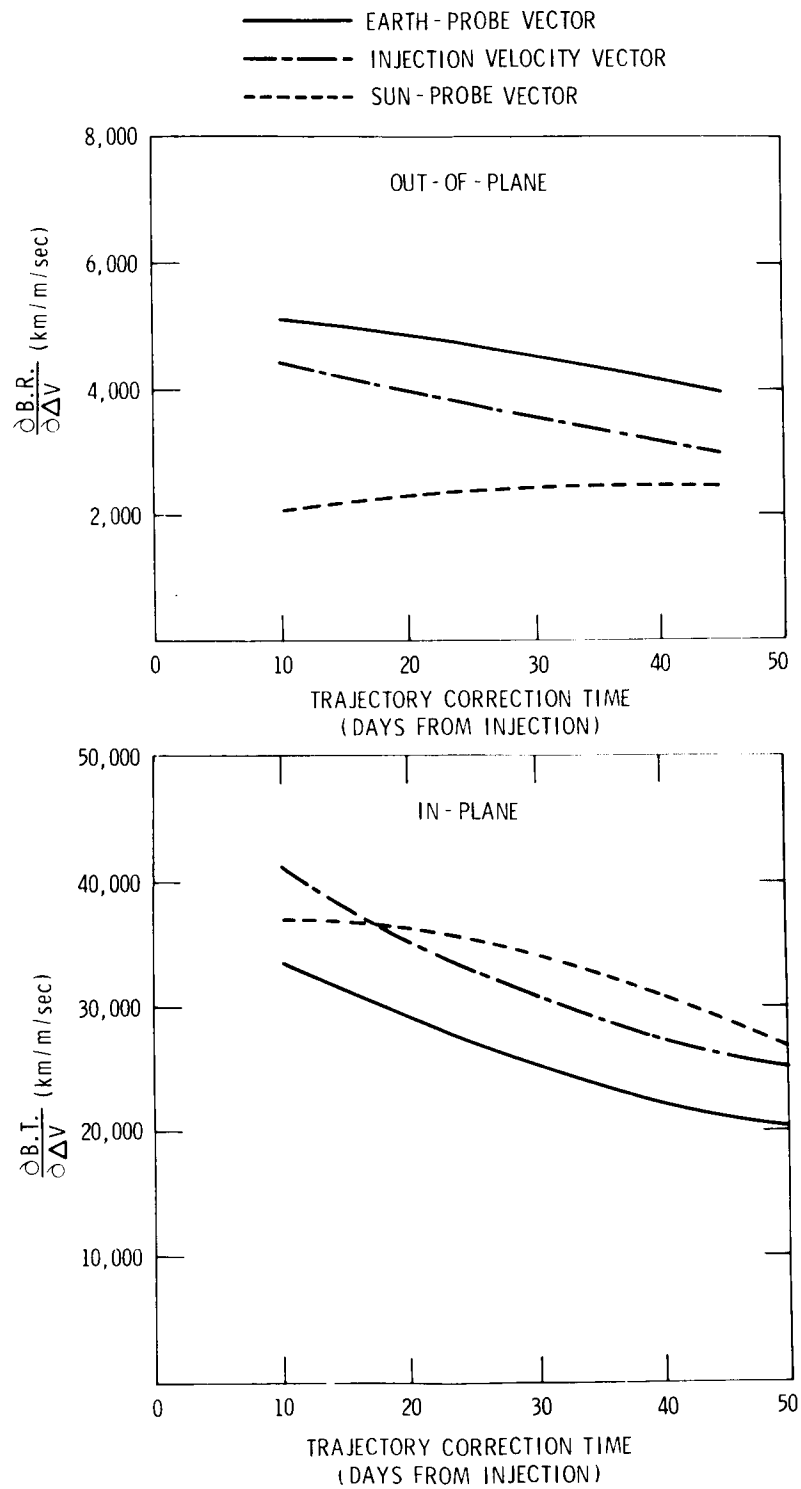


Figure III-24. Miss Parameters to a Velocity Impulse along the Restricted Axis

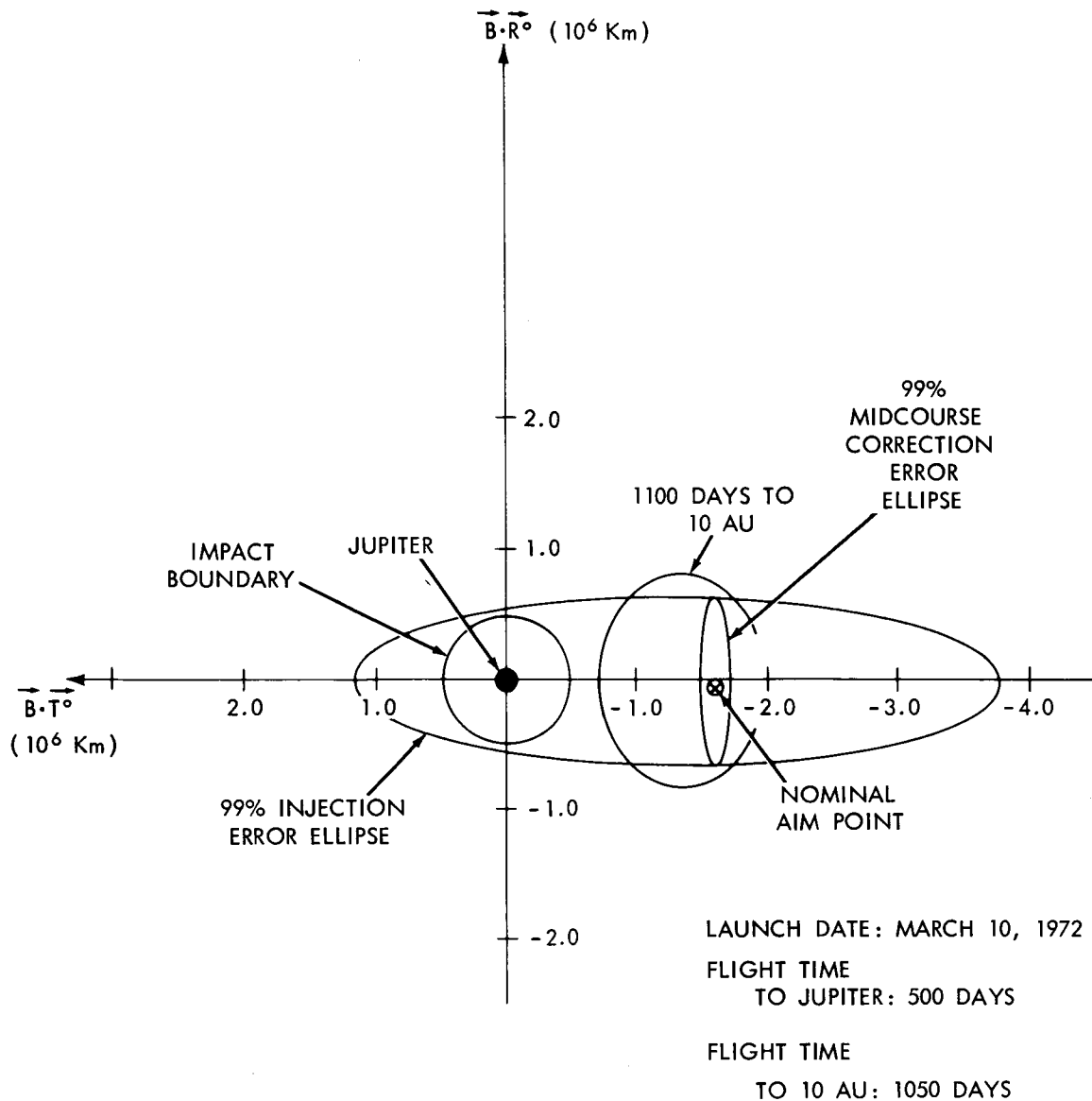


Figure III-25. Injection and Trajectory Correction Ellipses, Impact Plane Projection

midcourse requirements for a nominal 500-day flight to Jupiter, a launch date of March 8, 1972, and a covariance matrix of injection errors (TRW, Reference 2) for the Atlas-Centaur-TE-364), were computed using Monte Carlo techniques (References 12 and 13). This analysis assumes a perfect navigation system because results from the navigation error analysis were not available at the time this study was performed. A coordinated navigation error analysis where these effects are taken into account will be performed during Phase B. Corrections are assumed not to take place until 2.5 days after injection. From the

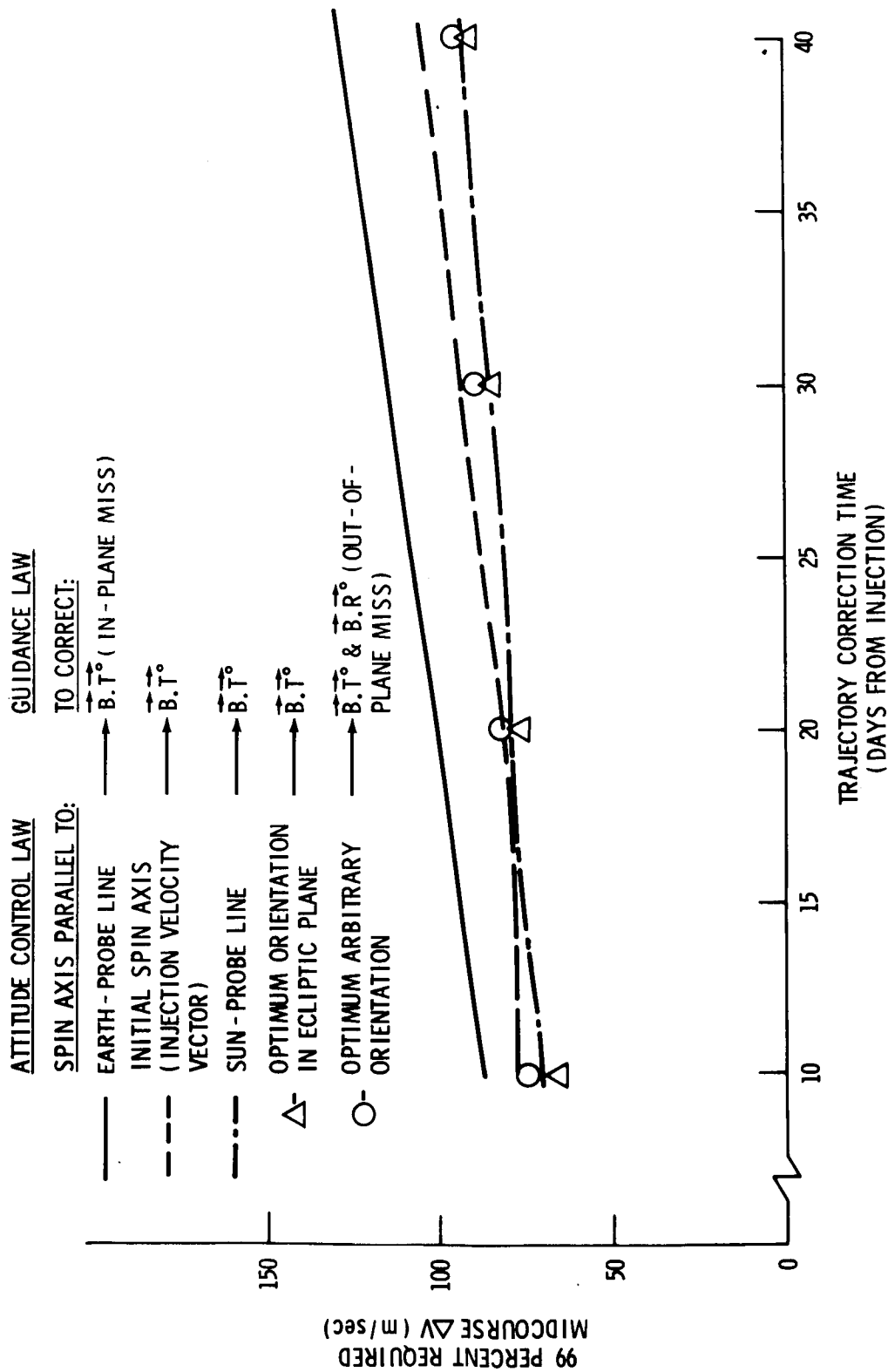


Figure III-26. 99% Midcourse Fuel Requirements Using the TE-364 (TRW Injection Errors)

2.5- to 40-day time period after injection, it becomes apparent that the required  $\Delta V$  increases with correction time for all guidance and attitude laws considered (see Figure III-26). It can then be concluded that the midcourse correction should be executed as soon as the trajectory can be determined accurately from the tracking data. Figure III-26 also shows that midcourse  $\Delta V$  requirements are 30 to 40 percent higher for an earth-pointing attitude control law than for the case using optimum ecliptic orientation. It should be noted that the required  $\Delta V$  for all restricted and optimum pointing, other than earth-pointing, is essentially the same to within 10 percent. It should also be noted that the  $\Delta V$  results are presented in terms of 99 percent probability for correcting the miss. This corresponds to a 2.3-sigma level in the control parameter  $-\Delta V$  for a bivariate normal distribution (uncorrelated). A conclusion is that a total correction capability of 100 meters per second should be sufficient for any of the foregoing attitude control and guidance laws if the midcourse correction can be executed within 20 days after injection.

The information in Figure III-27 was generated, using Boeing (Reference 11) injection errors, to show the effect of upper stage configuration for the required  $\Delta V$ . This figure shows that by using a Burner II upper stage with 3-axis stabilization and vernier velocity capability, the required midcourse  $\Delta V$  is slightly less than 50 percent of that required by use of the spin-stabilized configuration. This is but one of the factors that enters into selection of the upper stage configuration. Payload capability, spin table requirements, etc., also must be weighed against injection accuracy and the resulting reduced midcourse correction requirements.

The data in Figure III-28 are intended to provide a means of translating midcourse  $\Delta V$  requirements into required fuel mass for any propellant (where specific impulse is known). For example, a 500-pound spacecraft using hydrazine as a propellant ( $I_{sp} \approx 220$  sec) and requiring a correction capability of 100 meters per second will have a fuel-mass ratio of approximately 0.05; this requires approximately 20 pounds of propellant.

### 3. Navigation Accuracy From Tracking Data

The use of earth-based tracking data to determine position and velocity of the Galactic Jupiter Probe must be considered carefully. These data represent the only navigation measurements for this mission. Accurate trajectory determination is important to the mission from the points of view of the scientific experiments and guidance. Spatial correlation of scientific measurements (particularly in the vicinity of Jupiter) is desired. Early, accurate knowledge of the projected trajectory is necessary for determining midcourse corrections. An error analysis of the trajectory determination process using range, range

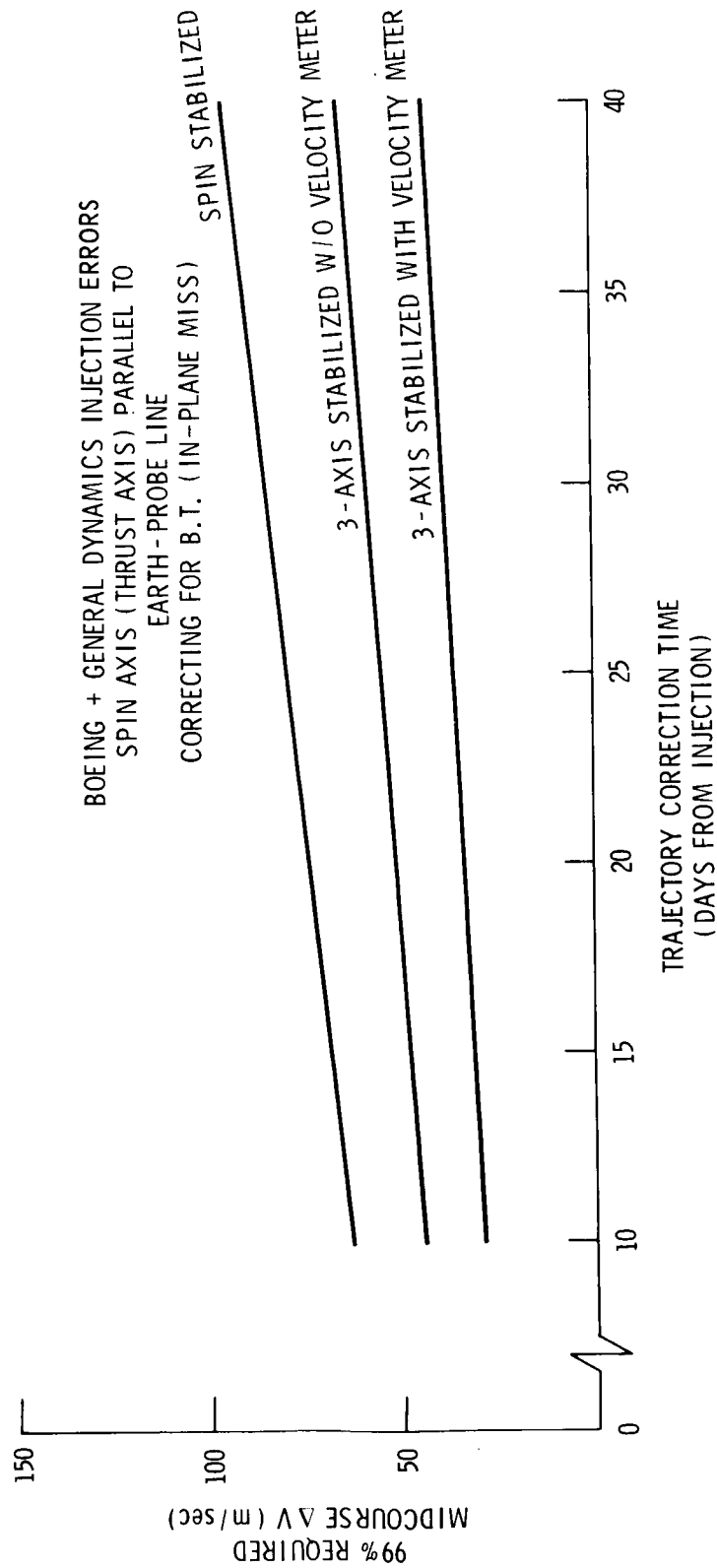


Figure III-27. Midcourse Correction Time (Days from Injection)

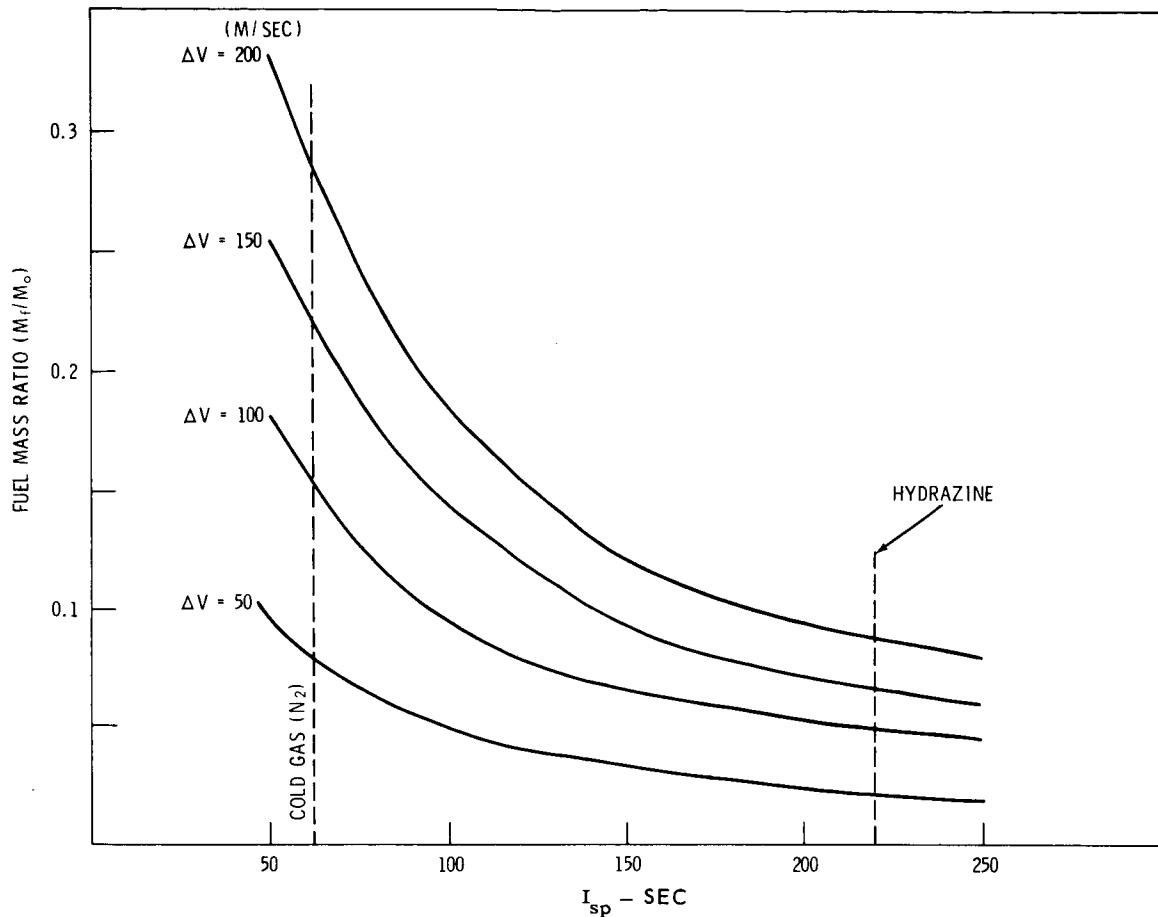


Figure III-28. Midcourse Fuel-Weight- $\Delta V$  Tradeoff

rate, and angular data, has been performed. It was made primarily to answer questions relating to midcourse corrections.

The following assumptions are used in this analysis:

- a. Postulated tracking schedule: heavy tracking early in the flight and much less tracking in the heliocentric portion of the flight.
- b. Tracking system errors: represented as Gaussian noise and biases in the physical measurements (Reference 14).
- c. Linear error propagation: adequately simulates trajectory determination process. (Reference 14.)
- d. Measurement uncertainties: assumed as follows:

<u>Measurement</u>	<u>Noise</u>	<u>Bias</u>
Range	$\delta R = 10m$	$\Delta R = 5m + R\left(\frac{\Delta C}{C}\right)^*$
Range rate (Injection to +1 hr)	$\delta \dot{R} = 3.65 \text{ cm/sec}$	$\Delta \dot{R} = 0.5 \text{ cm/sec}^{**}$
Range rate (+1 hr to +10 days)	$\delta \dot{R} = 0.06 \text{ cm/sec}$	$\Delta \dot{R} = 0.5 \text{ cm/sec}$
Azimuth and elevation	$\delta \alpha = \delta \epsilon = 0.8mr$	$\Delta \alpha = \Delta \epsilon = 1.6mr$

\* $\Delta C/C$  is the relative uncertainty in the speed of light, assumed to be  $3 \times 10^{-7}$  (Reference 15).

\*\*speed of light uncertainty is assumed to be the major part of  $\Delta \dot{R}$ .

e. Tracking schedule, measurements and stations utilized are as follows:

Injection to +1 hr - 1 measurement/sec including angles - Ascension, Tananarive (Malagasy Republic), Carnarvon (Australia), Madrid (Spain).

+1 hr to +10 hr - 6 measurements/hr, no angles - Ascension, Carnarvon, Madrid, Tananarive, Rosman (N. C.)

+10 hr to +10 days - 1 measurement/hr, no angles - Rosman, Ororral (Australia).

f. Other trajectory prediction uncertainties considered:

- (1) Astronomical unit (AU) to kilometer conversion,  
 $\Delta \text{AU} = 500 \text{ km}$  (Reference 16)
- (2) Astronomical ephemeris uncertainty - 1 arc second (Reference 17)
- (3) Solar radiation pressure uncertainty - 5 percent of total radiation pressure effect (conservative estimate)

The position and velocity of a space probe with respect to its target planet are a function of the quality and amount of tracking data and the techniques with which they are processed. Sources of trajectory position and velocity uncertainties are principally gravitational and those indicated in assumptions f. These and other possible sources of uncertainty occur when the trajectory must be predicted over significant distances in order to obtain target miss-vector components, as is the case for midcourse guidance.

Table III-2 shows the projected miss-vector uncertainties for a 500-day Galactic Jupiter Probe flight launched March 8, 1972. The table is based on tracking system and speed of light uncertainties only. Range-rate only, as well as range and range-rate, are considered for total tracking times of 2.5 and 10 days after injection.

Table III-2  
Miss-Vector Uncertainties (1 Sigma)  
Due to Navigation Errors

Uncertainty	RMS $\vec{B} \cdot \vec{T}^\circ$ (km)	RMS $\vec{B} \cdot \vec{R}^\circ$ (km)
$\dot{R}$ only (2.5 days tracking)*	3000	1500
$\dot{R}$ only (10 days tracking)*	2500	1400
$R + \dot{R}$ (2.5 days tracking)*	1500	600
$R + \dot{R}$ (10 days tracking)*	1200	600

\*angular measurements are included in the first hour of tracking.

Table III-2 shows that for tracking considerations very little difference exists between tracking 2.5 and 10 days. The addition of range measurements decreases the projected miss-vector uncertainties by a factor of two. Other uncertainties will be considered as mutually independent errors, and as such can be root-sum-squared with the uncertainties due to tracking. The independent uncertainties include the AU-to-kilometer conversion, astronomical ephemerides, and solar radiation. This will indicate an overall projected miss-vector uncertainty that can be compared to the expected midcourse execution errors projected to Jupiter. The midcourse execution errors are used to determine the feasibility of performing an early correction. It should be noted that other perturbations such as attitude control effects on the trajectory, propulsion system leaks, planetary gravitational anomalies, etc., have not been considered. In these cases, perturbations were found to be insignificant when compared to those already under consideration.

The approximate effects of these major trajectory prediction uncertainties on the total miss-vector magnitude,  $|\vec{B}|$  are as follows:

- a. The scale factor for the solar system - AU-to-km conversion uncertainty;  $\Delta AU = 500$  km or  $\Delta AU/AU \approx 3 \times 10^{-6}$ . Using the  $AU \pm \Delta AU$  with identical initial trajectory conditions, the resulting miss-vector uncertainty  $\Delta |\vec{B}| \approx 9000$  km (1 sigma).

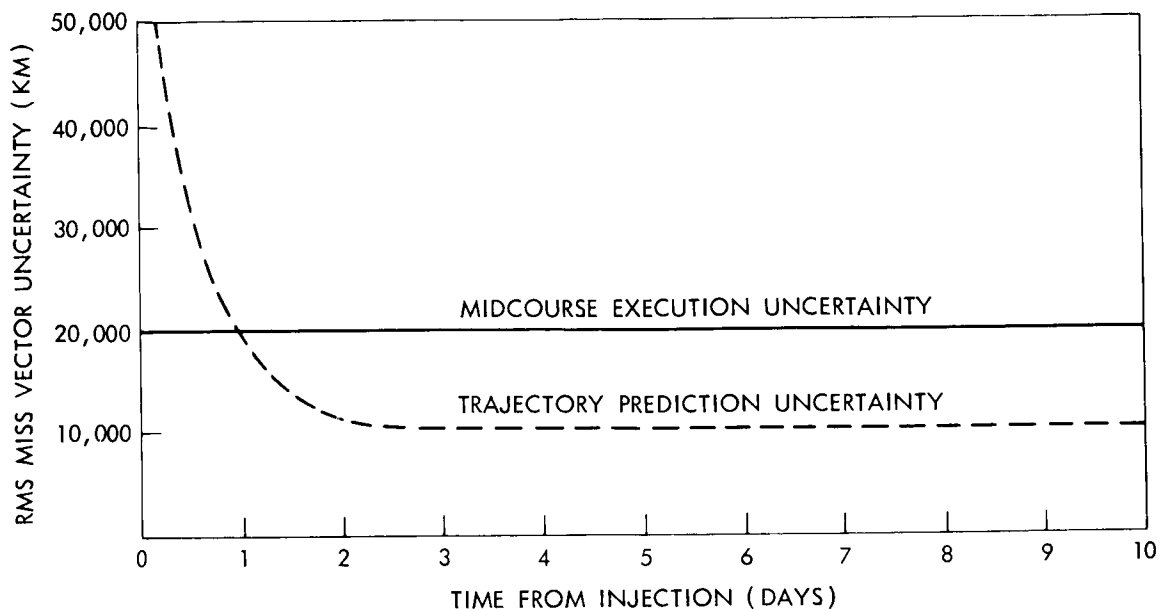


Figure III-29. Early Trajectory Correction Feasibility

- b. Astronomical ephemeris uncertainty of Jupiter; approximately 1 second of arc, which is equivalent to approximately 4000 km (1 sigma) in terms of  $|\vec{B}|$
- c. Solar radiation pressure ( $P_{SR}$ ) uncertainty; assumed to be 5 percent of the total effect or  $\Delta P_{SR} / P_{SR} = 1$  part in 20. Total effect for a 500-day flight to Jupiter has been determined to be equivalent to a miss-vector difference of 36,000 km. Thus, the uncertainty in  $|\vec{B}|$  is approximately 2000 km (1 sigma).

The root-sum-squared uncertainties, together with the previously discussed tracking uncertainties, result in total 1-sigma trajectory prediction uncertainties (in terms of  $|\vec{B}|$ ) that range from 10,100 to 10,600 kilometers. This includes all the tracking situations considered.

Midcourse execution errors, as discussed in the previous section, have been assumed to be represented by a proportional error (1 percent of  $\Delta V$ ), a resolution error ( $\sigma_{\Delta V} = 0.1$  m/sec) and a pointing error ( $\sigma_{\theta} = \sigma_{\chi} = 1^{\circ}$ ). If a 500-day, spin axis, earth-oriented mission has a single midcourse correction in which the in-plane miss ( $\vec{B} \cdot \vec{T}^{\circ}$ ) alone is corrected, then the resulting miss-vector uncertainty due to midcourse execution errors is approximately 22,000 kilometers (1 sigma). This uncertainty is for midcourse corrections performed at both 2.5 and 10 days from injection.

From these results (see Figure III-29), it can be concluded that a 2.5-day or earlier midcourse correction is feasible. This assures a reasonable fuel budget and a Jupiter flyby accuracy limited primarily to the execution accuracy of the midcourse guidance system.

#### REFERENCES

1. Quick Look Mission Analysis Program. Philco Corporation Report WDL-TR-2217, Palo Alto, California, 1964
2. Advanced Planetary Probe Study, Final Technical Report, vol. 2. TRW Systems Report No. 4547-60005-R0000, 1966
3. Launch vehicle performance data obtained from the Centaur Project Office at Lewis Research Center, 1967
4. Battin, R. H.: Astronautical Guidance, McGraw-Hill Book Company, 1964
5. Kaufman, F.; Newman, C. R.; and Chromey, F.: Gravity Assist Optimization Technique Applicable to a Variety of Space Missions. GSFC Document X-507-66-373, 1966
6. Minovich, M. A.: Utilizing Large Planetary Perturbations for the Design of Deep-Space, Solar-Probe, and Out-of-Ecliptic Trajectories. JPL Technical Report No. 32-849, 1965
7. Minovich, M. A.: The Determination and Characteristics of Ballistic Interplanetary Trajectories Under the Influence of Multiple Planetary Attractions. JPL Technical Report No. 32-364, 1963
8. Kizner, W. L.: A Method of Describing Miss Distances for Lunar and Interplanetary Trajectories. JPL External Publication No. 647, 1959
9. Vonbun, F. O.: Transfer Geometry, Communications Conditions and Definitions for Galactic Probe Analyses. GSFC/Mission Analysis Office Technical Study, 1965
10. Newman, C. R.; Kaufman, B.: The Effects of Jovian Encounter Geometry on the Post-Encounter Heliocentric-Trajectory. GSFC Report (to be published)
11. Letter from Mr. M. Gene Seath, The Boeing Company, dated March 14, 1967, (Atlas/Centaur/Burner II Escape Accuracies)

12. Groves, R. T.: Injection and Midcourse Correction Analysis for the Galactic Probe. Mission Analysis Office Technical Study, January 1966
13. Newman, C. R.; Groves, R. T.: Midcourse Guidance Analysis – Galactic Jupiter Probe. (to be published)
14. Kahn, W. D.; Vonbun, F. O.: Tracking Systems – Their Mathematical Model and Their Error – Part 2, Least Squares Treatment. NASA Technical Note D-3776
15. Missions and Navigation Systems Characteristics. Apollo Navigation Working Group, NASA KSC-GSFC Technical Report AN-1.2, Jan. 1967
16. Anderson, J. D.: Determination of the Masses of the Moon and Venus and the Astronomical Unit from Radio Tracking Data of the Mariner II Spacecraft. JPL Technical Report 32-816, July 1967
17. Lawson, C. L.: of JPL – Telephone Conversation with R. T. Groves (September 1967)

#### IV. GROUND NETWORK SUPPORT

##### A. Ground Network

##### 1. Function

The ground network complements the spacecraft in achieving the scientific objectives of the Galactic Jupiter Probe, (GJP). It has four principle functions each of which it accomplishes by radio links. They are:

- a. Receives data resulting from the scientific and engineering observations made by the on-board instruments,
- b. Tracks the spacecraft throughout its long flight,
- c. Maintains control of spacecraft functions via command, and
- d. Relays the received data to central control at GSFC.

##### 2. NASA Facility Availability

Due to the very long ranges associated with this probe, very large ground antenna apertures are required. The NASA has three ground networks possessing

such antennas: 1/ the Space Tracking and Data Acquisition Network, (STADAN), with 85 foot dishes at Rosman, N.C.; Canberra; Australia; and Fairbanks, Alaska; 2/ the Deep Space Network (DSN), with stations at Goldstone, California; Canberra, Australia; and Madrid, Spain; 3/ the Manned Space Flight Network, (MSFN), with 85 foot dishes at these same three sites. The stations in the DSN now have 85 foot dishes and one 210 foot dish at Goldstone. By late 1971 all three sites are scheduled to have operational 210 foot dishes. The STADAN station near Canberra is named Orroral; the DSN site is called Tidbinbilla; the MSFN site at this location is titled Canberra. Table IV-I summarizes this information:

Table IV-1  
NASA Big Dish Stations - 1972

Station	STADAN	DSN	MSFN
Rosman	85' X/Y		
Canberra/Orroral	85' X/Y	210' Az El 85' Hr-Dec	85' X/Y
Fairbanks, Alaska	85' X/Y		
Goldstone		210' Az El 85' Hr-Dec	85' X/Y
Madrid		210' Az El 85' Hr-Dec	85' X/Y

#### B. Station Description

##### 1. STADAN Data Acquisition Stations. Rosman and Orroral:

The Rosman II Data Acquisition Facility is located 35 miles southwest of Asheville, North Carolina 35° 12' 0.7"N, 277° 07' 4.23"E; Orroral is near the city of Canberra, Australia 35° 37' 52.718" S, 148° 57' 20.867"E. The Alaskan station is excluded henceforth because of its far northern location. The site selection, in natural shallow valleys, and other precautionary measures provide a noise free environment for good reception.

These stations now function as high-gain multi-frequency and wideband spacecraft communication terminals (Reference 1). The predominate characteristic is the 85' paraboloidal antenna shown in Figure IV-1. The antenna reflector is mounted on an X-Y type mount designed specifically for tracking spacecraft.

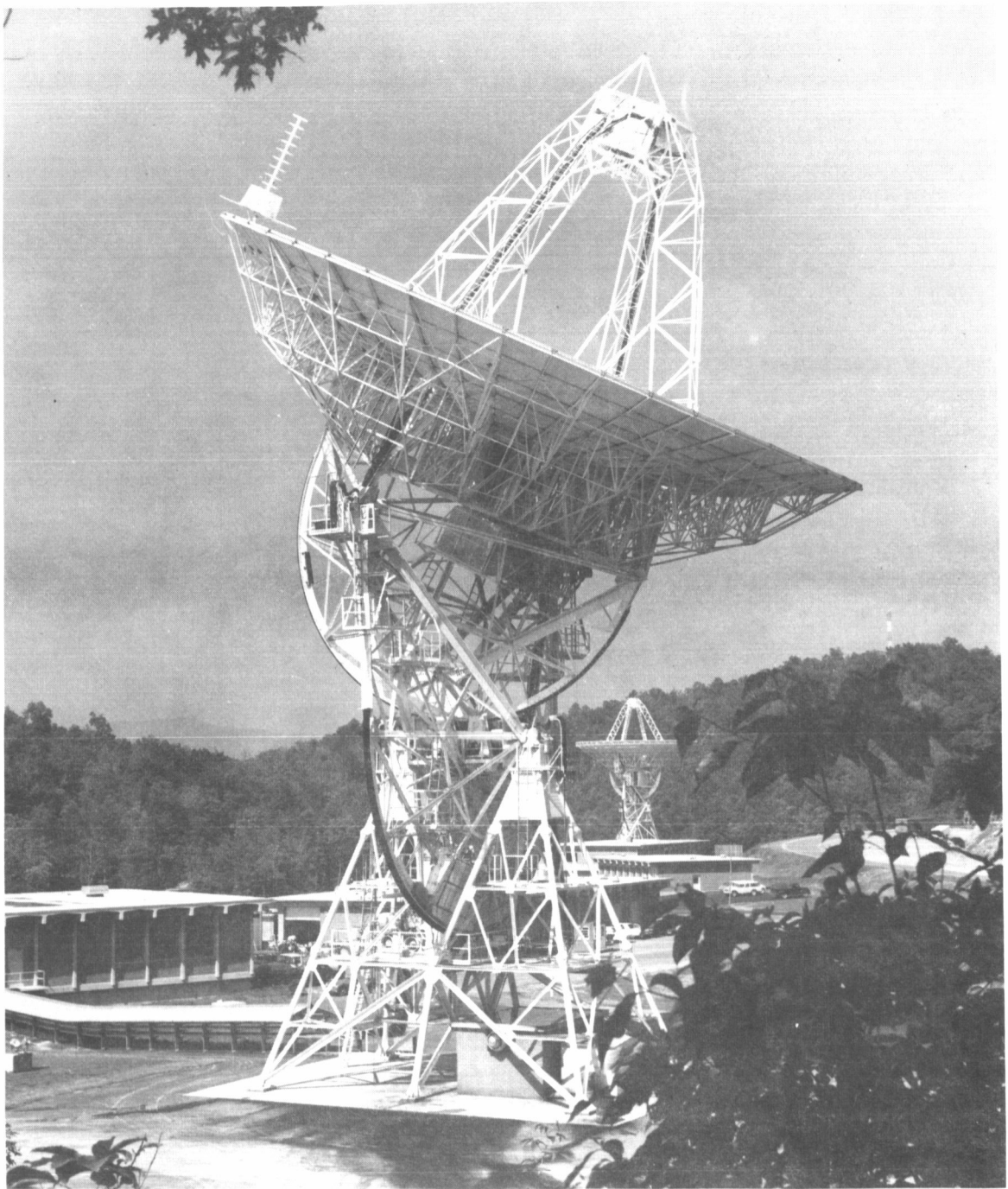


Figure IV-1. 85-Foot Data Acquisition Antennas Rosman, North Carolina

Having two transverse roll axes there is no gimbal lock positions in the sky area above the horizon; thus excessive shaft velocities in the antenna drive system are avoided. The antenna is capable of tracking at rates from  $0^\circ$  to  $3^\circ$  per second with acceleration up to  $5^\circ$  per/sec<sup>2</sup>. The pointing accuracy is 2 minutes of arc. It has five operational modes:

1. simultaneous lobing autotrack,
2. teletype drive-tape,
3. manual operation,
4. slaved to an acquisition antenna,
5. program search modes for initial acquisition.

At present, the Rosman II antenna is equipped with a cassegrain feed system operating at 4.1 GHz receiving and 6 GHz transmitting. This antenna can be modified for low temperature operation at 2.3 GHz. If it is found necessary to supplement the network, assuming Rosman II is modified for extensive GJP coverage, the 40' antenna now at Cooby Creek, Australia will be transferred to Rosman.

The stations also include major subsystems that give them extensive capabilities (Figure IV-2 is representative of these STADAN stations). The stations also employ precision time standards, and are linked with the NASA World-Wide Communications Network.

## 2. Deep Space Network 85' - 210' Data Acquisition Stations (Reference 6) Goldstone, Canberra, Madrid

These stations function as precision communication systems which communicate with and permit control of spacecraft designed for deep space exploration. The station implementation is similar to that of the STADAN stations except that the 85' antenna mounts are hour angle - declination types (Hr-Dec), and the 210' antenna mounts are Azimuth-Elevation (Az-El). With respect to gimbal lock, the Hr-Dec mount has approximately the same advantages as the X-Y mount employed by the STADAN. These stations operate at 2.1 GHz for uplink transmissions and 2.3 GHz for the down link.

The DSN employs the Unified S-Band concept, also envisioned for the GJP, which accomplishes both precision tracking and data acquisition on a single RF carrier.

One 210' dish is operational at the Goldstone site. Construction of two more 210' dishes for installation at Canberra and Madrid is scheduled to begin during fiscal year 1968 and will be operational by late 1971. Also scheduled is the installation of 100 or 400 kilowatt transmitters at these three sites. These

antennas do not have autotrack capability, that is, the monopulse feed arrangement whereby a signal is generated proportional to the angular difference between the antenna pointing direction and the direction of arrival of the received signals, and this error signal minimized by a closed loop servo system. Thus, accurate antenna programming will be required.

Although customary to employ autotrack on antennas used for space research the deterioration in system noise temperature resulting from the antenna feed configuration prohibits its use on high gain antennas which have as their predominant characteristic the ultimate in sensitivity. Table IV-2 lists the DSN station 85-foot and 210-foot antenna parameters.

### 3. Manned Space Flight Network 85' Unified S-Band Stations (Reference 7) Goldstone, Canberra, Madrid

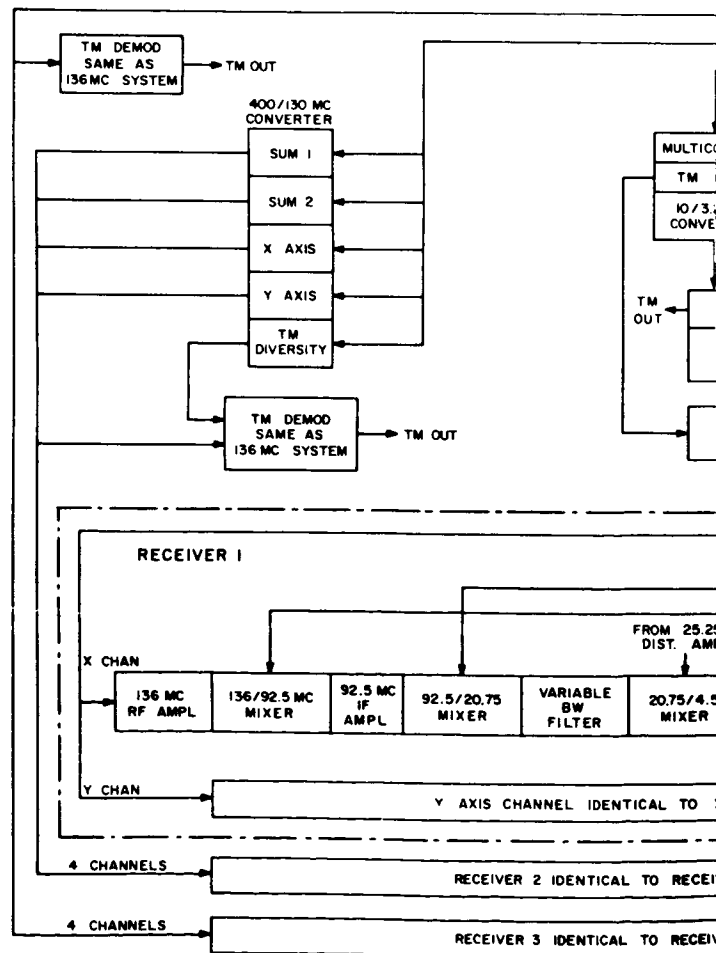
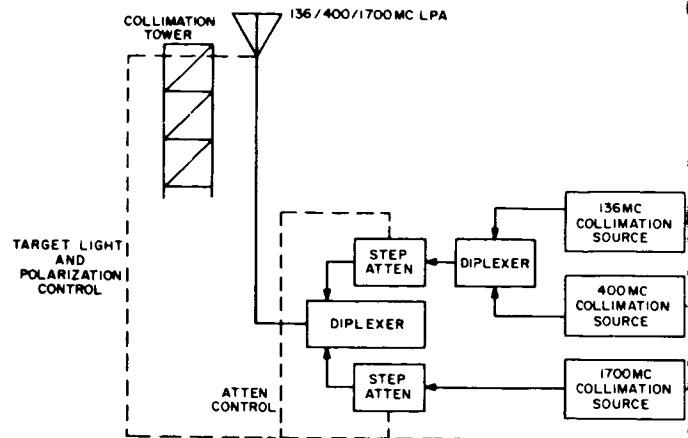
The 85' USB stations are located in the general vicinity of the Deep Space stations at these sites. These stations function primarily to provide wideband, highly sensitive and reliable two-way communications in the 2.3 GHz band with manned spacecraft. With respect to operation on the Galactic Jupiter Probe these stations have identical capabilities.

The 85' dishes at these stations are X-Y types very similar to those in the STADAN Network. Their receiving and transmitting instrumentation is very similar to that of the DSN. Their operation is limited to the 2.1 GHz up-link frequency band and the 2.3 GHz receiving band. The range and range rate system, data format and modulation are essentially identical to that used by the Deep Space Network. The command transmitters are similar to the 10 kilowatt units presently used in the DSN except that 20 kw instead of 10 kw is available. Using the two transmitters available at each site in a combined mode should permit nearly 40 kw output power levels. Lower transmitter powers are also available.

Cooled preamplifiers are scheduled for installation in the near future. The resulting system noise temperature will then be approximately 100°K. In addition a field operable hydrogen maser is scheduled for installation in 1969, which will drive the existing frequency synthesizers. The loop bandwidths in the coherent demodulator are adjustable to permit operation at 50 Hz, 200 Hz, and 700 Hz. The USBS Station ground communications is linked to the NASA Worldwide Communication Network.

With the installation of the Galactic-Jupiter Probe unique receivers, signal conditioners and some modifications to the frequency synthesizers, these stations will operate satisfactorily as backup on the Galactic-Jupiter Probe project.

# COLLIMATION SYSTEM



53A



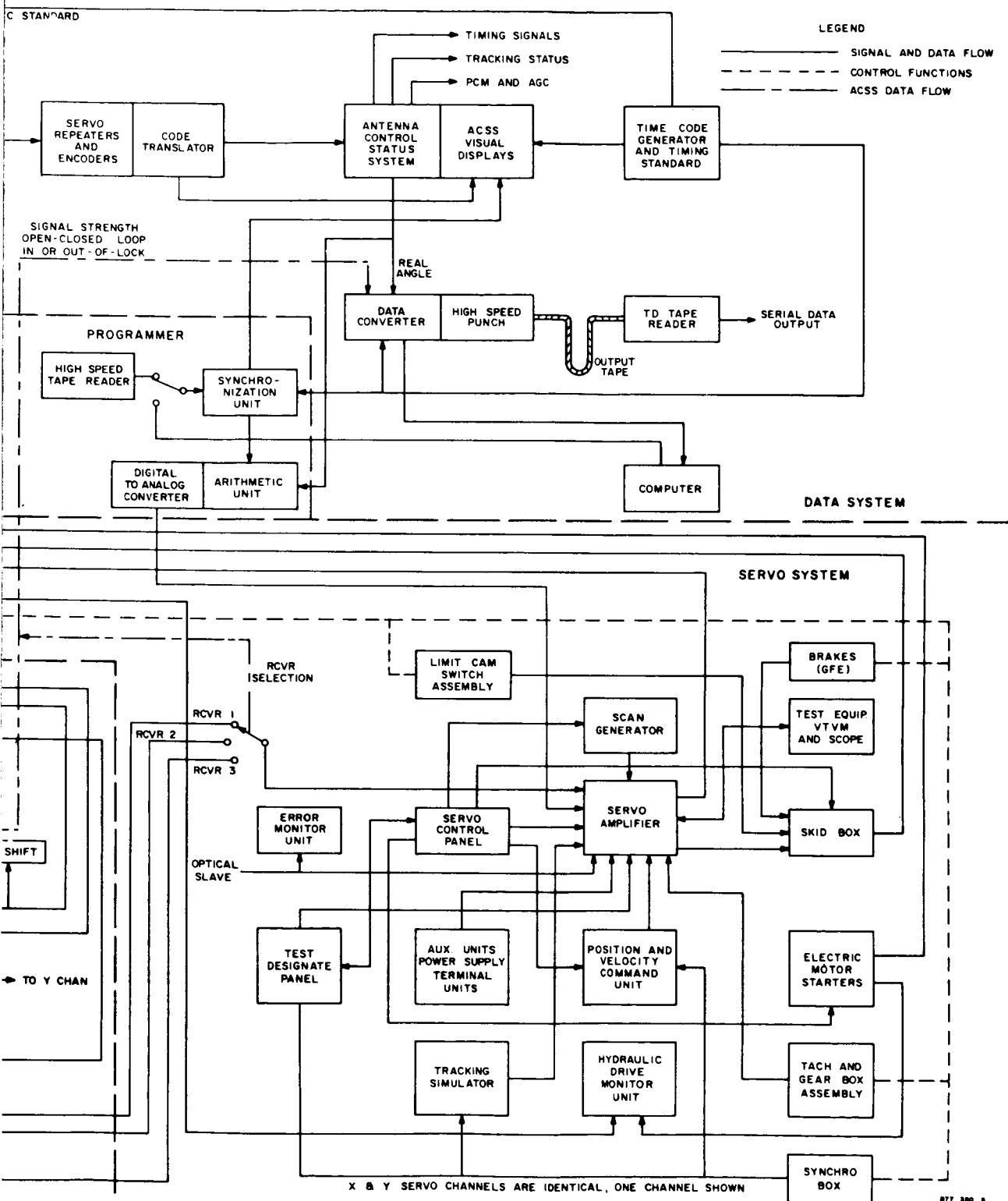


Figure IV-2. Rosman Data Acquisition Facility, Functional Block Diagram

Table IV-2  
Deep Space Network Parameters (Reference 5)

85-Foot Antenna Parameters		
Parameter	Receiver	Transmitter
Antenna gain	53.0 <sup>+1.0</sup> <sub>-0.5</sub>	49.6 ± 1.0 db
Antenna beamwidth	0.36°	0.36°
Axial ratio	0.75 ± 0.25 db	0.75 ± 0.25 db
Feed line loss to transmitter		0.18 ± 0.05 db
Antenna temperature (zenith)	16° ± 3°K	
Polarization	LC & RC*	LC & RC
Paramp system temperature (referenced to paramp input)	270° ± 50°K	
Maser system noise temperature	18°K ± 3°K	
Transmitter power		to 400 kw
Transmitter noise contribution	10°K	
210-Foot Antenna Parameters		
Parameter	Value	
Antenna gain	61.0 ± 1 db	
Antenna beamwidth	0.14°	
Axial ratio	0.5 db	
Feed line loss to LNA	0.02 ± 0.01 db	
System temperature	34° ± 5°K	
transmitter power	400 kw	
polarization	RC & LC	

\*LC—left-hand circular; RC—right-hand circular

### C. Station Selection

Careful planning is necessary in order that the big dish facilities at the various stations in the networks be judiciously allocated their appropriate

share of the T&DS workload. The selection of the facilities for the GJP involves both the coverage requirements and the necessary allocations of the network facilities to other flight programs.

### 1. Program Requirements

In order to determine which ground station facilities are the most appropriate for various phases of this project, the following three broad program requirements must be taken into consideration:

a. For the reason stated above, very high gain, low noise ground receiving instrumentation is required.

b. Continuous operation is required 1/ during launch and several weeks thereafter, 2/ for several weeks during Jupiter encounter and 3/ probably at intermittent periods during the long cruise phase when significant scientific events occur.

c. Daily coverage during the cruise phase of the order of 12 hours per day are required in order to fully satisfy scientific objectives. This last requirement is most significant and has a decided impact on the ground station selection.

Because the range is relatively low during the first few months after launch, 85 foot dishes provide sufficient performance to satisfy program objectives. After that time the use of 210 foot dishes, although not absolutely necessary, would be desirable.

### 2. DSN Advantages

From a technical and performance viewpoint, there are good reasons for selecting the DSN facilities as the ground terminals for the GJP. These stations are presently implemented to operate at the GJP frequencies, 2.3 GHz down and 2.1 GHz up, they are low noise highly efficient dishes at this frequency and they already possess some electronic instrumentation usable on this project. The available time that these facilities can be allocated to the GJP, however, is another matter.

### 3. Coverage Restrictions

From JPL Inter-Office Memo - 319/1834, "Deep Space Mission Parameter Analysis," and common knowledge of the planned NASA programs, it is recognized that an appropriate 210 foot dish allocation to the GJP, is in the

order of 8 hours per week during the later portion of the cruise phase. Continuous coverage could be supplied by the 210's during encounter.

Although two DSIF 85 foot facilities exist at both Canberra and Madrid the deep space programs now planned prohibit allocating 12 hours per day coverage daily to the GJP. It is important that the GJP project have at least one station that can be counted on to supply daily coverage on a continuing basis throughout the cruise phase.

#### 4. STADAN Use

A partial solution to this problem lies in the use of the STADAN 85 foot dish at Rosman. Rosman II can be shifted from the ATS program to the GJP. To fill in for ATS, the 40 foot transportable site, now in Cooby Creek, Australia, can be moved to Rosman. ATS will not require coverage in Australia in the 72 era. The scheduled loading on the STADAN is too heavy to consider tying up the existing 85 foot dish in Orroral. In addition, the multi-frequency operation prevents the attainment of the high performance demanded by the GJP requirements. Construction of such a facility is out of the question in view of the shortage of funding that exists today and the foreseeable future. Rosman II can supply coverage amounting to about 7 hours per day. Although impossible to definitely substantiate at this time, it is felt that the remaining 5 hours or so daily coverage can be supplied on the average by the various DSIF 85 footers. Interruptions will probably occur, however, for days or even weeks when conflicts occur with other programs.

#### D. Coverage

##### 1. Station Use vs. Mission Phases

In the light of the foregoing discussions it is considered appropriate that the coverage for the GJP be supplied by a combination of DSN and STADAN stations. The DSN stations would consist of 85 foot dish facilities at Madrid and Canberra and the three 210 footers at the three prime DSN sites. STADAN would supply an 85 foot facility at Rosman. Using these stations, the resulting coverage would be as shown in Figure IV-3. The two STADAN and the DSN 85 foot facilities would supply the required continuous coverage at launch. The DSN 210 foot facilities would supply the required continuous coverage for several weeks during encounter, and at intermittent periods during the cruise phase if permitted by their other commitments. Thus, during these crucial phases an increased bit rate and/or performance margin would be attainable. A daily coverage of about 7 hours per day would be supplied by the STADAN facilities at Rosman. The bit rates shown are approximate only and do not show the full

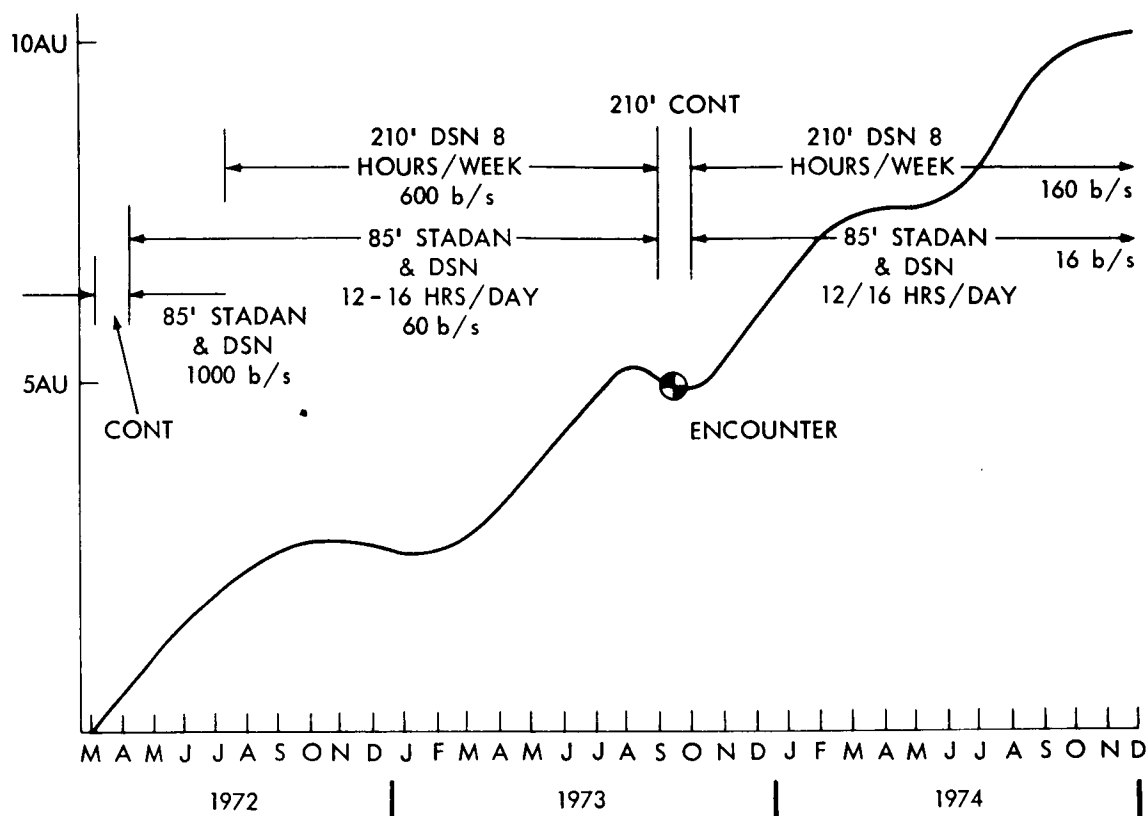


Figure IV-3. Tracking Coverage

capability of the communication system. The selection of the bit rate also depends upon practical factors associated with the data handling capabilities of the data processing equipment.

## 2. Trajectory

The sub-orbital trajectory shown in Figure IV-4 is that of a 550-day-to-encounter operation with a launch date in March 1972. With respect to the probe coverage problem, the trajectory is representative for launches in this era.

During the 1972 era, Jupiter is located in its orbit about the Earth in a position roughly orthogonal to the Earth's equinoctial line. The Earth's axis being tilted away from Jupiter results in the sub-orbital path being in the southern hemisphere close to the tropic of Capricorn. At encounter, about 18 months after launch, Jupiter has moved in its orbit about 45 degrees – the orbital period being about 12 years. This will cause the sub-orbital path to rise a corresponding amount. Since the spacecraft maintains roughly an alignment

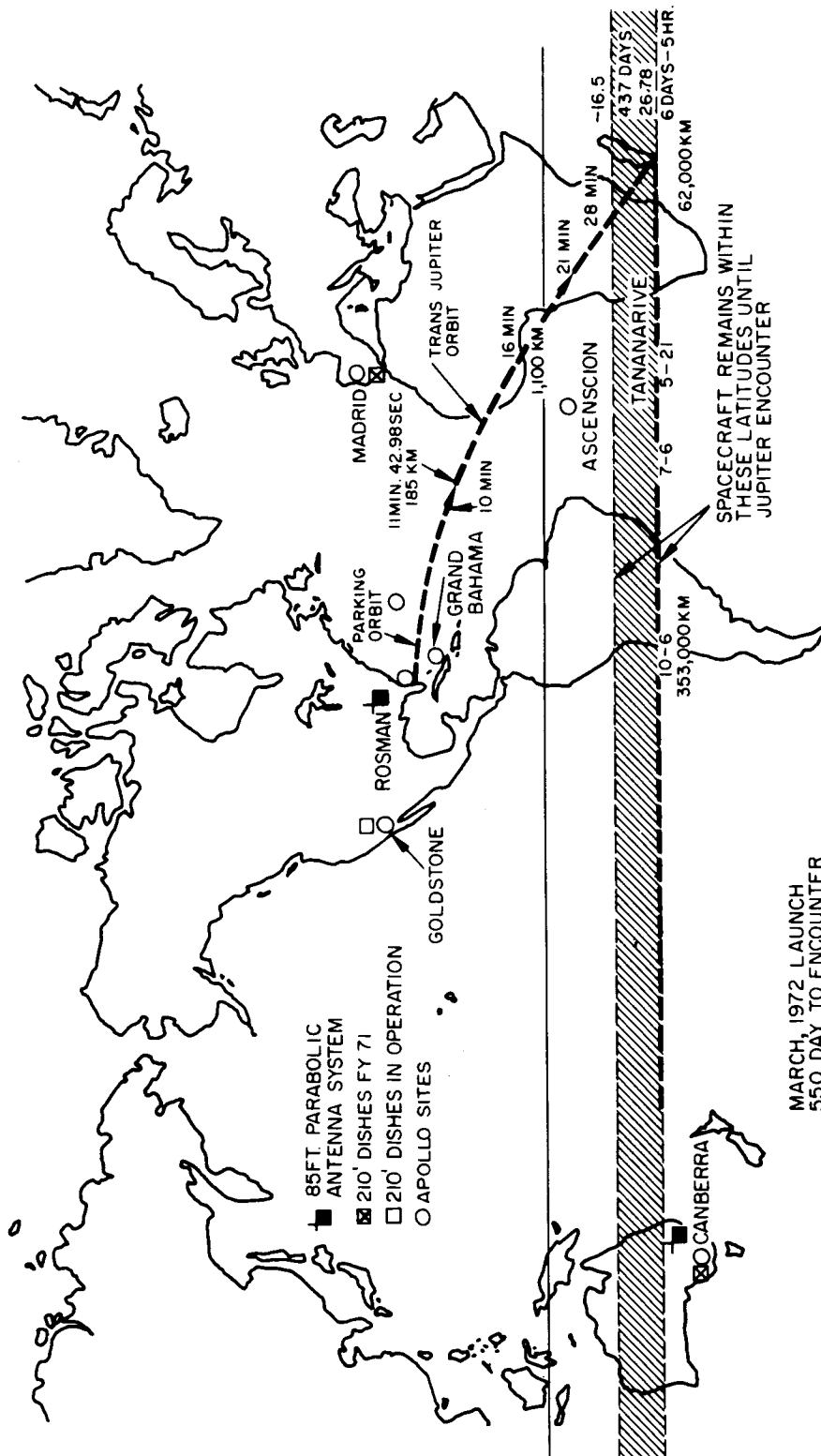


Figure IV-4. Sub-Orbital Trajectory - Galactic Jupiter Probe

between the Earth and Jupiter its sub-orbital path is similar. The cross-hatched area on Figure IV-4 represents the sub-orbital path between launch and encounter.

### 3. Launch and Near-Earth Operation

The launch azimuth is about 100 degrees. The spacecraft travels through a short parking orbit for about 11 minutes at which time injection occurs. The spacecraft then gains latitude rapidly and speed almost directly away from the earth with its sub-orbital point over Madagascar. The rotation of the Earth then causes the sub-orbital path to travel from East to West at a rate due largely to the Earth's diurnal rotation.

After only about two hours after launch, the predominate angular motion of the spacecraft with respect to the ground stations is that due to the Earth's rotation. This is corroborated by the probe visibility relationships shown in

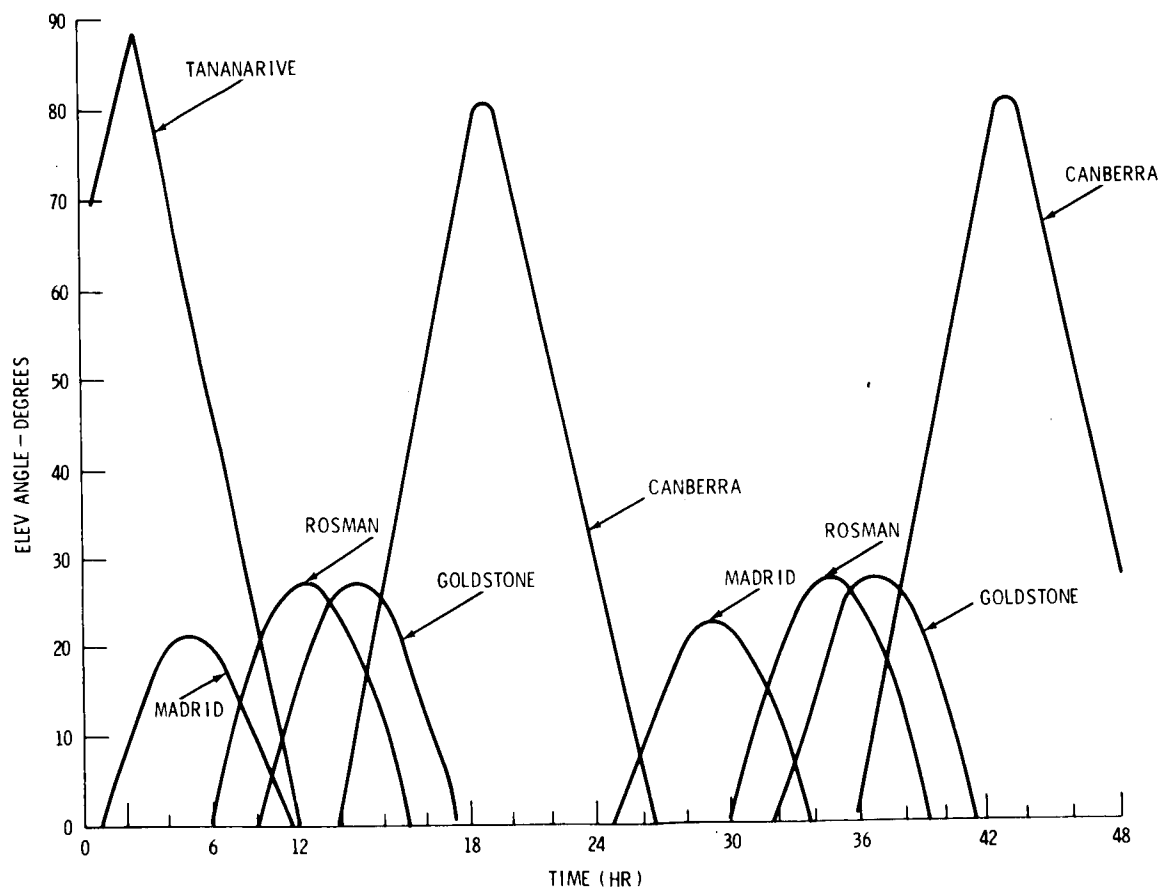


Figure IV-5. Probe Visibility 0 to 2 Days After Injection, March 1972 Launch

Figure IV-5. Note that the visibility curves for the first pass over the stations are nearly identical to those during the second (and subsequent) days.

The launch and near earth phases can be adequately covered by the ETR and MSFN C-Band radars at Patrick, AFB, Grand Bahama, Grand Turk, Antigua, Bermuda, Canary Island, Ascension, Pretoria and Tananarive; and by DSN and MSFN USB instrumentation at Cape Kennedy, MILA, Grand Bahama, Antigua, Canary Island, Ascension, Bermuda, Carnarvon, Tananarive, and Madrid. Angle measurements derived from the autotrack antennas at appropriate stations during the early hours will materially aid in the trajectory determinations.

#### 4. Visibility by Stations During Cruise

The Canberra station, at 35 degrees south latitude, will provide excellent coverage in the 1972 era; the Rosman and Madrid stations, located 35 degrees north latitude will provide similar coverage in the 1978 era. Figure IV-6 shows the coverage plot for a typical day during the cruise phase of a March 1972 launch.

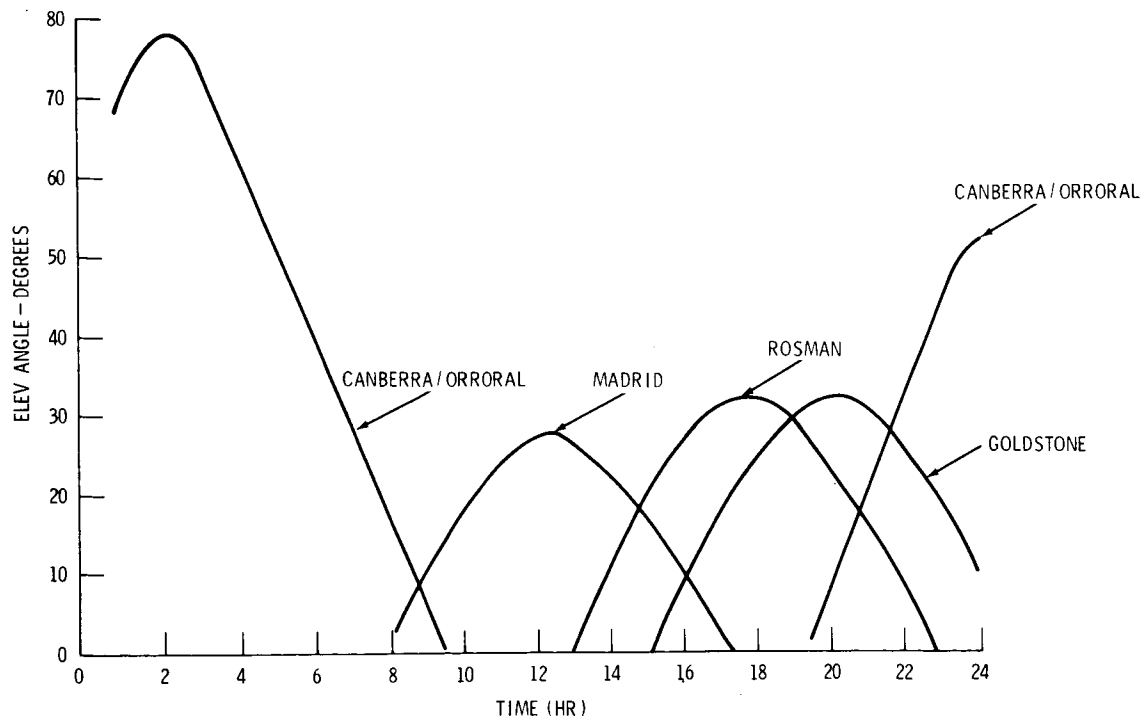


Figure IV-6. Probe Visibility 300 to 301 Days After Injection, March 1972 Launch

## E. Improvements to the Rosman Station

### 1. Frequency and Noise-Temperature

In support of the Galactic Jupiter Probe, the Rosman station will be improved for operation at the 2.3 GHz receiving and 2.1 GHz transmitting frequencies. Due to the long ranges associated with the mission and, consequently, the resulting space loss in the communications link, the best available system noise temperature must also be achieved. Therefore, the existing feed support structure at Rosman II will be replaced with a newly developed Cassegrain feed system that has an antenna noise temperature of 10.5 degrees K at Zenith (Reference 3).

The design goal for the system noise temperature of improved stations is less than 50 degrees K for elevation angles from 10 degrees to 20 degrees, and less than 40 degrees K for elevation angles above 20 degrees. System noise temperature as a function of elevation is shown in Figure IV-7. These design goals can be readily realized since the feed cone to be used has demonstrated successful operating noise temperatures in another system (References 3, 6). Maser preamplifiers with low noise temperatures of less than 10 degrees K will also be installed (Reference 4). With a feed line and diplexer loss of 0.18 db the

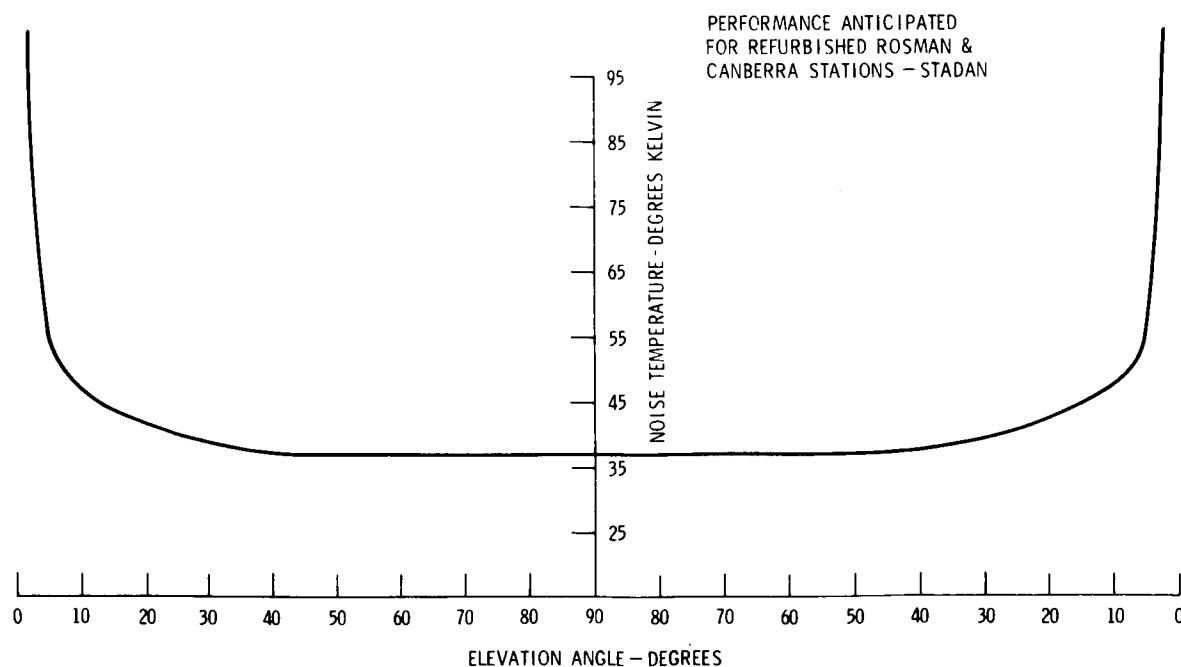


Figure IV-7. Noise Temperature Characteristics of Cassegrain Antenna With Maser Preamplifier

system noise temperature at Zenith is therefore  $37^{\circ}\text{K} \pm 9^{\circ}\text{K}$ . This becomes as high as  $47^{\circ}\text{K}$  when the command transmitter is turned on. To maintain low noise-temperature performance, it will be necessary to omit all autotrack capability. A simultaneous lobing autotrack feed consists of a group of four separate feeds. The result of this feed configuration is high side lobes, decreased antenna efficiency, additional losses due to the autotrack comparator network, and increased system noise temperature. Since tracking data will allow definition of the probe trajectory with a high degree of accuracy, autotrack will not be required for the Galactic Jupiter Probe mission. Programmed antenna pointing with an accuracy of less than 0.1 beamwidth can be readily achieved through trajectory predictions.

## 2. Receiving System Improvements

Due to the characteristics of the Galactic Jupiter Probe signals and the demand for maximum sensitivity, a special receiving system will be developed and installed at Rosmann II. A single system will provide the functions of both telemetry and tracking. All local oscillator signals will be generated through synthesis from the hydrogen maser frequency standard. The phase-lock-loop for the coherent detector will obtain its VCO signal from the maser synthesizer; a special digital VCO will be developed for this function. Frequency and phase stability is of great significance to the mission since the limitation in system sensitivity is determined by these parameters. The resulting achievable phase lock bandwidth is therefore as narrow as 0.3 Hz. Because such bandwidths have never been achieved as yet in the field a value of 4 Hz was used for communication link calculations.

## 3. Command Transmitter Installation

At present, command transmitters operating in the 2.1 GHz band do not exist at these stations. This function will be supplied by a 100-kw transmitter now under research and development. These high-power amplifiers, tunable over the band from 2090 MHz to 2120 MHz, will have an instantaneous bandwidth of at least 10 MHz. The RF Klystron and waveguide circuitry will be antenna-dish mounted, probably within the feed cone. The beam power supply will be housed in a building at the base of the antenna.

The transmitter exciter will coherently synthesize the carrier frequency and the required doppler extractor frequencies from the hydrogen maser. Phase modulation capabilities will be provided as well as provisions for programming out doppler during the course of the mission. Table IV-3 lists the STADAN station parameters after improvements for the Galactic Jupiter Probe mission.

Table IV-3  
Rosman II Station Parameters After Modification  
For the Galactic Jupiter Probe

Parameter	Value
Dish size	85-ft. diameter
Antenna gain	53 db <sup>+1</sup> -0.5
Antenna beamwidth	0.36°
Feed line and diplexer loss	0.18 ± .05 db
Antenna noise temperature - zenith	16°K ± 3°K
Maser noise temperature	10°K ± 3°K
System noise temperature	37°K ± 9°K
Circular polarization (transmit and receive)	LC or RC*
Phase-lock bandwidths	0.3 - 1 - 4 - 16 - 64 Hz
Ground transmitter power	Adjustable from 10 kw to 100 kw
Command transmitter noise contribution	10°K
*LC - left-hand circular; RC - right-hand circular	

#### F. Down Link Performance (Telemetry)

##### 1. Received Signal Levels

It is assumed that the scientific and engineering data will be telemetered to the ground stations by either a coherent carrier PCM/PM system or by a PCM/PSK system where the carrier component is completely suppressed. The latter provides the advantage that all the transmitted power is useful - that is, is composed entirely of information. On the other hand, to avoid SNR deterioration the ground detector must perform its function coherently, which requires the re-generation of the missing carrier component. Because of the keyed 180 degree phase shifts in the transmitted signal, multiplying by 2 (squaring) results in the sideband components combining to form a spectral line at twice the frequency of the absent carrier component. Frequency dividing and narrow band filtering this signal by a phase-lock-loop provides the necessary ingredient to attain the required coherent demodulation.

In a coherent system of either of the above types the predominate system limitation is the carrier phase-lock-up by the ground terminal. For the PCM/PM system, therefore, one-half the total radiated power is allocated to the carrier component. This component does not contain telemetry information. However, this carrier component can be counted on to be a very precise and stable signal which is of paramount importance for the phase-lock function. For the PCM/PSK system the carrier component must be regenerated from sideband components which entails some uncertainty with respect to its resultant spectral composition. In short, the PCM/PSK system has the potential for improving the sensitivity of the down link by a valuable 3 db; however, test and evaluation of the phase lock-up operation remains to be performed. The telemetry link performance using the PCM/PSK system is shown in the Communication and Data Handling Section of this report. For the purpose of establishing boundary conditions leading to the requirements for phase and frequency performance, the down link performance shown below will be based on the PCM/PM system.

Using this modulation format the resulting relationship between probability of error  $P_e$  and the ratio of signal energy per bit to the noise power per unit bandwidth,  $ST/N_o$ , is shown in Figure IV-8 (Reference 8).  $S$  is the received signal level,  $T$  is the bit period, and  $N_o$  is the effective input noise level per Hz. This figure also includes the curve showing the effect due to the 3 db reduction in side band power due to the carrier component.

For the Galactic-Jupiter Probe program a probability of error of  $2 \times 10^{-4}$  is considered adequate. As seen from the figure, this corresponds, for the Convolutional coding and power division modulation system described above, to a  $ST/N_o$  of 4.9 db.

The received signal level depends upon the ground station and spacecraft parameters which are summarized for the worst case as follows (see Communication and Data Handling Section):

Spacecraft:

Transmitter Power Level . . . . .	10 watts
Antenna Gain . . . . .	31.6 db
Pointing Loss . . . . .	3 db
Cable Loss . . . . .	2 db
Aperture Blockage . . . . .	0.5 db

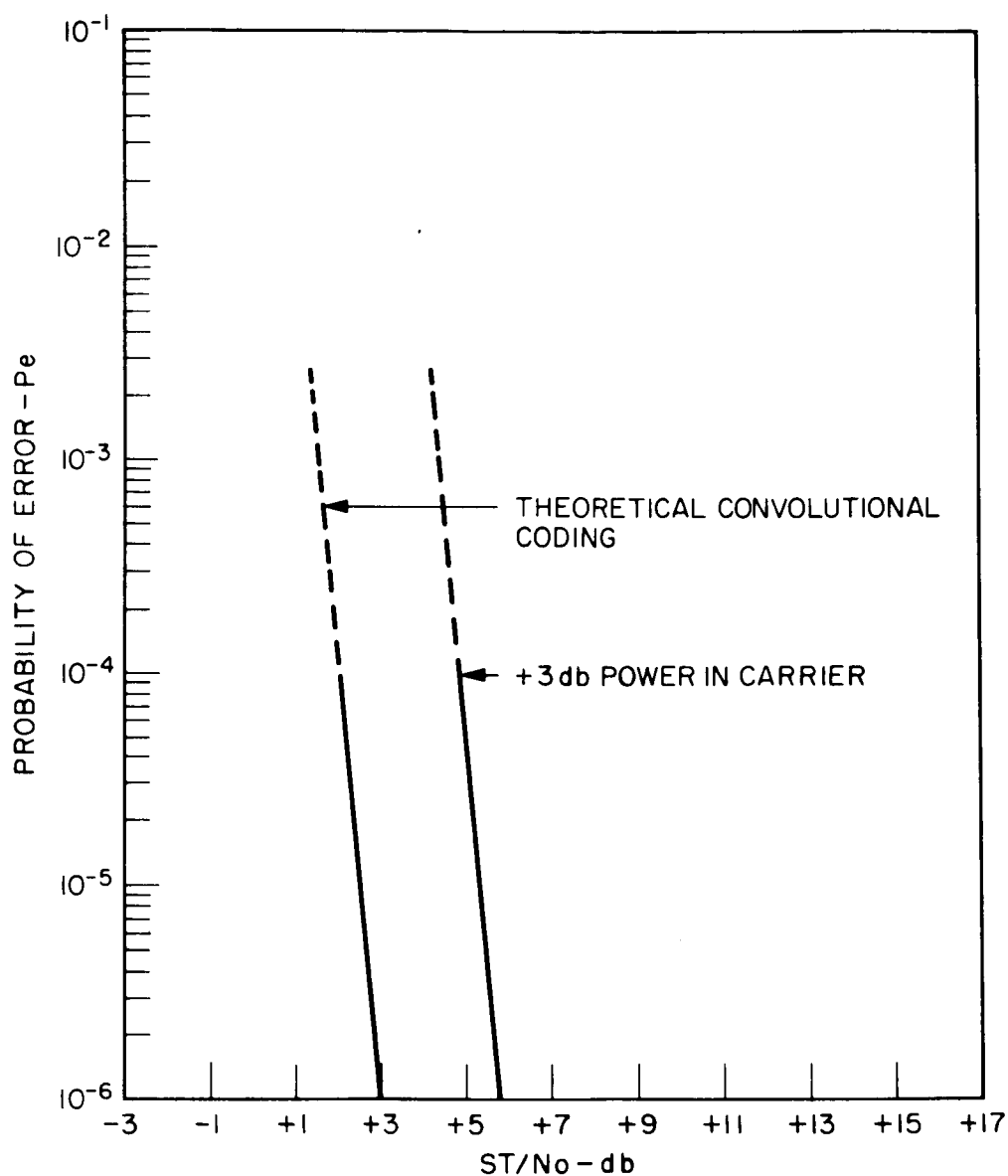


Figure IV-8. Received Signal to Noise Ratio  $ST/N_o$  (db)

Ground Terminal, 85 foot dish

Antenna Gain . . . . . 52 db

System Noise Temperature . . . . . 55°K (max)

Ground Terminal, 210 foot dish

Antenna Gain . . . . . 61 db

System Noise Temperature . . . . . 35°K  $\pm$  10°K

The received signal level as a function of range is:

$$P_r = P_t G_t G_r L \left( \frac{\lambda}{4\pi R} \right)^2 ,$$

where

$P_r$  is the received signal level

$P_t$  is the transmitted power level

$G_t$  is the transmitting antenna gain

$G_r$  is the receiving antenna gain

$\lambda$  is the propagating wavelength at 2.3 GHz

$R$  is the range in the same dimension as  $\lambda$ , and

$L$  is the pointing Loss.

Then for the 85 foot dish ground station at 1 AU:

$$P_r = 40 \text{ dbm} + 52 \text{ db} + 31.6 \text{ db} - 263.6 - 3 \text{ db} - 2.0 - 0.5 \approx 145.5 \text{ dbm}$$

Figure IV-9 is a plot of the received signal level as a function of range for both the 85 and 210 foot antennas.

From the relationship between  $P_e$  versus  $ST/N_o$  and the received signal level versus range, the allowable bit rate,  $f_b$ , can be derived. From Figure IV-8, the theoretical value of  $ST/N_o$  corresponding to a  $P_e$  of  $2 \times 10^{-4}$  for convolutionally coded PCM/PM is 4.9 db, where  $T$ , the bit period,  $= 1/f_b$ . With reference to the input terminals of the receiver:  $N_o = KT_e = -181.2 \text{ dbm}$ , where  $K$  is Boltzmann's constant,  $T_e$  is the effective system noise temperature. Allowing a 1 db detector loss,  $L_d$ ,  $f_b = P_r + KT_e - ST/N_o - L_d = P_r + 175.3 \text{ db (bits/sec)}$ . From the results of Figure IV-9,  $P_r$  versus  $R$ , the bit rate,  $f_b$ , can be determined as a function of range. Figure IV-10 shows these results. Note, that at 5 AU, (the approximate Earth-Jupiter range at encounter for the assumed 600 day mission), the allowable bit rate, for the PCM/PM system, is approximately 38 bits/sec using the 85-foot antenna. This corresponds to 76 bit/sec for the PCM/PSK system.

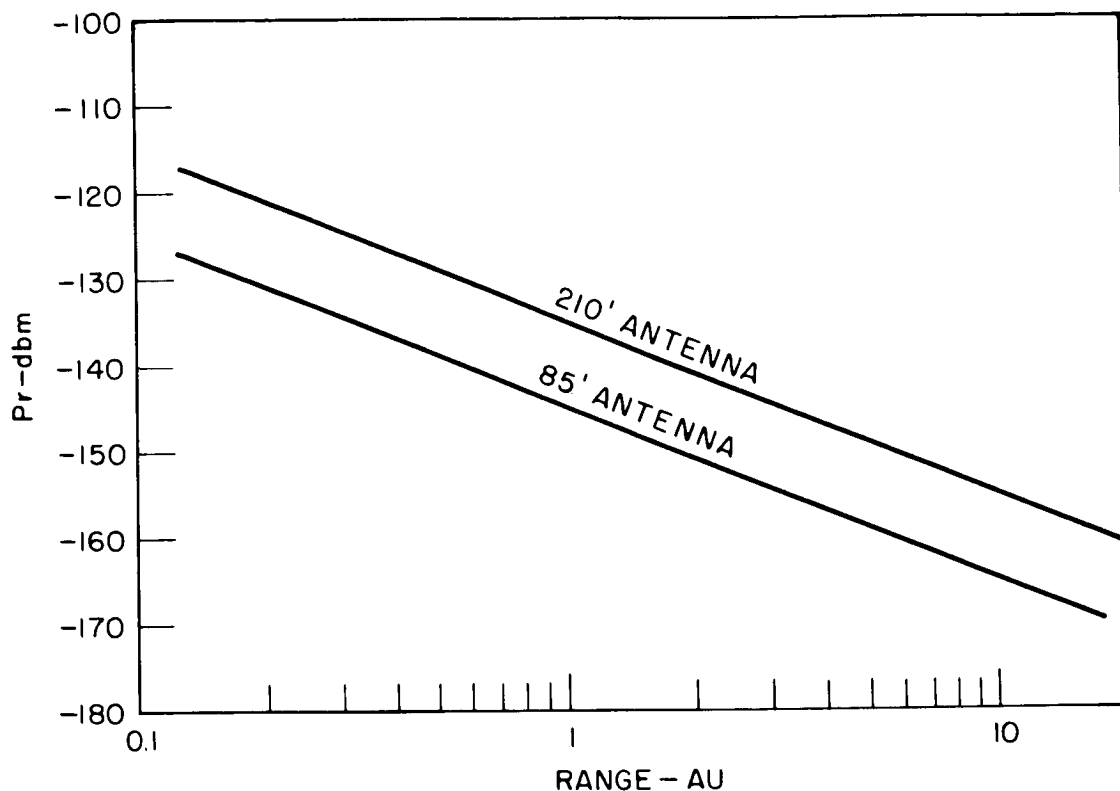


Figure IV-9. Received Signal Level

## 2. Phase and Frequency Stability Performance

Thus far, any possible loss in the system due to imperfect demodulation of the received modulated carrier has been ignored. Without careful design, this source of sensitivity degradation could be substantial. The considerations leading to the removal of these effects will now be discussed.

The SNR at the output of a perfectly coherent detector is equal to the input SNR. As the SNR of the received carrier component decreases with range, the noise within the phase lock loop, (PLL), associated with the coherent detector reaches a value where perfect coherency can no longer be maintained. Further reduction results in the PLL not able to retain lock-up at which time data trans-ferral ceases.

The deterioration in the SNR of the demodulated signal due to noise in the loop is only about 0.4 db at  $\sigma_{\phi} = 20^{\circ}$  rms (Reference 9). Thus, this deterioration is not serious until the loop begins to skip cycles; this begins to occur at about loop phase variations,  $\sigma_{\phi}$ , of about  $30^{\circ}$  rms. The problem, then, can be

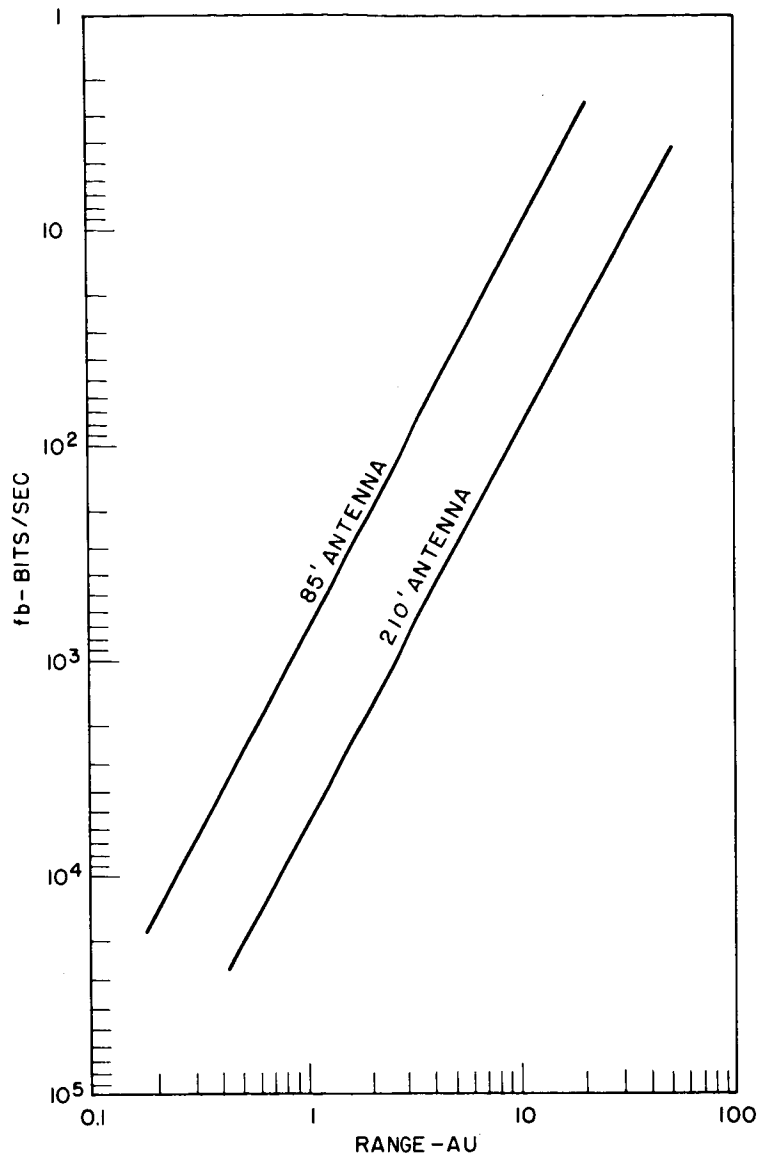


Figure IV-10. Allowable Bit Rate Versus Range

viewed as one of establishing and maintaining phase lock in the ground receiver in spite of the very low received signal levels.

Loop phase-error variations are caused by two sources; (1) the additive receiver noise, and, (2) oscillator instabilities. The effects from the additive noise is a function of the loop noise bandwidth,  $B_n$ , and the received signal level,  $P_r$ . The resulting loop phase variations,  $\sigma_\phi$ , from this source is (Reference 10):

$$\sigma_{\phi_a} = \frac{N}{\sqrt{2} S} = \left( \frac{K T_e B_n}{2 P_{rc}} \right)^{1/2}$$

radians rms, where  $P_{rc}$  is the level of the received carrier component =  $P_{tc} G_t G_r (\lambda/4\pi R)^2$ . Since, as stated previously, one-half the power transmitted is in the carrier component:  $P_{tc} = 5$  watts. Figure IV-11 shows the loop phase error from additive noise as a function of the noise bandwidth for received SNR applied to 85-foot antennas in terms of range from 0.1 AU to 40 AU.

The loop phase variations due to oscillator instabilities,  $\sigma_{\phi_o}$ , is given by:  $\sigma_{\phi_o} = (C/B_n)^{1/2}$  (Reference 11), where, C is a constant dependent on the noise level. This relationship has been verified for a large number of oscillators. For this analysis, an oscillator was chosen having a noise spectrum representative of oscillators rated between the best available and the latest high Q types.

Superimposing the additive noise and composite oscillator stability relationships as shown in Figure IV-11, shows that the optimum loop bandwidth for a coherent detector with the described oscillators is a compromise between the two sources of loop phase variations. In addition, it is seen that at ranges of 10 AU, lock-up cannot be reliably achieved with the system parameters given. Figure IV-12 contains the same data as Figure IV-11 except as applied to the 210-foot antennas.

Two alternatives are available to overcome this limitation; (1) the carrier component level can be allocated a greater proportion of the total transmitted power, (2) the oscillator instability effects can be reduced. The first alternative has severe limitations. If all of the power were allocated to the carrier component, an improvement of only 3 db would result, with, incidentally, the total removal of all information side bands. Only minor improvements can be achieved by attempting to improve further the short term stability of crystal controlled oscillators. The hydrogen maser, however, does exhibit characteristics that make a substantial improvement in this area possible.

The stability characteristics of the hydrogen maser/synthesizer output signals are not limited to the  $C/B_n$  characteristics displayed by crystal VCO's. The flicker noise and  $1/f^2$  perturbations on these signals is negligible. Therefore, considering this error source only, the loop bandwidth,  $B_n$ , can be reduced almost without limit with a resulting reduction in loop phase noise as shown by Figures IV-11 and IV-12. The additive noise curves only, then apply. Experimentation now in process in the Advanced Development Division of GSFC has confirmed this concept. Phase Locking to the 1.4 GHz Hydrogen Maser Signal, translated by synthesis techniques to 5 Mc, results in only about  $5^\circ$  loop

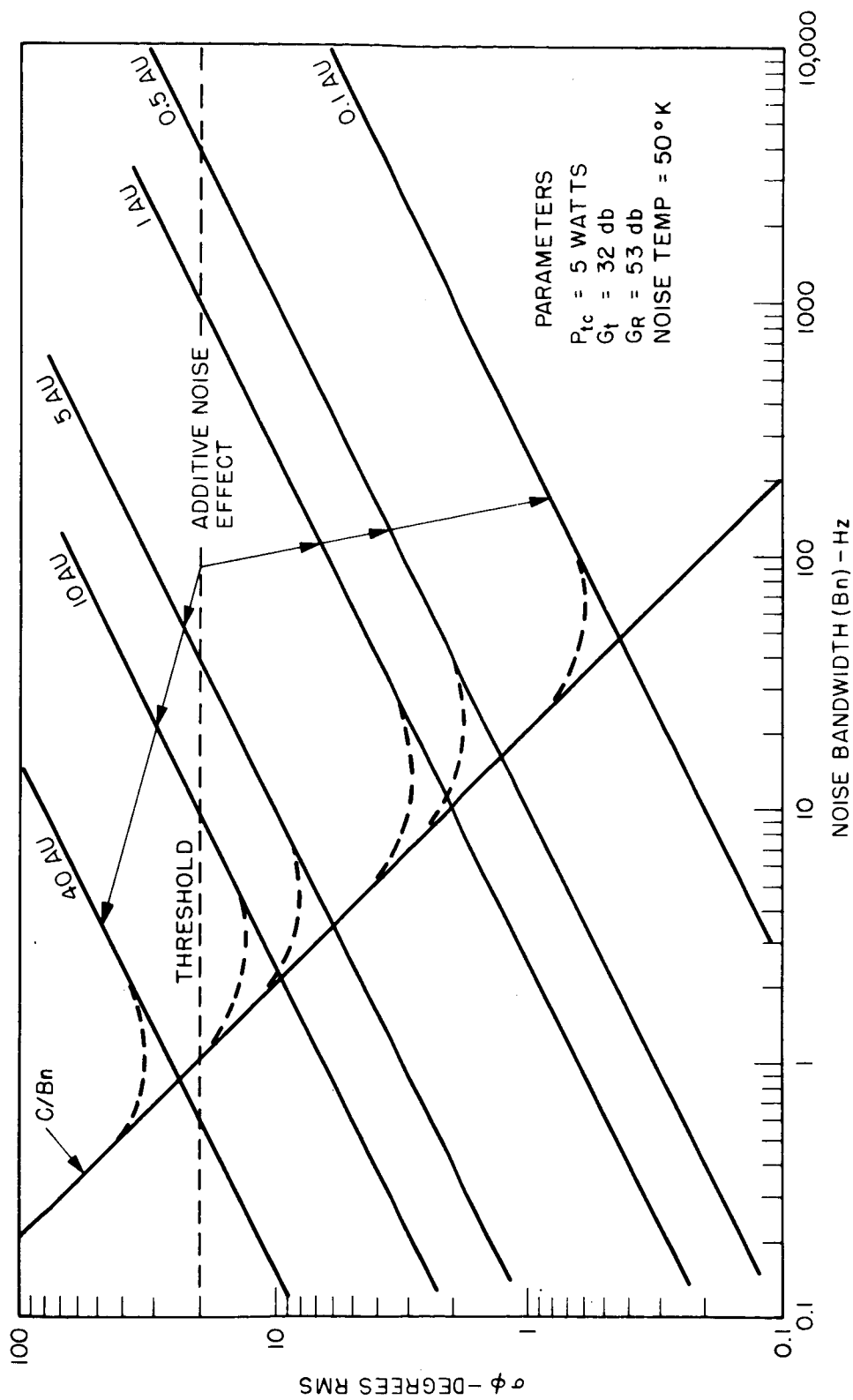


Figure IV-11. Ground Receiver Coherent Detector Loop Noise - 85° Antenna

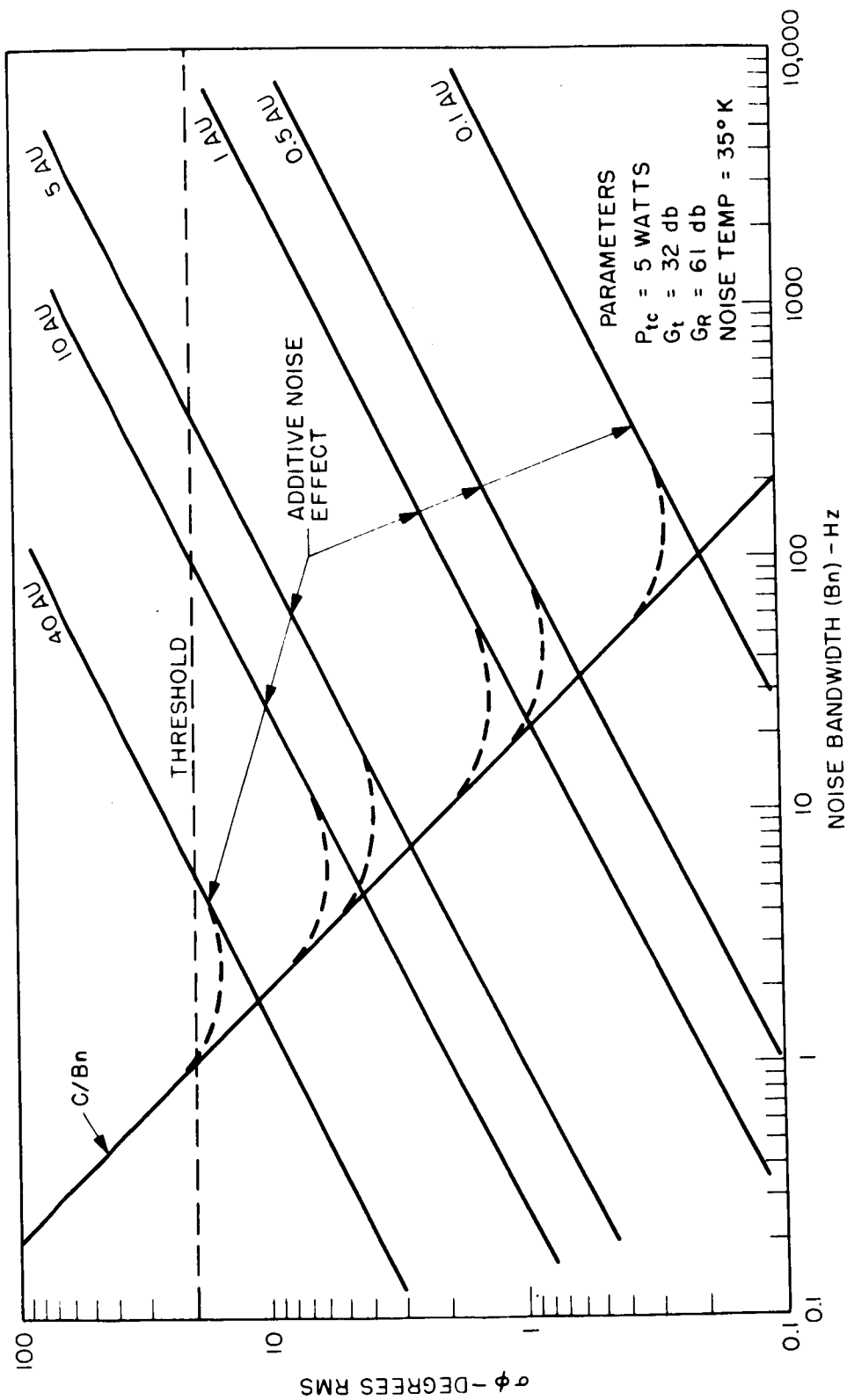


Figure IV-12. Ground Receiver Coherent Detector Loop Noise - 210' Antenna

phase fluctuations for a tracking bandwidth of about 0.3 Hz. In practice, the acquisition time required and instrument bias errors would probably prohibit narrowing the loop to less than 0.1 Hz. The lower limit has not yet been experimentally derived.

Figure IV-13 is a block diagram of the communication system showing the use of the hydrogen maser frequency standard in stabilizing the system's local oscillators. To achieve the removal of the  $C/B_n$  characteristic, it is necessary to supply all the ground receiver translator oscillators as well as the VCO for the coherent demodulator. Through experimentation in the Advanced Development Division of Goddard Space Flight Center such VCO's are being developed and show promise of meeting the requirements for this function (Reference 12).

The narrow loop bandwidths and resulting improvement in system sensitivity cannot be attained unless the spacecraft transmitted signal is also free from the characteristic phase jitter of even the best crystal controlled oscillators. Thus, if down-link transmissions only are being performed, the narrow loop bandwidths cannot be used because of the instability of the transmitted signal.

The ground transmitter can, however, stabilize the spacecraft oscillator so that during this operational mode the lower loop bandwidths can be used. Figure IV-14 shows the loop phase noise in the spacecraft transponder, thus the radiated down-link signal. At 10 AU the total phase variation is only about 1 degree. At 40 AU it is only about 3 degrees. This amount of phase noise will not disturb the operation of the ground receiver beyond a negligible amount.

Assuming that the ground phase-lock demodulator operates according to the theory described above, communications from the spacecraft to ground is not limited even with 85 foot dishes at the ground terminal at ranges as great as 30 AU. The bit rate, would be, as shown in Figure IV-10, only 1 bit/sec. With the 210 foot antenna this bit rate corresponds to a range of over 100 AU. Although such deep space travel is not envisioned in conjunction with this project, the excess performance can be viewed as a comfortable margin.

#### G. Command System Performance

The function of the command system for the Galactic-Jupiter Probe is to provide a highly reliable ground to spacecraft link suitable for controlling the on-board experiments, midcourse maneuvers, communication system parameters, etc. Due to the importance of highly reliable, error free command the assumptions regarding system parameters have been made on the conservative side.

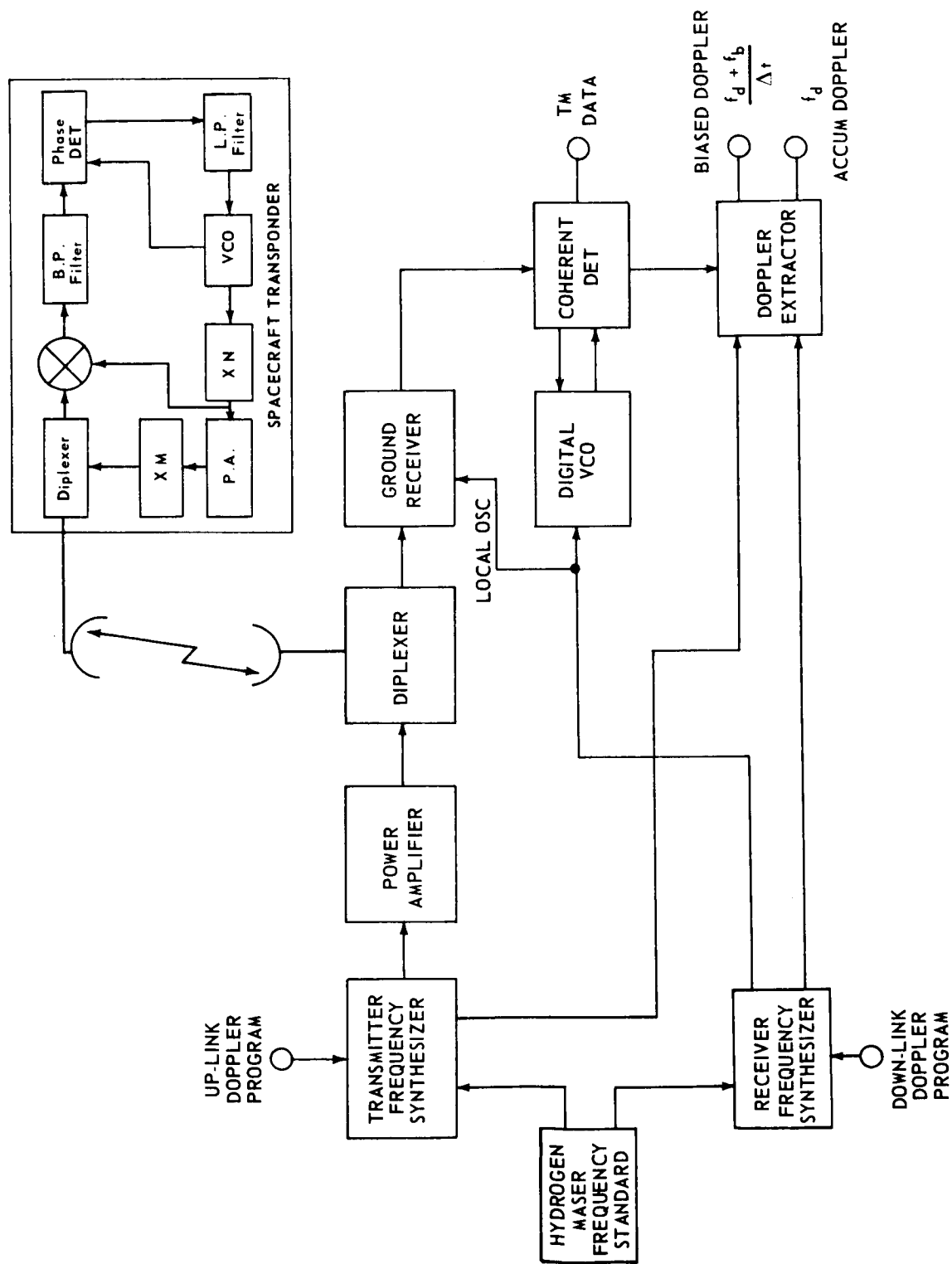


Figure IV-13. Communication System Block Diagram

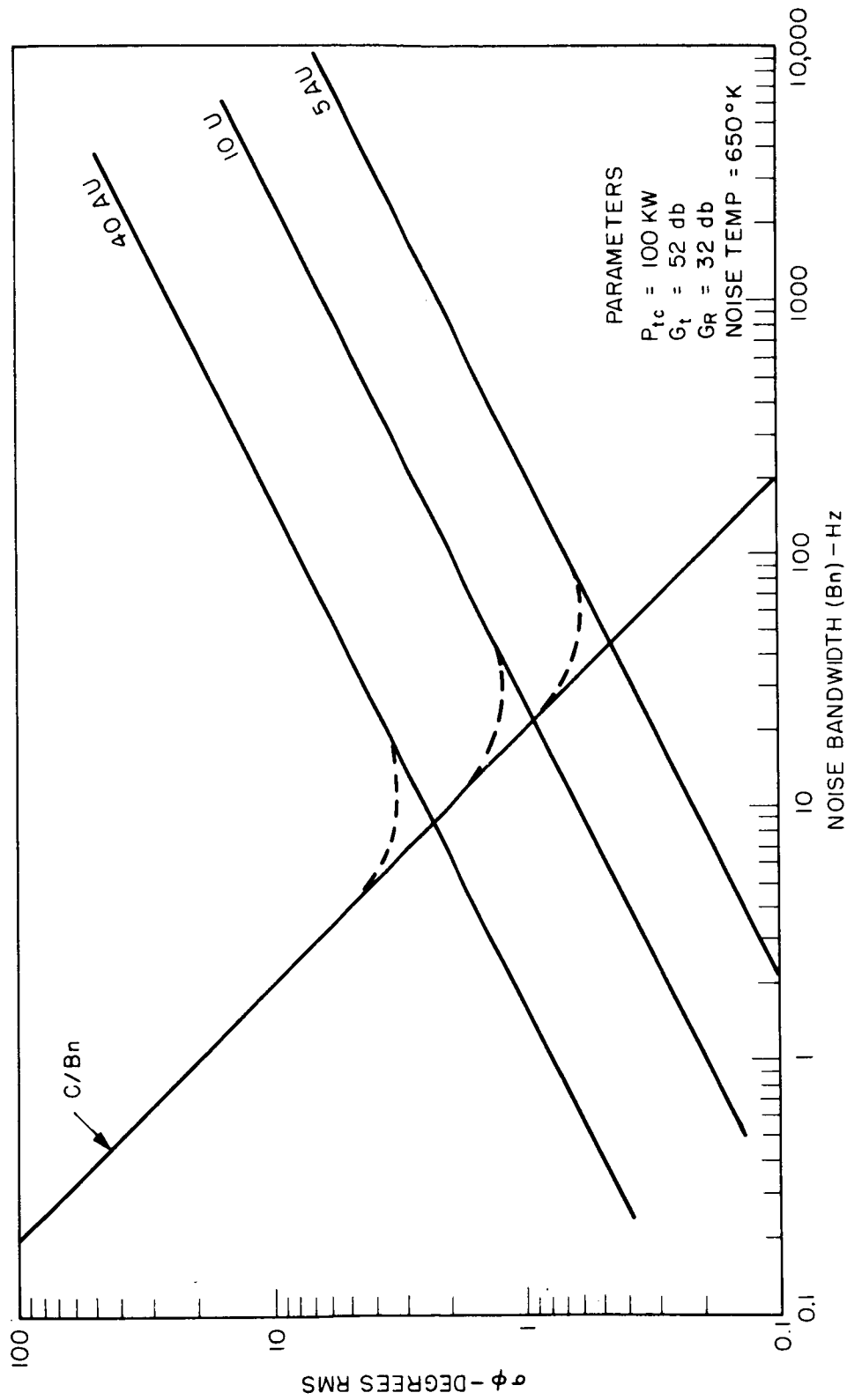


Figure IV-14. Spacecraft Transponder Loop Phase Noise

The command system proposed for the Rosman ground station is illustrated in Figure IV-15. Since the command frequency is 2.1 GHz, the existing command facilities of the MSFN and the existing and proposed facilities of the DSN are applicable and will be included in this analysis. The spacecraft may employ three separate antenna systems suitable for command reception; an 8 foot dish, a horn, and an omnidirectional system. The command link will be low bit rate (1 bit/sec) PCM/FSK/PM with the phase deviation of the carrier adjusted to 70° so that 50% of the up-link power remains in the carrier.

### 1. Power and Antenna Gain

By 1972, the Rosman II facility will be equipped with 100 KW power amplifiers. Each of the 85 foot antennas in the MSFN is presently capable of dual frequency 20 KW operation. These stations could be modified to produce 40 KW for a single frequency transmission. The 85 foot antennas in the DSN are presently equipped for 10 KW operation and one station (Venus, Goldstone) is capable of 100 KW operation.

The power output and antenna gains projected for the various stations in the network are summarized below.

#### 1972 Command Capability Summary

<u>Station</u>	<u>RF Power</u>	<u>Antenna Gain</u>
Rosman	100 KW	52 db
Canberra/MSFN	20 KW (40 KW)	52 db
Goldstone/MSFN	20 KW (40 KW)	52 db
Goldstone/DSN/Venus	100 KW	52 db
Madrid/MSFN	20 KW (40 KW)	52 db
Goldstone/DSN/Mars	100 KW	60 db

#### Spacecraft Parameters

<u>Antenna</u>	<u>Gain</u>	<u>Receiver Noise Figure</u>
High Gain (8' dish)	32 db	5 db (2 db (Reference 13))
Medium Gain (horn)	15 db	5 db (2 db (Reference 13))
Low Gain (OMNI)	0 db	5 db (2 db (Reference 13))

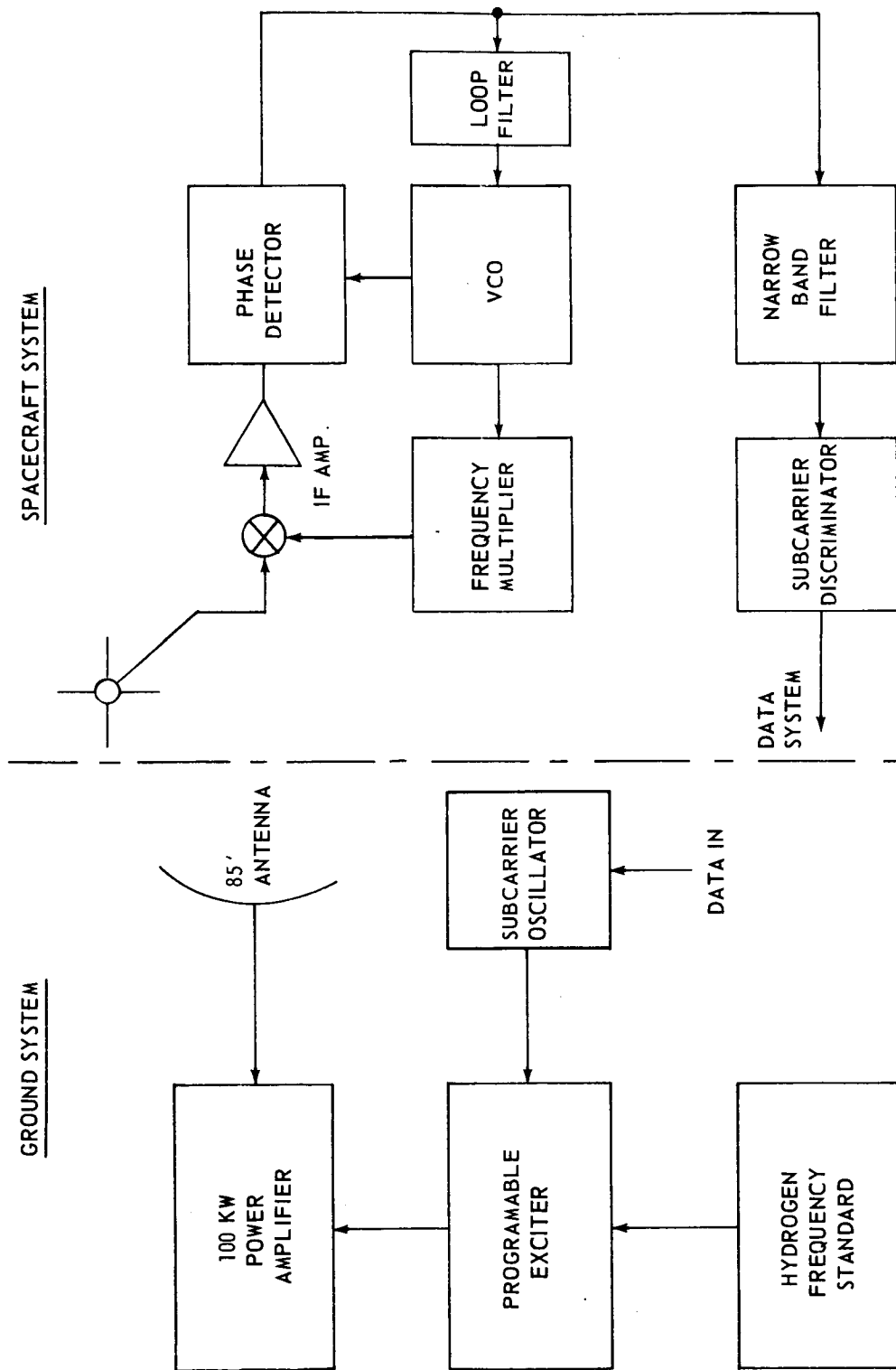


Figure IV-15. Command System

## 2. Exciter Characteristics

The transmitter exciter for the Galactic-Jupiter Probe will coherently synthesize the required transmitter frequencies from the station master frequency standard, the atomic hydrogen maser. The stability of this standard is summarized below (Reference 14).

<u>Averaging Time</u>	<u>RMS Deviation</u>
1 sec	$5 \times 10^{-13}$
10 sec	$1 \times 10^{-13}$
100 sec	$8 \times 10^{-14}$
1000 sec	$6 \times 10^{-14}$
$10^5$ sec (1 day)	$3 \times 10^{-14}$

The absolute resettability of atomic hydrogen standards which employ automatic tuning will be better than 5 parts in  $10^{-13}$ .

The exciter/synthesizer design will be very similar to a multi-band exciter currently under development at GSFC (Reference 15). This design permits discrete frequency steps as small as 0.4 Hz if necessary for continuously programming out the up-Doppler. However, because of the long two way travel times encountered in the Galactic-Jupiter Probe, holding the up-link frequency constant for the duration of a ranging operation or even a day is considered more appropriate, easier to implement, and more accurate than that achievable by continuously varying the up-link frequency. This is due to the fact that the extraction of doppler is accomplished by subtracting the ground transmitter frequency from the transponded received signal frequency. When continuously programming, a method would have to be devised to subtract a frequency which existed in the past. Thus the transit time would have to be known very accurately.

The apparent liabilities associated with holding the frequency constant during a ranging operation are: the VCO in the spacecraft must accommodate a wider frequency range which might reduce its stability, and the spacecraft predetection filter bandwidth must be widened to allow the wider frequency variation to pass. This might cause dynamic range problems in that the relatively wideband noise could overwhelm the signal at the input to the phase detector causing loss of fidelity in the detected signal and product detector drifts that finally obviate lock-up.

Both of these apparent liabilities are, in fact, negligible in their effect on the system operation. The change in Doppler over an entire day's operation is due primarily to the diurnal rotation of the earth which at 2.1 GHz amounts to only about plus and minus 3.5 kHz. Allowing for uncertainties in the spacecraft

circuitry, the spacecraft VCO is still only required to vary about plus and minus 5 kHz. Even very stable crystal controlled oscillators, when referred to the 2 GHz frequency region, do not have their stability degraded beyond a negligible amount when required to be pulled by this amount (Reference 11). Thus the stability of the spacecraft VCO, whether pulled in frequency by 10 Hz or 5 kHz, remains essentially the same.

With respect to the predetection filter bandwidth problem phase-lock-loops can be, and in fact are usually, constructed with a mixer frequency translator in the loop as shown in Figure IV-15. Since the predetection IF strip is now within the loop and follows the incoming signal frequency, a narrow bandpass filter can be employed which virtually eliminates this problem.

### 3. Up-Link Margin Calculations

Assumptions:

Up-link Frequency . . . . .	2.1 GHz
Receiver Noise Figure . . . . .	5 db
Carrier Loop Noise Bandwidth . . . . .	20 Hz
Carrier Loop SNR required in $2B_{10}$ . .	8 db
Receiving Circuit Losses . . . . .	1 db
	1 AU $\rightarrow$ 263 db
Path Loss . . . . .	5 AU $\rightarrow$ 277 db
	10 AU $\rightarrow$ 283 db

For a noise figure of 5 db, the system temperature is 630°K. Therefore the noise power spectral density is -170 dbm per Hz. The results of these assumptions for various system configurations are plotted in Figure IV-16.

This figure shows that the limiting range for reliable command transmission using the 100 KW-85' ground system and the omnidirectional spacecraft antenna is 3.5 AU. The use of 210' antenna with a 100 KW transmitter will extend the useful range of command through the spacecraft omnidirectional antenna to 9 AU. If the spacecraft is oriented so that either the horn or 8' antenna can be used the situation is considerably improved.

### H. Tracking System Performance

Because Doppler frequency, thus range rate, can be measured with extreme accuracy (Reference 16) the trajectory of the Galactic Jupiter Probe will be

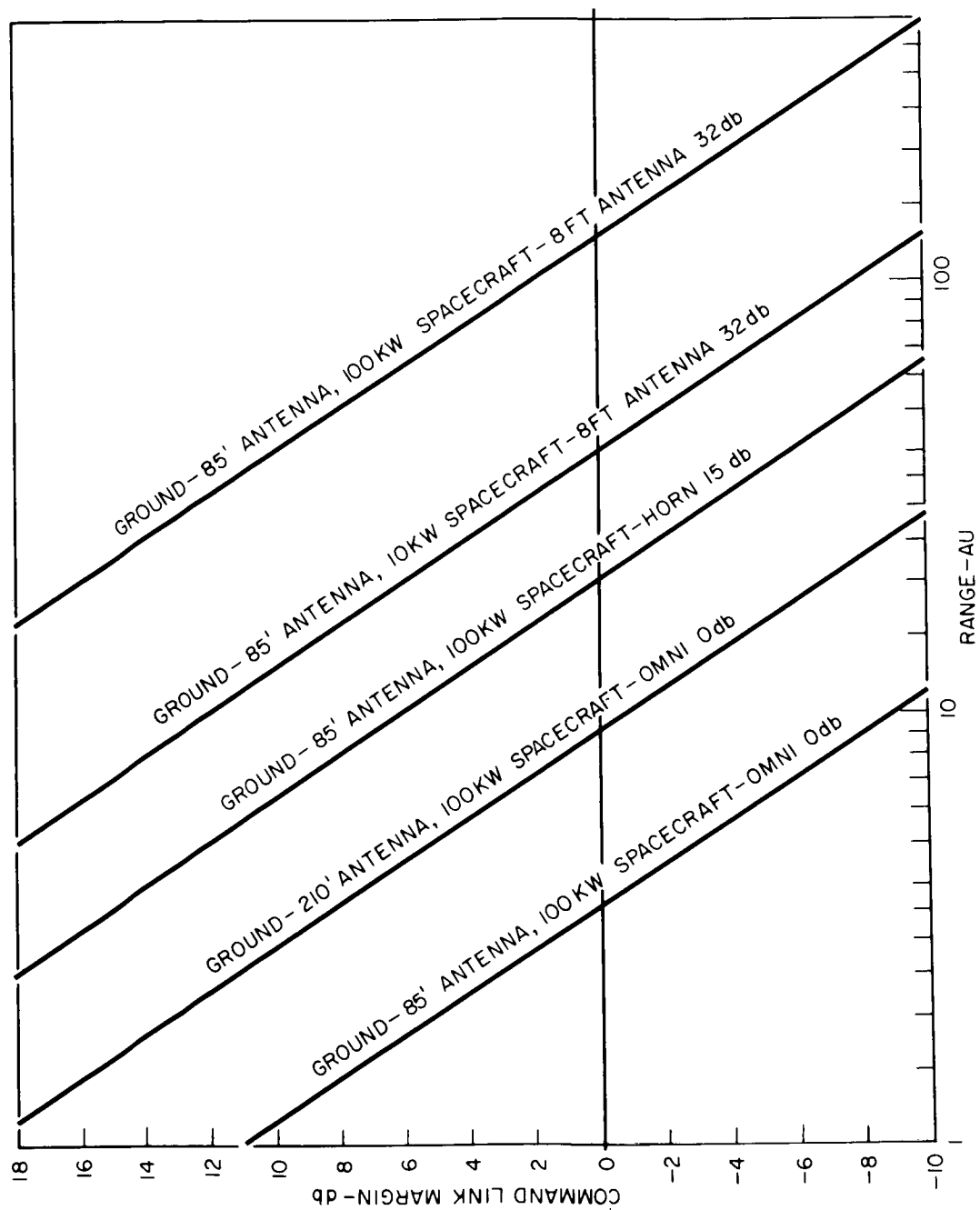


Figure IV-16. Command Link Performance from Various Antenna and Power Combinations

determined by means of two-way range-rate measurements made periodically throughout the life of the probe. Such range-rate systems are used extensively by all three NASA ground networks. The radial range-rate information,  $\dot{r} = dr/dt$ , is obtained through accurate measurements of the Doppler shift on signals transmitted to the spacecraft and back to the ground station. The operation of such systems is well described in the literature (References 17, 18, 19, 20, 21). Briefly, the operation is as follows: a highly frequency-stable signal is transmitted to the spacecraft, received there, off-set in frequency by a specific ratio, (exactly reproducible at the ground site), and then retransmitted to the ground site. The ground receiver amplifies the signal, mixes it with the transmitting signal and adjusts the result by the off-set ratio employed in the spacecraft. The resulting signal has a frequency equal to the two-way Doppler. As shown by B. Kruger (Reference 22), this frequency, for the case where the transmitting antenna coincides with the receiving antenna, is related to the radial range-rate as,

$$\frac{dr}{dt} = \frac{c \frac{\omega_d}{\omega_t}}{2 + \frac{\omega_d}{\omega_t}}$$

where

$\omega_d$  is the two-way Doppler frequency

$\omega_t$  is the transmitting frequency, and

$c$  is the speed of light

### 1. Instrumentation Accuracy Requirements

It is shown in Chapter III, Section B-3 that a limitation in the range-rate accuracy is the relative uncertainty in the speed of light,  $\Delta C/C$ , which is herein assumed to be  $3 \times 10^{-7}$ , (Reference 23). The uncertainty in  $\dot{r}$  pertaining to the assumed uncertainty in the speed of light,  $\Delta c$ , is,

$$\Delta \dot{r} = \dot{r} \frac{\Delta c}{c}$$

where

$\dot{r} \approx 10^6$  cm/sec for that phase of the flight preceding mid-course guidance which imposes the most stringent requirements on the tracking system.

Then

$$\Delta \dot{r} = 10^6 \times 3 \times 10^{-7} \approx 0.3 \text{ cm/sec.}$$

In order to avoid diluting the range-rate determinations further, it is desirable to limit the instrumentation uncertainties to a small part of this uncertainty – say 1/10 as much or 0.03 cm/sec.

## 2. Galactic Jupiter Probe Range-Rate System

To reduce range-rate instrumentation uncertainties for this project to such low values it will be necessary to incorporate new features into the ranging system. These features can be identified by an examination of instrumentation error sources listed as follows:

- (1) Frequency variations of the ground transmissions during signal round trip transit time.
- (2) Additive receiver noise.
- (3) Quantization uncertainties in the Doppler measuring instrumentation.
- (4) Phase noise due to tracking filter cycle skipping.
- (5) Local oscillator noise.
- (6) Phase drifts in the system's receivers.
- (7) Phase changes through the receivers as a function of applied signal frequency variations.

Probably the most important of these error sources is the ground transmitting source frequency variations over the transit time interval.

The frequency stability requirements for the ground signal source can be determined by recognizing that any variation in the frequency of this source during the transit time appears as an error in the Doppler. Since only small variations are involved and  $\omega_d/\omega_t$  is  $\lll 1$ , the range-rate equation can be simplified for the purposes here to:

$$\dot{r} = \frac{C}{2} \frac{\omega_d}{\omega_t}$$

differentiating,

$$2 \frac{\Delta \dot{r}}{C} = \frac{\Delta \omega_d}{\omega_t}$$

but considering the ground signal source stability only,

$$\Delta\omega_d = \Delta\omega_t$$

then

$$2 \frac{\dot{\Delta r}}{c} = \frac{\Delta\omega_t}{\omega_t},$$

which is the fractional stability of the range-rate transmitted signal. Letting

$$\dot{\Delta r} = 0.03 \text{ cm/sec}; \quad \frac{\Delta\omega_t}{\omega_t} = \frac{3 \times 10^{-2}}{3 \times 10^{10}} = 10^{-12}.$$

Such a stability, for the transit times involved, can be supplied only by the hydrogen maser frequency standard (References 24 and 25).

The hydrogen maser will also reduce other system uncertainties. Through synthesis, it is planned to derive all system local oscillators from the hydrogen maser signal source, therefore, oscillator noise will be reduced to a very small value. The system sensitivity is inversely proportional to the bandwidth of the tracking filter which operates on the received signal prior to the counting operation. By exploiting the short term stability of the hydrogen maser, which is significantly better than crystal voltage controlled oscillators, the tracking filter bandwidth can be reduced from the 10 Hz area, presently being used for S-band signals on deep space probes, to a fraction of a Hz.

Quantization uncertainties will be reduced by utilizing nondestructive continuous cycle counting techniques presently being employed in the Apollo and DSN range-rate systems. At present, counting technique in these systems count whole cycles only and ignore the fractional part of a cycle which occurs just prior to the read-out time. A technique developed by D. Curkendall (Reference 26) avoids this quantization error by counting, in addition, a high frequency signal which is gated for the duration of the remaining part of the last cycle counted.

Because of the slowly changing Doppler variations of probes of this type, bias errors due to the phase vs frequency characteristics of the receivers and other instrumentation involved can be reduced to negligible values without undue difficulty.

The instrumentation errors for a proposed Galactic Jupiter Probe range-rate system have been analytically determined. This is the subject matter of GSFC Report X-523-67-386 (Reference 27) to be published. This report shows that, for the measuring intervals allowed by the Galactic Jupiter Probe spacecraft dynamics, the range-rate instrumentation uncertainties can be made small in comparison to the effects resulting from the uncertainty in the speed of light.

#### REFERENCES

1. "Space Tracking and Data Acquisition Network Facilities Report, STADAN," X-530-66-33, Goddard Space Flight Center, Dec. 1965.
2. Potter, Phillip D., JPL - TR - 32-653, The Design of a Very High Power, Very Low Noise Cassegrain Feed System for a Planetary Radar, 8/24/64, Contract NASA 7-100-NASA-CR-58674.
3. JPL Space Programs Summary, The Deep Space Network, No. 37-41, Vol. III, Sept. 1966, p. 86.
4. Johnson, C. C., The Maser Experiment, Proceedings of the Fourth Space Congress, April 1967, Section 16, p. 31.
5. Deep space Station Parameters: Jupiter Flyby Application, EPD-358, May 1966, p. 5-7.
6. JPL Space Programs Summary, The Deep Space Network, No. 37-43, Vol. III, January 1967, p. 1-2.
7. Proceedings of the Apollo Unified S-band Technical Conference, NASA SP-87, Goddard Space Flight Center, 1965.
8. Sos, J. Y. and Saliga, T. V., "A Coded PCM Telemeter for IMPs H I and J," GSFC Memo from Authors to Rochelle, R. W., May 1, 1967.
9. Lindsey, W. C., "Optimum Design of one-way and two-way Coherent Communication Links," National Telemetry Conference Proceedings, May 1966, p. 42-48.
10. Gardner, Floyd M., "Phaselock Techniques," John Wiley and Sons, Inc., New York, 1966, p. 24.
11. Sydnor, R., "Frequency Stability Requirements for Space Communications and Tracking Systems," Feb., 1966, IEEE Proceedings, p. 233.

12. GSFC Progress Report, "Digital Voltage Controlled Oscillator," R&D Quarterly, April 1 to June 30, 1966, Report No. 4, p. 2-4.
13. Recent work with the image enhancement mixer technique shows promise of achieving a 2 db system noise figure at S-Band. See EEE, April 1967, Vol. 15, No. 4 p. 22-30.
14. A. O. McCoubrey, "A Survey of Atomic Frequency Standards," Proceedings of the IEEE, Vol. 54, No. 2, p. 129.
15. GSFC Progress Report "Multiband Transmitter Exciter," R&D Quarterly January 1 to March 31, 1967, Report No. 4, pp. 3-5.
16. Vonbun, F. O., "Space Trajectories and Errors in Time, Frequency, and Tracking Station Location," GSFC X-507-67-163, November 1966.
17. Habib, E., et al, "Development of a Range and Range-Rate Spacecraft Tracking System," NASA TND-2093, June 1964.
18. Kronmiller, G., et al, "The Goddard Range and Range-Rate Tracking System: Concept, Design and Performance," GSFC X-531-65-403, Oct. 1965.
19. Baghdady, E., "High Accuracy Satellite Tracking Systems," Second Quarterly Report, NAS5-1187, Sept. 1961.
20. JPL Technical Report No. 32-694, "Ranger VII Flight Path and Its Determination from Tracking Data," December 15, 1964.
21. Kruger, B., "The Doppler Equation in Range and Range-Rate Measurement," GSFC X-507-65-385, Oct. 1965.
22. *ibid*, P. 5.
23. *Op cit* (16), P. 8.
24. McCoubrey, "A Survey of Atomic Frequency Standards," Proceedings of the IEEE, Vol. 54, No. 2, Feb. 1966, p. 125.
25. Johnson, E. H., T. E. McGunigal, "Hydrogen Maser Frequency Comparison with a Cesium Beam Standard," NASA TN D-3292, April 1966.
26. Curkendall, D. W., To be published in JPL SPS No. 37, Volume III.
27. Simas, V. R., T. E. McGunigal, "A Range-Rate System Appropriate for the Galactic Jupiter Probe," GSFC X-523-67-386.

## V. THE GALACTIC JUPITER PROBE COMMUNICATION AND DATA HANDLING SYSTEM

### A. Introduction

The design of the Galactic Jupiter Probe (GJP) Communications and Data Handling System (C&DHS) is strongly influenced by three factors. They are:

- The 10 Astronomical Unit (AU) communication range
- The minimum mission time of 5 years
- The large number of "unknowns"

The proposed C&DHS design accounts for each of these. The performance characteristics are summarized as follows: A worst case communication capability from the GJP to the earth (using a 210-foot diameter antenna) of 480 bits per second at Jupiter encounter (for an assumed 600-day mission) and of 120 bits per second at 10 AU. 76 bits per second are available through the 85-foot ground antennas at Jupiter encounter. These smaller facilities will carry the GJP through most of its mission while the 210-foot facilities would be used at extreme ranges and during special events such as Jupiter encounter. Command, at the rate of one bit per second, is possible at ranges up to 9 AU utilizing an omnidirectional spacecraft antenna and a 100 KW ground transmitter with a 210-foot dish. On-board data processing will be employed to achieve as much information per bit as possible.

The primary concern of the long mission times is the required spacecraft reliability. The C&DHS design contains enough options and redundancy so that a "few" failures may occur and still allow most of the data to get through. "Single point" failures that can completely disable the system are held to an absolute minimum. It is recognized that in a complex system, some failures may occur in a period of five years.

The "unknowns" referred to above are of two kinds. First are those related to the uncharted environments such as Jupiter radiation belts and the asteroid hazard. The other kind is associated with random failures or degradations in other spacecraft equipment. For instance, the communications capacity devoted to a degraded experiment could be increased or decreased depending on the situation. This requires the ability to optimally reassign communication capacity to all communications users to minimize the effect of a degraded experiment or other equipment on the overall mission.

The various subsystems that make up the C&DHS System are covered in detail in the following sections. The communication subsystems are taken up first.

These include the antennas, the design of the command or up-link, the design of the data or down-link and the data coding used with these links to improve communications fidelity. The Data Handling Subsystems are taken up next and these include on-board data processing, storage, and formatting and the ground data reduction. The significant improvement in information per bit through on-board processing is also discussed. Two related functions that also use the communications links are then discussed. These are the tracking function and spacecraft spin axis orientation determination function.

The breakdown of the C&DHS into these smaller pieces is primarily for clarity of presentation. The philosophy of the design is to unify as many subsystems as possible so that maximum usage of all hardware, both spacecraft and ground, may be achieved. A natural byproduct of this approach is a system with multimission capability and consequently a lower cost per mission.

Figure V-1 is a simplified block diagram of the spacecraft-ground C&DHS. This may be folded out for reference throughout the system discussion.

## B. Communications System

The communications system is comprised of two radio frequency links in the 2100 to 2300 GHz (S-band) region. The link from the ground to the spacecraft is the command or up-link. The link from the spacecraft to the ground is called the data or down-link. Each link is comprised of an encoding device, a transmitter, a transmitting antenna, a receiving antenna, a receiver and a decoding and error checking device. The generation of actual spacecraft data to be sent over the down-link and the commands to be sent over the up-link are discussed in detail in the section on Data Handling.

The prime function of the communication links is to transfer information (bits) both ways between the GJP and the Earth with a low number of errors.

The command or up-link will be covered first followed by the data or down-link. The tracking function and the spacecraft spin orientation use of these links are covered in a later section.

### 1. Command or Up-Link

The S-band link is used to control the functioning of the spacecraft. The GJP is a spinning vehicle whose spin axis is oriented towards the earth. A high gain dish (32 db) and a medium gain horn (15 db) are both oriented along this spin axis. An omnidirectional antenna system is also included, which permits the entry of commands should the spin axis not be aligned towards the earth.



Figure V-1. Block Diagram of the Spacecraft-Ground Communication and Data Handling System

When using a 100 k watt transmitter and 210-foot dish, commands may be entered over the omnidirectional antenna out to a distance of about 9 AU. If the earth is within the beam of the horn, beamwidth of 12 degrees, command reception to a range of about 50 AU may be accomplished. Command reception beyond this range requires that the GJP be aimed at the earth to within about 2 degrees so that the high gain antenna may be used. The equivalent ranges using a 100 k watt transmitter and the 85-foot dish facility are: 3.5 AU for the omnidirectional antenna; 20 AU for the horn; and 126 AU for the high gain dish (8-foot diameter).

The command message is first encoded with suitable error detecting bits. This is done so that the spacecraft will not accept or act upon a command message which contains detectable errors. This message, at the coded bit rate of two bits per second, is modulated onto a subcarrier at approximately 10 kHz which in turn phase modulates the S-band transmitter. The degree of phase modulation is chosen so that approximately equal power is given to the carrier and to the sidebands (50 k watts each for a 100 k watt transmitter). This power is aimed at the spacecraft by either an 85-foot or 210-foot parabolic dish antenna.

On-board the spacecraft, a phase lock receiver is connected to each antenna (omnidirectional, horn and 8-foot dish) and logic scheme is used to pick the receiver with the best received signal to noise ratio. This receiver's output is fed to a subcarrier detector. This is followed by an error check circuit and, if it passes the check, the command is entered into the command system and acted upon.

- a. Encoding - Bit encoding is applied to the command bit stream so that errors may be detected on board the spacecraft. The encoding consists of simply sending the command followed by the complement of the command. A bit-by-bit error check is performed on-board. This technique is about the simplest to implement in the spacecraft and provides nearly perfect detection of errors. It catches every single bit error (all odd number of errors) and it catches 97.3 percent of all double errors if the command word is 18 bits long and 98.6 percent of all double errors if the command word is 36 bits long. The most useful length for command words has not yet been determined, but it will fall in the range of 18 to 36 bits. The one bit per second rate referred to elsewhere in this study is the actual usable command message rate. The coded command message rate is a two bit per second bit stream since after coding, two bits are transmitted for every bit of the command message.
- b. Modulation-Subcarrier - The command message must be placed onto a subcarrier. The bit rate is so low that modulation sidebands would

interfere with the spacecraft receiver's phase lock loop if the data directly modulated the carrier. A frequency shift keying (FSK) subcarrier modulation was chosen since this is very simply detected on-board the spacecraft. A phase shift keying (PSK) technique could be used, but this would require another phase lock loop circuit. This more complex (and efficient) detector could certainly be implemented, but only if the higher bit rate of 4 bits per second was determined to be necessary.

- c. Modulation-Carrier - The S-band ground transmitter is phase modulated by the FSK subcarrier modulation. The total modulation system may then be described as PCM/FSK/PM.

The PM carrier modulation was picked since the phase lock spacecraft receiver has near optimum performance for this mission and because the phase lock receiver is needed for range rate tracking. Both AM and FM could be used, but each have drawbacks which make them less suitable than PM. AM would be disturbed by any irregularities in the spinning spacecraft antenna pattern since that would also produce an AM modulation on the received signal. Both PM and FM are essentially insensitive to this effect, but FM has an earlier threshold which severely limits its effectiveness at extreme ranges.

- d. Transmitter - The command link analysis below indicates that a 100 k watt transmitter is needed at both the 85 foot and the 210 foot dish sites. Under normal spacecraft operating conditions and with the earth in the beam of the horn spacecraft antenna, the 85 foot dish sites will be able to command out to a range of almost 20 AU. The 210 foot dish site under the same conditions can go out to about 50 AU. Under abnormal spacecraft conditions, such as a gross misorientation of the spacecraft with respect to the earth, the 85 foot sites can still command through the omnidirectional spacecraft system at ranges of about 3.5 AU and the 210 foot dishes at ranges up to 9 AU. This capability is considered essential since, with a few commands under such unfavorable aspect angles, one could "steer" the GJP from the ground to correct the misorientation and possibly save the mission.

- e. Spacecraft Receivers - In order to reliably service all of the spacecraft antennas, a phase locked receiver is connected to each. A "lock-unlocked" signal is available from each receiver as well as an analog voltage to indicate its signal to noise ratio. A simple decision circuit turns the command decoder circuits on if any receiver indicates it is phased locked and routes it to the command decoder. Under normal conditions, several receivers may lock up. In that situation, the "best" receiver is picked for command processing. Each receiver has a noise temperature

of 5 db. Six (6) db was used in the calculations to allow for some degradation. A loop bandwidth of 25 Hz was assumed for purposes of calculating receiver threshold ranges. Six (6) db noise figure is presently obtainable using a transistor device. Other flight preamplifiers are under development using other techniques, but in general they each require more power. A 2.5 db noise figure can be obtained with an uncooled paramp but with an additional power consumption of 4 watts. All threshold ranges quoted for the command system could be multiplied by a factor of 1.7 if such a low noise preamplifier were used.

- f. Subcarrier Detectors - The best receiver output is gated into a redundant pair of subcarrier detectors. Except for the low bit rate, the detection technique is the same as used in the OGO spacecraft. While this type of detector is 6 db from perfect PCM performance, it is very simple to implement using two narrow filters to detect the two transmitted subcarrier frequencies. The OGO scheme has a sinewave at the bit rate modulating (AM) the subcarrier. This clock signal takes only a small fraction of the available sideband power and saves considerable decoder complexity.

If a more optimum system were built, such as a phase locked detector, the command rate could be increased from one (1) bit per second to 4 bits per second. Alternatively, one could stay at one bit per second and put slightly more power into the S-band carrier. The threshold of the spacecraft receiver's phase lock loop is the limiting factor in the system. Note, however, that if all the power were put into the carrier, the range at which one could get phase lock would increase only 40 percent.

- g. Command Coding Check - The output of the subcarrier detector is clocked into a shift register that is one bit longer than the command in length. As the second word or the command pair is clocked into the register, it is compared bit-by-bit to the first word and as long as the second word is an exact complement of the first word, the command is accepted. Any disagreement is grounds for rejection and a notification of rejection is transmitted to the ground. The ground then retransmits this word to the spacecraft. The need for retransmission should be quite infrequent since even at spacecraft receiver threshold, only one bit in a million will be decoded incorrectly.
- h. Decoding - After the word passes the error check, it is partially decoded to determine if it is to be acted upon immediately (real time command) or if it is to be read into command storage for future execution (stored command). If it is a real time command, it is further decoded to

determine if it is to be decoded by the spacecraft decoder (discrete command), or if it is to be used on a binary number by another piece of spacecraft equipment (proportional command). There are up to 64 "on-off" functions that are decoded by the spacecraft and used for such functions as controlling power to spacecraft equipment or switching between redundant equipment. Each function requires two discrete commands.

The proportional commands are routed to the appropriate user equipment as a binary number. The user equipment then decodes the number as appropriate. This "proportional" feature allows for wide variation (mission-to-mission) in the control complexity without causing a similar wide variation in spacecraft decoding equipment complexity. The extra complexity is only built into the equipment that needs it.

The stored commands are acted upon at the spacecraft time specified along with the command. Any of the command functions both discrete and proportional may be stored for delayed execution. One use for these commands is during periods of time when the ground stations are not in contact with the spacecraft. Another use is when it is desired to have several functions executed simultaneously. At one bit per second, about 3-1/3 commands per minute may be received and executed. By specifying the same future time with several commands, all would be executed together. Beside the simultaneous capability, a complex sequence may be stored and verified as correct prior to execution. Because of the round trip delay of 16 minutes per AU of range, it is impractical to send one command at a time and require verification prior to sending the next command. Memory capacity for about two hundred commands is planned.

The command decoder and error check circuits are small units. A pair of units will weigh less than 0.5 pound and consume less than 0.5 watt total. The units are turned on only when at least one receiver is in phase lock.

- i. Command Operation - When it is desired to send a command to the GJP, the 100 k watt transmitter is turned on and the ground antenna aimed at the probe. The carrier is not modulated and its frequency is slowly swept  $\pm 5$  Kc around a calculated center frequency. The calculated frequency accounts for the relative motion between the probe and the transmitting antenna (Doppler) so that the spacecraft receiver(s) will be able to lock up properly. The round trip communication time per AU is about 16 minutes. During the early phases of the mission one would not start sending a command message until the telemetry data from the probe indicated receiver lock up. At long ranges, it might be required that the

command message be started after sweeping the transmitter frequency a few times but before obtaining confirmation over the telemetry link of spacecraft receiver lock up. The time required to achieve lock up would be known with a degree of certainty from prior experience and "blind" operation should not present any unusual complications. The subcarrier modulation was chosen in the 10 kHz range for two reasons. First, it is far enough away from the carrier so as to prevent the receiver from locking up on this sideband. Secondly, it allows for good range data without compromising the command function. The use of the command subcarrier for range data is discussed in Section V-C.

## 2. Data or Down-Link

This S-band link is used to return Spacecraft and Scientific data from the GJP to the Earth. The Data Handling system which processes this data is discussed in Section V-D.

The down-link consists of a data encoder, a transmitter, a spacecraft antenna system, a ground antenna, a receiver, and a decoder. The object of the down-link is to produce at the output of the ground decoder a faithful replica of the data that was generated by the spacecraft data handling equipment. Another use for the link is to complete the two way tracking link. Tracking is covered in detail in Section V-C.

- a. Link Performance - The GJP has "limited" power capability, so the down-link transmitter is only a ten watt unit. This low power is partially made up by the very low noise ground receiving system, efficient coding-decoding schemes (6 db gain) and optimum modulation techniques. The Figure V-2 shows "worst case" link performance as a function of range and antenna combination. It is seen that at Jupiter encounter (for an assumed 600-day mission) using the 8-foot spacecraft antenna and the 210-foot dish a bit rate of 480 bits per second is possible. 76 bits per second is available using the 85 foot dish at that range. It is also seen that the other spacecraft antennas are effective only at ranges less than 3 AU. Therefore the 8-foot dish must be used to receive data from Jupiter distance and beyond. The use of the up-link with an RF interferometer on the spacecraft and various other aspect sensors allow this accurate ( $\pm 2^\circ$ ) orientation. The interferometer aspect sensors are described in Appendix A.
- b. Spacecraft Transmitter - Power Amplifier - It is imperative that the transmitter be as efficient and reliable as possible. It is the largest DC power load in the spacecraft (50 watts nominal). The proposed technique is to use solid state amplifiers in all stages (including the final) and to

Figure V-2. Telemetry Link Performance with Various Antenna Combinations

have standby transmitters built in. Figure V-3 is a block diagram of this transmitter. Each of the 4 power amplifiers will contribute 5 watts to the S-band output whenever its DC power is turned on. Thus, the rated 10 watt transmitter power may be obtained with any two transmitters on and the other two in a standby condition. If just one 5 watt transmitter is on, only 30 watts of DC power is required and operations could be carried on with 1/2 data rate. This mode could be supported even if one RTG failed. Conversely, with both RTG's operating and all power amplifiers operating, the transmitter would achieve a 20 watt output. This requires about 85 DC watts and would require turning off some of the other

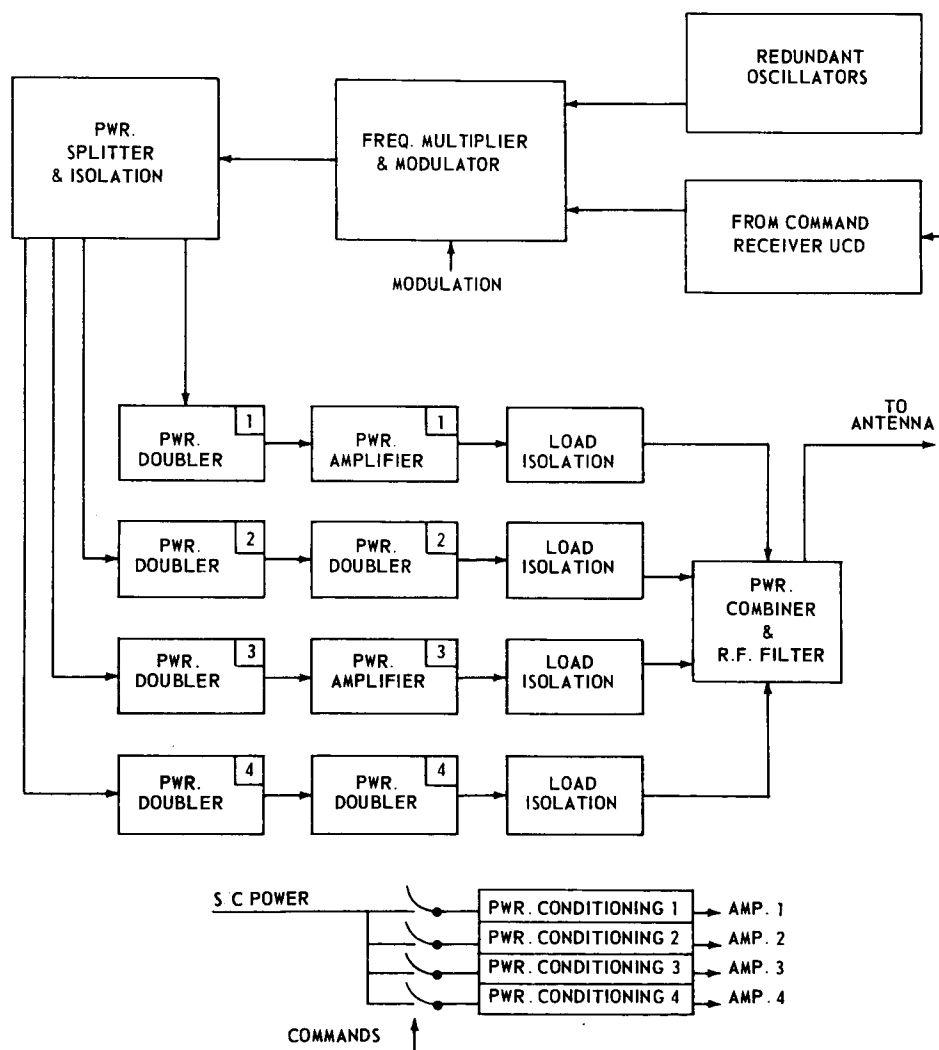


Figure V-3. Block Diagram of Spacecraft Transmitter

spacecraft loads. It would also at least double the possible bit rate. A 20 watt transmitter extends the spacecraft to earth range for a given bit rate by 41 percent. This adjustable RF power output concept allows one to optimize spacecraft operations to get maximum data return.

The power consumption figures include DC to DC conversion losses and are based on a newly developed transistor (RCA type TA 2751) operating at one half the output frequency and then power doubling with a varactor diode to S-band. However, if a transistor that operates directly at S-band that is now under development (NAS 5-10066) should become available in time, the DC to RF efficiency of the transmitter using this device will be better than for the TA 2751 with a varactor. Since this device is still under development, mission feasibility using the existing TA 2751 was proposed for this study demonstration since a suitable transmitter for GJP could indeed be built using this device at the DC power consumptions quoted. Other S-band amplifiers that might be considered use the various vacuum tubes of which the TWT is the best candidate. TWT's have been flown in spacecraft with success, but they require high voltage power converters (1 to 2 K volts), use an electrically heated filament which has a "wearout" mechanism, and have a magnetic problem. The magnetically clean TWT is possible, but its magnetic shielding weight and the extra weight of the high voltage power converter is expected to be at least double the solid state power amplifier weight (8 pounds versus 4 pounds).

- c. Antenna Switching - Solid state RF power switches will be used to feed the transmitter to one of the three spacecraft antenna systems. During launch and prior to spin axis orientation, the omnidirectional system is used. After a coarse orientation of the spacecraft toward the earth, the medium gain horn antenna will be used. When the spacecraft is aligned to within two degrees of the earth, the high gain dish may be used.
- d. Transmitter Modulation - Phase Shift Keying (PSK) modulation is used for this transmitter since near theoretically optimum results may be obtained with this technique. An unmodulated carrier is also available. Since the carrier is completely suppressed (-30 db down) all the transmitter power is available for transmission of information. The PSK approach has two major advantages over other modulation techniques. The first is the higher data rate possible - in some cases as much as a factor of two over conventional PM approaches. The other is that the data is modulated directly on the carrier. This means that a subcarrier is not needed and any losses due to the demodulation of the subcarrier are not incurred. A ground receiver that operates with suppressed carrier is being developed.

The unmodulated carrier is also available. This will be used as an aid in acquiring receiver lock up when in a PM mode and may also be used when tracking (Doppler) measurements are being performed.

Although the theory for the performance of PSK has been published several years ago (Reference 1), it has not been implemented in the STADAN or DSIF. The demonstration of near theoretical performance for PSK with actual hardware has not yet been accomplished. It is anticipated that such actual demonstrations will occur during Phase B study for this mission. It must be emphasized that should such techniques not work, the mission can still rely on the normal phase modulation (PM) techniques presently used in both networks. The performance of various PM modulation indices is also shown in the Figure V-2. Appendix B gives an analysis of the PSK and other PM modulation and demodulation techniques.

- e. Transmitter Oscillator - The frequency source for the transmitter is a redundant pair of crystal oscillators contained within a proportional oven isolated by vacuum and aluminized mylar film from the spacecraft thermal environment. This isolation technique requires very little oven power and has been successfully used on the GEOS, Anna, and other satellites. A long term stability of one part in  $10^8$  per day is realized. This represents an aging factor of 8 kHz per year at 2300 MHz. The oven's thermal stability is better than  $\pm 1^\circ\text{C}$ . In order to achieve two-way doppler tracking and also to achieve better short term frequency stability for the down-link, an interconnection between the command receiver's VCO and the transmitter is provided. This feature may be selected or locked out by command. The up-link has the spectral purity of a hydrogen maser and, with sufficient signal to noise in the spacecraft receiver tracking loop, the VCO can achieve comparable stabilities. A smooth switch over from the crystal oscillator to the VCO is achieved as follows: After a spacecraft receiver locks up, the VCO frequency is compared to the crystal frequency using a phase detector. When the two frequencies are very nearly the same, the switch over is made. (The VCO will be following the slow frequency sweep of the up-link and will pass through the down-link crystal oscillator frequency.) This technique will allow the ground receivers to remain in lock through the transfer. When spacecraft phase lock is lost, the transmitter reverts to the crystal oscillator. This will give a frequency discontinuity, which will require reacquiring phase lock. Normally, however, the spacecraft is no longer in ground contact and in this case, the frequency transition is of no consequence. The use of the spacecraft receiver VCO for the down-link frequency source serves two purposes. First, it completes the two-way Doppler signals needed for range rate measurements and second, it

assures that 4 Hz ground receiver loop bandwidths may be used. Loop bandwidths are presently limited by transmitter crystal oscillator stability to about 12 Hz.

The stability of the spacecraft receiver VCO when used for control of the down-link transmitter frequency will be almost as good as the ground transmitter source (hydrogen maser) stability. The noise contribution to the VCO instability will be very small since the spacecraft receiver phase lock loop signal to noise ratio is at least 18 db better than the ground receiver phase lock loop signal to noise ratio. This may be shown by noting that the differences between the up and down links are: (1)  $\pm 10$  db due to transmitter power, (2) -11 db due to system temperature differences, (3) -8 db due to phase locked loop bandwidth differences, and (4) -3 db since the up-link may be modulated with command while the PSK receiver uses all the down-link power. All other parameters are virtually the same for both the up and the down links since the antennas used at each end are common and spacecraft pointing errors are also common. If the ground receiver is at phase lock loop threshold (9 db), then the spacecraft receiver's signal to noise ratio is 27 db. The rms phase error associated with a phase lock loop operating at a signal to noise ratio of 27 db is .032 radians. When this small error is added to the extremely small error of the up-link hydrogen maser stabilized transmitter frequency, it is seen that a 4 Hz ground receiver phase lock loop bandwidth is feasible. It is quite possible that the 4 Hz loop bandwidth can be extended downward by the time GJP flies, but for purposes of this study, 4 Hz was used as the lowest loop bandwidth for the ground receiver phase lock loop and all threshold versus range calculations are based on this bandwidth.

- f. Ground R.F. System - The ground end of the down-link is composed of a large aperture antenna (either 85 foot or 210 foot) each equipped with a low noise maser amplifier (see Chapter IV). The antennas are pointed using computed spacecraft position (drive tape mode) and polarization diversity is used. A communication link analysis at 5 AU is shown in Figure V-4 and a bit rate versus range is shown in Figure V-2 for both the 85 foot and 210 foot dishes in combination with the three spacecraft antenna systems. Note that a -7.9 db tolerance is included in these curves thereby giving a worst case picture.

PSK/PM receivers will be installed at each GJP receiving site. The primary difference between these receivers and our present receivers will be in the very high frequency stability required. The PSK feature is of nominal cost over the cost of a PM receiver. Both PM and PSK will be provided since a PSK receiver may easily be switched into a normal

Link Parameters:		Nominal Case		Tolerance		Worst Case	
Transmitter Power	10 W	40 dbm				40 dbm	
Antenna Gain	8'D	32.6 db		-1.0 db		31.6 db	
Cable Losses		- 1.5 db		-0.5		- 2.0 db	
Aperture Blockage		- 0.5 db		-		- 0.5 db	
Trans. Atn. Pointing Loss		- 1.0 db		-2.0 db		- 3.0 db	
Path Loss	5 AU	277.6 db		-		277.6 db	
Receiving Ant. Gain	85' D.	53 db		-1.0 db		52 db	
Receiving Ant. Pointing Loss		0 db				-	
Polarization Loss		0 db				-	
Receiving Sys. R.F. Losses			(Included In System Temperature)				
Received Signal Power		-155 dbm				-159.5 dbm	
Noise Spectral Density	$T_{sys} = 25^{\circ} K$	-184.6 dbm	$55^{\circ} K$	-3.4 db		-181.2 dbm	
Modulation Loss		0				0	
Detection Losses		- 1.0 db		0		- 1.0 db	
S/No Received		28.6 db				20.7 db	
ST/No Required for Uncoded $P_e = 2 \times 10^{-4}$		8 db				8 db	
Bit Rate Capability, Uncoded		115 b/s				18.6 b/s	
Coding Gain (Conv./Seq., $n = 2$ )		6.1 db				6.1 db	
Bit Rate Capability, Coded		470 b/s				76 b/s	
Modulation Loss		0 db				0	
Filtering Loss		1.0 db				1.0 db	
Available Loop Signal Power		-156 dbm				-160.5 dbm	
Loop Noise Power ( $B_n = 2 BL = 4 Hz$ )		-176.8 dbm				-173.4 dbm	
S/N In Loop		20.8 db				12.9 db	
S/N Loop Threshold		9.0 db				9.0 db	
Loop Margin		11.8 db				3.9 db	
Value tolerance:						-7.9 db	

Figure V-4. Telemetry Link Performance At Jupiter Mean Distance (5AU) PCM/PSK (NRZ), Coded ( $n = 2$ )  $\beta = \pm 90^{\circ}$

PM mode. Thus this receiver will be able to handle any type of phase modulation for any other mission.

- g. Down-Link Data Coding and Decoding - It is proposed to improve the data transmission capability by at least a factor of 4 (6 db) by convolutional coding of the data prior to transmission and then optimally decoding after reception on the ground. The key to this coding and decoding is that the received noise is integrated over many information bits rather than just over one bit time. This type of coding has been demonstrated at Ames Research Center and may be implemented for future Pioneers. If used on these missions, one would be insured of operational use of this type of coding prior to the GJP mission. In the Ames demonstration equipment, the decoding is performed using a small general purpose computer. It is proposed that a small computer be installed at each GJP site to perform this decoding function. This is judged to be a small cost compared to achieving 6 db system improvement in any other way.
- h. Ground Communications - It is planned that a GSFC control center will be in two-way real time contact with each ground receiving terminal (see Chapter VI). This capability presently exists at all sites considered for this mission. These links use various error checking and correcting techniques and virtually error free data is now transmitted. This will be the prime method of communicating data between GSFC and a remote site. It will be backed up by magnetic tape recordings sent through the mails. This is the reverse of our normal data handling methods, but is justified by the need for rapid response. One cannot wait weeks to find out the spacecraft is not functioning as desired and then acting. One actually would like to have instantaneous ground data processing and decision making, since the long round trip communications time (16 minutes per AU) already severely limits ones ability to give rapid response.

The ground data links will also be used when it is necessary to back up the remote computer for coding detection. This could be done in one medium sized computer located at GSFC but it would require a higher (at least a factor of 10) communication data rate from the station to the GSFC. At the highest spacecraft bit rates, this capability is not presently available for real time communications. When the capacity becomes available, it may be more economical to eliminate the field computers.

### C. Tracking Function

Both range and range rate are provided for tracking the GJP. Range rate is achieved by using a two-way Doppler technique. The spacecraft transmitter

frequency may be controlled by the spacecraft receiver VCO. Thus by comparing the transmitted up-link frequency to the received down-link frequency, one can extract the relative velocity between the probe and the ground antenna. This two-way Doppler measurement is available at all times simultaneously with up-link command and down-link data transmission.

Ranging accurate to  $\pm 150$  meters rms due to instrumentation error is available by substituting the output of the spacecraft receivers for the normal down-link telemetry data. The up-link is then modulated with various range tones one at a time. These modulation tones are varied in such a way that all ambiguity may be resolved down to the cycle of the highest frequency, in this case 10 kHz. The phase of this frequency is then determined to about  $\pm 1\%$  accuracy or, at 10 kHz, about  $\pm 1$  microsecond round trip delay period. This is an accuracy of  $\pm 300$  meters in two-way range or  $\pm 150$  meters in range.

The technique presented allows virtually any type of modulation to be returned to the ground for range determination. In this way techniques other than the proposed multitone approach may be used without changing spacecraft hardware.

Note that this range function is achieved with very little complication on the spacecraft. The ground phase lock loops are straightforward and are similar to the devices used with the Goddard Range and Range Rate. When the spacecraft is close to the Earth, it is expected that even better performance can be achieved since the signal to noise will be considerably improved. The range limitation under these conditions will be the various bias errors estimated to total about 20-30 meters.

No down-link telemetry will be possible while the range data is being transmitted. Note that after a few good range measurements are obtained at the beginning of a pass, range rate may be continuously integrated to update the range measurement. Tracking is of prime importance early in the mission to determine the midcourse correction needed and to verify the midcourse maneuver performance. Accurate tracking in the vicinity of Jupiter is also needed to satisfy various scientific requirements such as improving the accuracy of the Jupiter Ephemeris and the accuracy of the mass of Jupiter itself.

#### D. Data Handling System

##### 1. Introduction and Functional Description

The GJP mission is not a static mission, but one which has various phases superimposed on a decreasing communication capability. The spacecraft data handling must be performed in a manner that maximizes the scientific return

with a "reasonable" amount of electronics on-board. Analysis and experience indicate that three small programmable processors (2 on standby) implemented with large scale integrated circuits (LSI) will provide a reliable implementation for the five year mission. Some data storage ( $\sim 450$  K bits) is provided so that continuous data coverage may be obtained even when the probe is not in contact with the ground. In addition, a simple hard wired multiplexer and A to D unit is provided to backup the programmable units. This will provide less than the optimum on-board data system, but will allow some data recovery should all else fail.

- a. Examples of Processing Gains - The objective of the on-board processing of data is to maximize the information content of the bits that are communicated to the ground. It is estimated that through a variety of processing techniques, at least a ten to one (10 db) improvement in information sent over the channel may be realized. Some of these techniques are illustrated below.

- (1) Logarithmic Compression

Logarithmic representation is very useful in handling wide dynamic range measurements to a fixed accuracy. Thus a 22 bit accumulator register may be represented to 1% accuracy with an 11 bit number. This is a 3 db savings.

- (2) Spin-Related Data

Spin-related data functions are quite amenable to processing. For instance, if the detector is directional, perhaps only the maximum and/or minimum or some other statistical description is more meaningful than many raw data points. Also the spacecraft detector may scan over a detectional source and send only that data back. It might also be desirable to "build up" a sample through an integration process over several spin cycles. Each instance cited could result in a 10 db reduction in the number of bits required to describe the measured phenomenon.

- (3) Pulse Height Spectrum

More extensive processing than any of the above illustrations holds the promise of still greater data rate reductions. An illustration of this would be the on-board construction of a pulse height spectrum. Present techniques would encode each pulse event into, say, 256 (8 bit accurate) pulse heights and then transmit each sample to the ground. If 16,000 consecutive pulses were taken

and a spectrum generated (that is a histogram of the number of pulses in each of 256 possible heights) a minimum of 128,000 bits would be processed. (In actual practice, a larger number of bits are required because the telemetry must sample at a high enough rate so as to not miss too many pulses. Thus at the highest data pulse rates, some pulses are missed while at low data pulse rates, many zeros will be transmitted.) The spectrum may be represented by 256 nine (9) bit numbers or only 2304 bits. If generated on-board the spacecraft, almost no events need be missed and the meaningless zeros are simply not counted. The ratio of 128,000 to 2304 is better than 17 db.

The key to on-board processing is to eliminate that information that does not interest the experimenter and transmit only that information that matters. Thus when a series of zeros are transmitted in today's systems, it tells the experimenter that nothing was happening. This is useful information, but is not what he wants to base a paper on. When each pulse height is transmitted, it not only tells of a given pulse's height, but also tells the time sequence in which the various pulses occurred. This time sequence is lost in producing a histogram, but if a histogram is to be the end product anyway, the time history is unimportant and this information may be eliminated.

## 2. Spacecraft Services

In order to make the most use of the experiments, several spacecraft services are provided. These are used by the experiments and other spacecraft equipment and include: spacecraft time, spin angle, a programmable processor, a memory bank and a command processor. Each of these are discussed in a section below.

- a. Spacecraft Time - This is an eighteen bit word which is incremented every 4 seconds and thus takes about 12 days to recycle. This clock is used for normal sequencing and programming functions and is fine enough for most time related functions. Finer resolution of spacecraft time as well as accurate frequencies are available in the clock unit and will be provided to users as required. A drift rate of less than one part in  $10^8$  is possible by using the transmitter temperature controlled crystal oscillator and this results in about a one second error in 1200 days.
- b. Spin Angle Determination - A signal from the attitude control system will be used to generate a 9 bit number which indicates spin phase angle to  $0.75^\circ$  (480 increments). This allows convenient look angle determination for pointed or directional experiments and allows them to take

advantage of the spacecraft spinning motion to effect a scan over some specified portion of the heavens. The phasing and period of the spin will be accurately determined (on-board) in terms of spacecraft time and thus one may relate measurements in one time frame to measurements in the other. Attitude maneuvers, solar light torques, magnetic eddy current damping and micrometeor impacts will all act to change the spin rate. These effects may be quite small, but the spin rate stability will probably be several orders of magnitude below the spacecraft clock. The correlation between the spin and spacecraft clock will be made frequently.

- c. Programmable Processor - It is proposed to implement the spacecraft processor in as flexible method as possible within the major constraint of achieving high reliability. It is anticipated that all logic will be constructed of Large Scale Integrated (LSI) bipolar circuits which will afford a high degree of reliability coupled with very small size and low weight. The extent of complexity that is desirable has not yet been determined, but as a minimum, the multiplexers will be programmable, the bit rate may be varied in discrete steps and certain data manipulation functions may be performed. These items are discussed below.

The data formats may be programmed (and reprogrammed) by loading commands into particular memory locations. Up to six formats are tentatively proposed and a single command will select the format to be used. The reprogramming feature will allow the processor to ignore a failed sensor or to concentrate on some especially interesting unexpected phenomenon to the exclusion of other functions or to emphasize the Jupiter experiments near Jupiter and to de-emphasize them when in interplanetary space. It is necessary to have several selectable modes for the efficient command change from one format to another. It is not desired to reprogram the formats any more than that necessary to accommodate unanticipated conditions. If everything were exactly as predicted, no reprogramming would be needed - only format selection.

In order to maximize the data return, selectable bit rates which nearly match the available communication capability are required. Except for periods of particular interest, the spacecraft will not be in continuous communication with a ground station. This is particularly true after several GJP spacecraft have been launched and are on their way to Jupiter and beyond. It is expected that continuous coverage will still be obtained by storing the data on-board for future playback. The ground large dish sites would then dump the on-board storage from each spacecraft at its prevailing maximum bit rate and would take real time data as contact time allowed. During periods of special interest, the large 210 foot dishes would be used as necessary to supplement the 85 foot dish

coverage. Sixteen bit rates covering the range from one to 4096 bits per second are proposed. At the very low bit rates, 1.5 db steps are used. At high rates, 3 db steps are used and the last step is 9 db. The highest rate is used during spacecraft checkout and for the near Earth phases of the mission. The very lowest rates are used at the most extreme ranges. The bulk of the mission will be handled by the intermediate bit rates.

- d. Data Manipulation - It is proposed that certain simple data manipulation functions be implemented as part of the data processor. This would include such things as scaling, logarithmic compression, integration and comparison. The use of these functions would be called up by the multiplexer program as subroutines associated with the various experimenter data samples.
- e. Memory - A plated wire memory of 442,368 bits capacity is proposed for data storage on-board the spacecraft. After setting aside storage capacity for format control, delayed command storage (described in the next section) and for experiment subroutine programs, about 400,000 bits remain for data storage. This permits storing at an average rate of 28 bits per second over a four hour period. Two stations on opposite sides of the Earth each would have about an eight hour contact time with a spacecraft and the four hour period between contacts would go into data storage. If part of the eight hour real time contact were not available because the station was tied up on a second GJP for instance, then proportionally fewer bits per second could be accommodated.

The memory unit proposed is similar to one now under development (NAS 5-10077) and would actually be three 8192 by 18 bit word randomly addressed memory units. The present total size, weight and power consumption for the three units is 486 cubic inches, 20 pounds and less than one watt respectively. It is anticipated that future versions of this memory will be somewhat lighter.

Besides the operational flexibility afforded by the on-board storage, certain other advantages are apparent. There will be periods when the spacecraft is occulted by the Sun or by Jupiter and no ground station will be able to get real time data from the probe. Another possible use is to insure some data return in spite of a spacecraft power system degradation. The transmitter (the largest single power consumer) could be turned off and the experiments would load data into storage. Then the experiments would be turned off and the transmitter turned on to unload the data storage. This flexibility, although complex in itself, actually boosts

the overall spacecraft system reliability by providing an alternate data path.

- f. Command Processing - This equipment handles the entire commanding load for the spacecraft and is built into redundant units which are always on. There are two basic types of commands and each type may be executed either upon receipt or at a future specified time after receipt.

The first type of command is the simple on-off function command and is utilized primarily to control power to the various users, but may be employed wherever a simple magnetic latching relay is suitable. There will be up to 64 functions that may be accommodated, but generally only those that are actually to be used on a particular mission will be flown.

The second kind of command is a binary number or proportional command which is used as a number by an experiment or by a spacecraft function. For instance, the loading of a new format into memory would be accomplished with this kind of command. The command contains bits which identify it as being a proportional command and which user the word is destined for.

Either type of command may be placed into a memory location for future execution. In this case, a time identification is included with the stored word and when this spacecraft time occurs, the command will be executed. The delayed or stored commands are required to permit setting up a complicated maneuver in advance of the maneuver and verifying that all commands were accurately received by the spacecraft. It also allows the execution of commands in rapid sequence (essentially simultaneously) which is not possible in a real time mode since only about 3-1/3 commands can be sent per minute. If spacecraft verification is required after each command prior to the sending of the next command in a sequence, the round trip time delay costs 16 minutes per AU of range. It is clear that this could be a very time consuming process without command storage. The entire list would be sent, stored, and then verified and, at the specified time, executed step by step. Another use for the storage will be to backup the command link in the event of a real time command system failure. Thus commands with execution times of 10 days could be stored. These would normally never be reached and executed unless command contact were lost for 10 days. They could put the spacecraft into a mode and bit rate to allow the collection of some data for many months, for instance. The exact emergency command sequence and execution times would be revised and updated at frequent

intervals (less than a few days) and will insure extended data coverage and spacecraft lifetime in spite of a command failure.

The exact form of the command storage memory is not yet frozen. It could be assigned a portion of the main data memory bank, but since this is shared with other users, the possibility exists for an accidental write operation changing a stored command. This possibility may be circumvented by using a separate storage device just for this function. Use of the large data memory bank, however, allows one to easily size the command storage needs for each mission and further the location of this block of storage may be easily located and relocated in the memory bank (by changing the block address). This would retain this essential feature even after some memory failure. Memory write interlocks could be employed to get around the problem of an inadvertant word being written over a stored command. A resolution of this question will be obtained during the Phase B study.

### 3. SRT for the C&DH Subsystem

Much of the proposed design does not involve any additional SRT effort but only an extension of present techniques and developments now underway. The more significant areas for additional SRT effort are outlined below.

- a. Spacecraft Oscillator - A high reliability, very stable oscillator and the interconnection and selection technique of the various receiver VCO's used in generating the down-link carrier must be developed. This is critical to the entire communication and tracking system.
- b. Transmitter - The redundant interconnection of several solid state power amplifiers and the improvement of power amplifier efficiency requires extension of present SRT effort in these areas.
- c. S to X Band Multiplier - A study as to the use of X band for the down link to supplement the proposed S band link is desirable. Thus the S band power would be multiplied to X band with a varactor diode to realize higher gain with the 8 foot spacecraft dish. If the spacecraft control system can aim this narrower beam at the Earth, a 6 to 8 db system improvement would be realized. The 85 foot dishes have been operated at these frequencies for ATS. The 210 foot dishes have not been instrumented at X band since they are not precise enough at that frequency. It should be noted that an 85 foot dish facility operated at X band is within a few db of the data rate capability of the 210 foot dish facility at S band.

## VI. SPACECRAFT FLIGHT OPERATIONS

### A. Assumptions

The technical consideration given a mission must necessarily include much material directly related to flight operations. It is not intended that the following presentation be complete within itself, but rather, that reiteration be employed for continuity and augmentation for completeness. The areas of operational consideration to be highlighted are as follows:

Tracking and Telemetry  
Command  
Scheduling  
Communication  
Control Center  
Personnel  
Analysis

Certain rather general assumptions have been made with respect to the spacecraft flight operations in support of the Galactic Jupiter Probes. These are based upon previous experience and are employed to eliminate unnecessary detail. It is assumed that operational control will be centralized. This includes routine continuing activity following prescribed criteria as well as the decision making required of the experiment and spacecraft managers. It also includes the handling, processing and distribution of data and mission related information.

Another assumption is that the technical capability of supporting facilities will be adequate and a state of operational readiness maintained. In addition, considerations of capability and readiness have been addressed in the detailed technical portions of the study.

There will be occasions calling for the resolution of conflicting requirements to support this or another mission stemming from unique conditions or emergencies. In general, there are established criteria; however, management decision may also be involved. It is assumed that the Galactic Jupiter Probe will have or be given sufficient priority to be protected and achieve mission results.

### B. General Considerations

The operational support of the Galactic Jupiter Probes will require the use of facilities associated with the Space Tracking and Data Acquisition Network (STADAN), the Deep Space Network (DSN), the Eastern Test Range (ETR), the NASA Communications System (NASCOM) and the Goddard Space Flight Center (GSFC).

The spacecraft capabilities during launch and the extremely rapid pace of the flight will necessitate a maximum support effort by ground facilities such as down range stations and ships and STADAN dish sites during the early mission operation. Useful engineering data will be available from the time of shroud separation. Early orbit determination is essential. Such support will be a one-time-only exercise, since, the attitude and range will quickly preclude continuance. The assignment of uniquely qualified personnel and some technical augmentation is to be expected.

The long term spacecraft operations will call for support by the Rosman, North Carolina 85-foot dish link of the STADAN and the three 210 foot facilities of the DSN. Mission oriented personnel and some technical augmentation will be necessary at all locations.

The 85-foot dish facility will be prime to Jupiter encounter with the DSN 210 foot dishes taking over by task assignment for the encounter and the late mission support. The DSN will be called upon for unique or emergency support as required. Other facilities may be called upon to provide emergency backup and multiple mission capability.

At present, the planned facilities; augmented for the Galactic missions; appear adequate.

The extended nature of the missions, the long duration passes, multiple mission potential and the normal communication delay due to distance will be the basis for keeping all ground support functions in as near a real-time mode as practicable. A Mission Operations Control Center, direct center-to-station communication, and on line processing of data will be employed.

A potential operational limitation imposed by the use of a 100 KW or larger transmitter is that it may not be possible to use the same antenna for simultaneous transmit and receive. This is due to the fact that the operation of such a large transmitter will degrade the receive system noise temperature. This does not appear to be a serious limitation however, because of the long two-way travel times encountered when the high power up-link is required. Instead of a diplexer, a transmit/receive capability could be used for alternate transmit and receive periods. Another possibility would be the use of another station in the network for receiving the down link transmissions when the 100 KW up-link is operating.

### C. Tracking and Operational Scheduling

#### 1. Projected Loading.

A review of the 20 year Plan, the 5 year Plan, the NASCOM Plan and current program documents indicate continuing workloads approximating those

currently supported. This would indicate a good capability for Galactic Jupiter Probes; however, it must be remembered that higher frequencies and longer duration passes are also potentials for other projects. Thus, the use levels of large dishes will rise to some extent. The impact of this mission upon the prime facilities is considerable since 30-40 percent of their availability can be used almost indefinitely. The use level will be proportionately greater during portions of the multiple missions.

## 2. GJP Support

Telemetry support will be provided and includes both tracking information from doppler extraction and spacecraft data. Data coverage is inclusive of experiment and housekeeping information.

Tracking operations will produce the range-rate information required for orbit determination. Another form of tracking operations is that of antenna pointing. Except for early mission operations, antenna control will be programmed. There is a possibility that auto-track may not be available on the prime dishes due to the precision feed limitations.

The acquisition of doppler, spacecraft and experiment data will require long periods of transmission and reception on the spacecraft link. This necessitates careful planning and continuing orientation of operations personnel.

Given adequate on-board storage, single pass operation could provide coverage during routine flight. Unique events and emergencies will require the sequential scheduling of several stations. Additionally, multiple missions will require simultaneous support by at least two stations for extended periods.

The normal housekeeping functions will be predicted upon the application of predetermined operational criteria. Thus, it will be handled as a routine of the Mission Operations Control Center and the scheduled station.

The prime stations will require some housekeeping control capability for emergency use in addition to the normal functions required of all supporting facilities. Operations related information will be controlled and dissipated from the control center.

The control center will be the schedule source for all operations including spacecraft, experiment and ground processing functions. Thus, there will be information inputs and outputs including displays, remotes and reports.

### 3. Attitude Determination and Control

The normal attitude determination and control function will include the processing of data and a continuing evaluation of the spacecraft pointing error. When the error reaches a predetermined value, possibly 1 degree, a command for programmed correction by the spacecraft will be generated.

Special operations will be required during the early mission, midcourse and any unique experiment requirements. Special attention will also be directed toward operations at encounter and during times of spacecraft emergency.

### 4. Orbit Determination

The details related to continuous orbit determination have not been studied at this time; however, there are no apparent severe difficulties or anomalies. The planning will be accomplished at a later time as required.

### 5. Command

The determination of need and scheduling of commands will be a function of the Control Center. Particular attention will be required in planning for support during the early mission, mid-course correction, attitude control, and experiment control operations.

Specific criteria for routine housekeeping commands will be necessary. The criteria should include operations supporting the spacecraft, communications, experiments and the power system.

At long ranges, it may be required that the command message be started after sweeping the transmitter frequency a few times but before obtaining confirmation over the telemetry link of spacecraft receiver lock up. The time required to achieve lock up would be known with a degree of certainty from prior experience and "blind" operation should not present any unusual problems.

### 6. Scheduling

The GJP mission is not a static mission, but one which has various phases superimposed on a steadily decreasing communication capability. The spacecraft data handling must be performed in a manner that maximizes the scientific return with a "reasonable" amount of electronics on-board. Some data storage is provided so that data coverage may be obtained even when the probe is not in contact with the ground.

Scheduling in the operational sense will begin well in advance of flight operations and include consideration of personnel orientation and training, system simulation, and readiness assurance.

Operations for flight support may be scheduled to commence at shroud separation.

In terms of the spacecraft, scheduling will be inclusive of single link support, dual or multiple link support and unique/emergency backup. It will also account for the single and multiple mission cases.

Scheduling for ground communications presents no particular problem since it is and will be largely a matter of simple call up procedure.

Unique events will require special scheduling exercises, but the planning must be based upon detail which will not be developed until quite late in the project.

#### D. Communications

Ground communication support does not present a problem. With the low data rates, the existing network is capable of support; and improvements, now planned, will enhance this capability.

It is planned that a GSFC Control Center will be in two-way real-time contact with each ground receiving terminal. This capability presently exists at all sites considered for this mission. These links use various error checking and correcting techniques and virtually error free data is now transmitted. This will be the prime method of communicating data between GSFC and a remote site. It will be backed up by magnetic tape recordings. The ground data links may also be used when it is necessary to back up the remote computer for coding detection. This could be done in one medium sized computer located at GSFC but it will require a higher (factor of 10) communication data rate from the station to the GSFC and at the highest spacecraft bit rates, this capability is not presently available for real-time communications.

#### E. Control Center

The detailed development of the Control Center will be a requirement later in the project. It will have processing, command, display, communications and analysis capability. An approximation of the size and physical attributes is available in the current OSO Operations Control Center.

#### F. Personnel

Preliminary estimates of manpower requirements show approximately 15 people for the Control Center and 8 people at a prime station with one or two specially oriented personnel at each of the other supporting facilities. This allows for the first single mission. With multiple mission requirements, the Control Center may increase to 20 and the stations double. The amount of joint use will also be a factor in station manning.

#### G. Training

Consideration will be given the assignment of a unique operational cadre to be indoctrinated during the late period of project development. Training for additional personnel and the replacement of attrition is anticipated as on-the-job orientation. Separate and unique course work will not be a requirement.

All supporting personnel should be exercised regularly to assure continuing capability and readiness.

#### H. Analysis

A review and analysis will be prepared later in the study. Much of the procedure and technical detail is closely related to other parts of the study.



PRECEDING PAGE BLANK NOT FILMED.

## VII. APPENDICES

### APPENDIX A

#### Spin Axis Direction Determination for the Galactic-Jupiter Probe (Reference 1)

The antenna for the envisioned spin stabilized Galactic-Jupiter Probe is an 8-foot body fixed paraboloid which at the 2.3 GHz down link frequency transmits a  $4^\circ$  pencil beam toward the earth. The spacecraft spin axis which is concentric to the antenna beam must be precessed periodically to enable the antenna to follow the earth as it travels in its orbit about the Sun.

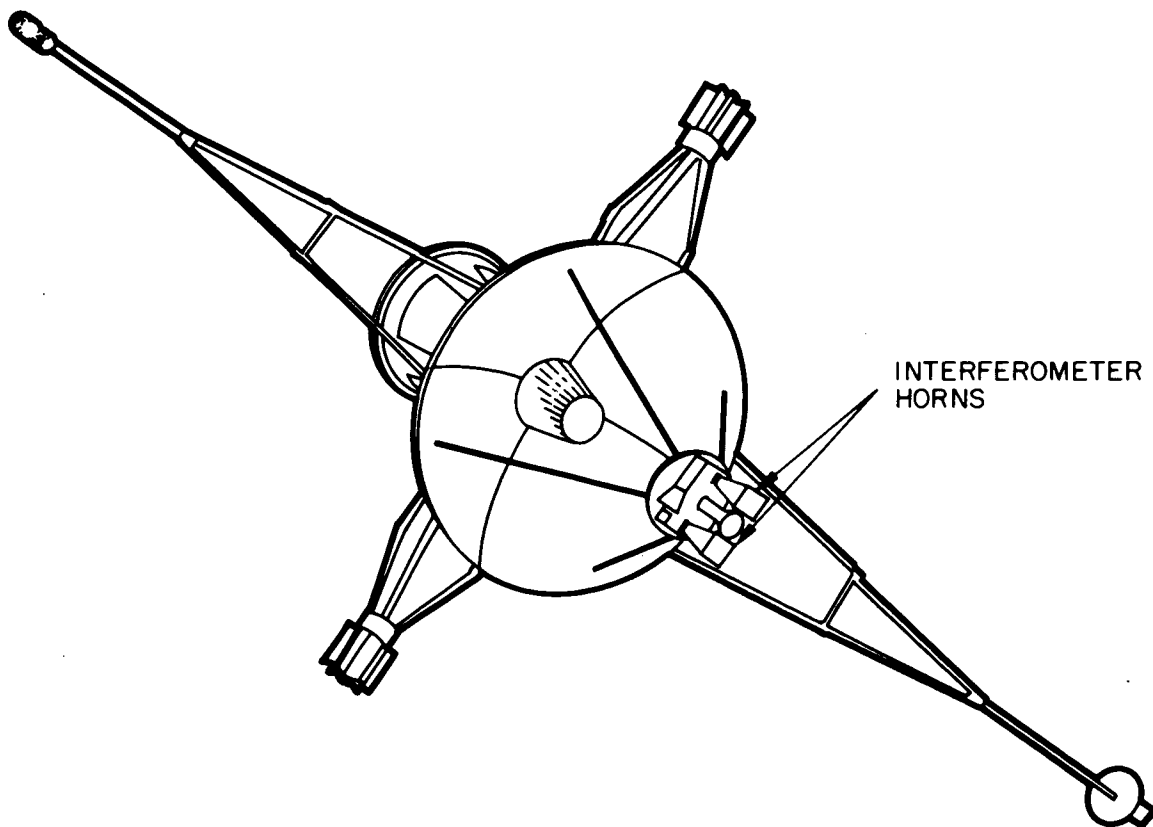


Figure A-1-Interferometer Antennas for Attitude Control

The described (spacecraft) Spin Axis Direction Determination System is a 2 wavelength single baseline radio interferometer with its two antennas mounted symmetrically with respect to the spin axis. Figure A-1 shows the interferometer



Horn antennas mounted at the focal point of the 8-foot dish. The system's acquisition beamwidth is  $24^\circ$ . Operating on a received 2.1 GHz beacon signal radiated by earth stations the system employs phase monopulse techniques to derive a sinusoidally varying voltage synchronous to the spin rate. The Block diagram of the phase measuring system is shown in Figure A-2. The amplitude of this voltage is proportional to the angular boresight error,  $\epsilon$ ; the phase,  $\psi$ , denotes the direction of the error and supplies timing signals for activating the series of propulsion pulses necessary to precess the spin axis in the proper direction to correct the error. Figure A-3 shows the geometrical relationships involved with the spinning spacecraft. From the determination, by the system, of  $\phi$  which is equal to  $\cos \alpha$  the values of  $\epsilon$  and  $\psi$  can be derived.

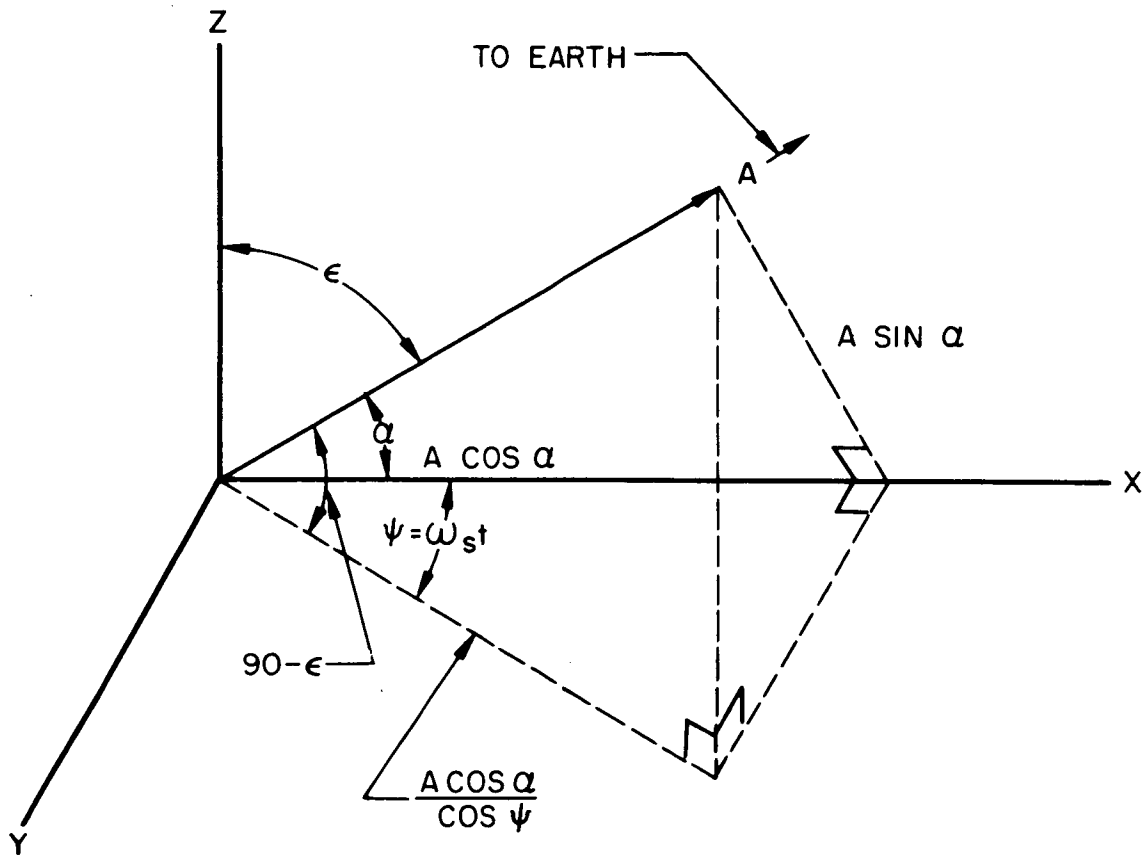


Figure A-3—Interferometer Spin Geometry

When  $\epsilon$  exceeds the prescribed threshold value of  $1^\circ$ , a programmed attitude correction sequence is initiated by command from earth. At a range of 5 AU and a power level of 10 kw radiated by an 85 foot dish the values of  $\sigma\epsilon$  and  $\sigma\psi$  at  $\epsilon = 1^\circ$  are calculated to be  $0.018^\circ$  and  $1.02^\circ$  respectively which are satisfactory for the mission.

The following table summarizes the system parameters and analytically derived performance results:

#### SYSTEM PARAMETERS

Antenna Beamwidth	$24^\circ$
Antenna Gain	15 db
Oper. Freq.	2110 MHz
SNR of Vo.	$(2\pi B)^2 \epsilon^2 (S/N)^2 c$
Coherent Detector SNR	18 db
Loop Bandwidth	25 Hz

#### Assumed Operating Parameters:

Power Transmitted	10 KW
Range	5 AU
Noise Fig. of Spacecraft Receiver	5 db
$\sigma\epsilon$ at $\epsilon = 1^\circ$	$0.018^\circ$
$\sigma\psi$ at $\epsilon = 1^\circ$	$1.02^\circ$

Locating the interferometer antennas near the focal point of the parabola compounds the multipath problem due to received energy being focused onto the back lobes of the horns. Careful design will be necessary to sufficiently reduce reception in the back direction.

#### Early Attitude Control and Resulting Received Signal Levels:

The spacecraft attitude with respect to the earth probe line is shown in Figure A-4. (Reference 1). The attitude at insertion is about  $90^\circ$ , rapidly increases to about  $180^\circ$ , then to  $160^\circ$  at about  $T + 5$  hours. After this time the attitude remains almost constant for long periods. From the viewpoint of attitude-control propulsion conservation no attitude correction should be made previous to  $T + 5$  hours. Nor is any correction necessary since the received signal levels are very high

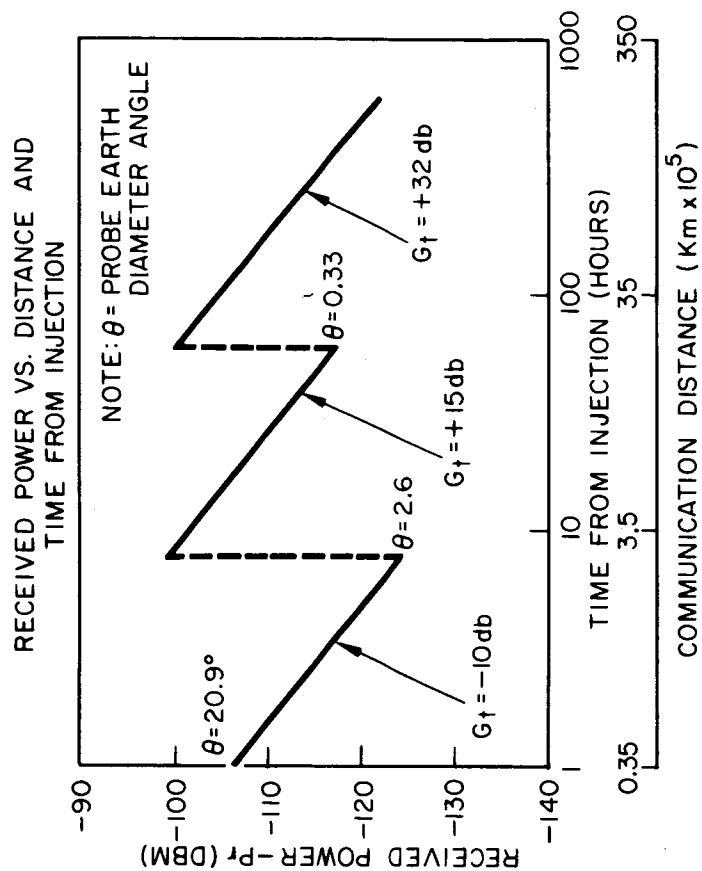
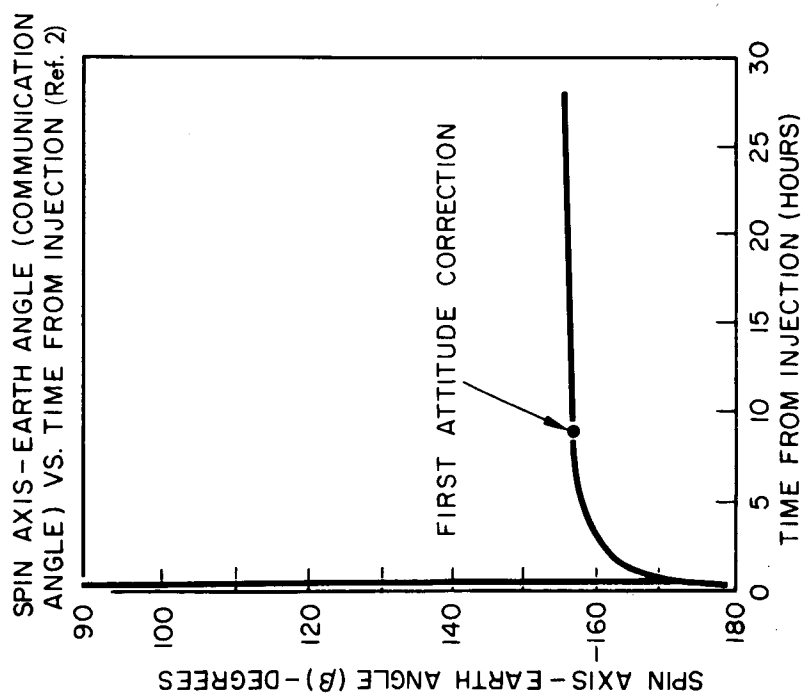


Figure A-4—Attitude Control for Early Mission Communications

even with the omni-directional antenna which, to be conservative, is considered to have a gain of -10 db. This gain factor takes into consideration, nulls in the spacecraft omni antenna pattern which are unavoidable due to the relatively short wavelength of the propagated signal in relation to the spacecraft physical dimensions.

At  $T + 8$  hours, the received signal, assuming 10 watts radiated by the omni, falls to about -123 dbm. This is still a very substantial signal level; however, in consideration of the anticipated demand for high data rates during the early portion of the flight, it is considered an appropriate time to make the first attitude correction. The probe-to-earth-diameter angle is still several degrees at this time. Thus, although a switch-over to the high gain spacecraft antenna with its  $3.8^\circ$  beamwidth is permissible, plenty of signal level and a great deal more safety results if the switch-over is made to the medium gain spacecraft antenna which doubles as the antenna element for the radio attitude error determination system. The signal level is thereby increased by about 25 db.

As the range increases with elapsed time to about  $T - 60$  hours, the earth's diameter finally presents an angle to the spacecraft that is sufficiently small for reliable operation with the high gain system.

#### REFERENCES

1. Simas, V. R., "Spin Axis Direction Determination for the Galactic-Jupiter Probe," X-523-67-122, March 1967.
2. Coady, R. E., "Preliminary Trajectory Data to be Used in Communications Design for the Galactic Probe," Mission Analysis Office Technical Study, Goddard Space Flight Center, October 20, 1965, Figure 6c.

## APPENDIX B

### The Modulation/Detection Method

#### A.1 Rationale

Sections of the study document show that significant improvements in the efficiency of the telemetry data system can be achieved through the use of advanced coding techniques, and especially by the application of some degree of on-board compaction or processing of the data. It should be made clear, at the outset, that lesser improvements are possible with improved modulation detection methods. It is none the less essential that care be exercised in the choice of the modulation/detection method to be used for the Galactic-Jupiter Probe. None of the hard-earned gains achieved in other parts of telemetry systems should be wasted through less-than-optimum modulation and detection.

The modulation method proposed is a phase-shift-keyed (PSK) system. This is a special case of phase modulation in which all the power resides in the sidebands and the carrier is completely suppressed. For binary PCM data, this spectrum characteristic is obtained when the modulation index ( $\beta$ ) is  $\pm 90$  degrees. Except at extreme ranges, this modulation technique is optimum. With a small increase in complexity, the transmitter can also be modulated at a much lower index, such as  $\pm 18$  degrees, which would be used only at extreme range. Performance obtainable with various other modulation indices is shown by the family of curves of Figure 5-2 (page 29 of the text).

The reasons for this choice are supported by the considerations treated in the following sections.

#### A.2 Scope of Consideration

Performance criteria and other known requirements immediately eliminate a wide variety of systems which, while entirely suitable to other applications, would not meet requirements for a mission such as that of the Galactic-Jupiter Probe. No purpose would be served by an analysis of the comparative performance of all such systems.

Rather, we take advantage of the results of several exhaustive analytical studies conducted during the last decade. (References 1, 2, 3). The consensus of recognized authorities is that the best technique for digital data transmission

is a phase-modulated coherently detected signal (treated in an optimum manner). Its use results in a lower data-error-rate over a given R.F. power link than any other modulation/detection technique currently realizable. Furthermore, a pulse code modulated, phase-shift-keyed (PCM/PSK) signal, optimized for the channel, is the specific optimum method.

Such systems are not difficult to implement both in the spacecraft and on the ground. Their characteristics are well understood and their performance can be accurately predicted. PCM/PSK has been shown in theory (12) to exceed the performance of its nearest competitor by about 3 db. In actual practice the margin is somewhat better, due to the relatively high thresholding level of most of these other detection methods.

### A.3 PCM Phase Coherent Systems

There are several variations or types within the general class of phase coherent systems which have been very closely examined and compared. Three principal types which were selected for comparison and their salient characteristics are tabulated below:

#### A.3.1 Classification of Types

##### Type I PCM/PM (Power divided between carrier and information)

PCM/PM will be referred to as "conventional" typical of telemeters used in S-6, AE-B, OGO's, OSO's, and OAO. (Actually a PSK system but with the modulation index always less than  $\pm 90^\circ$ ).

- A. Phase modulation of the R.F. carrier by the information
- B. Phase deviation ( $\beta = \pm 45^\circ$ ).
- C. Modulating waveform, serial PCM.
- D. Coherent detection, by a conventional carrier tracking phase-lock-loop (PLL) detector synchronized to the coherent carrier component of the signal.

##### Type II PCM/PSK (Using Bi-phase ( $\pm 90^\circ$ ) modulation)

Special techniques required to coherently demodulate. See References (4), (5), (6), and (7).

- A. PSK Bi-phase modulation of the R.F. carrier.
- B. Phase deviation  $\pm 90^\circ$  (no carrier component).
- C. Modulation waveform, serial PCM.
- D. Coherent detection, by a special carrier regenerating tracking loop detector.

### Type III PCM/PSK/PM

Exemplified by JPL Mariner Mars (1964). See References (8) and (9).

- A. PSK Bi-phase modulation of a subcarrier by the information.
- B. PSK Bi-phase modulation of a second subcarrier by PN-code sequence to provide word and bit synchronization at the ground.
- C. PM modulation of the carrier by the combined subcarriers, A and B; deviation much less than  $90^\circ$ .
- D. Coherent detection of the R.F. carrier and synchronous demodulation of the two subcarriers.

#### A.3.2 Relative Performance at Jupiter Mean Distance, 5 AU with 85-Foot Antenna

The performances of the three modulation/detection systems are compared in Table B-1, for a received total signal power of -159.5 dbm and a noise power spectral density of -181.2 dbm/cps which results from a (assumed worst case)  $55^\circ\text{K}$  effective system noise temperature. The received total signal power of -155 dbm is the nominal value; for the cases considered, a 7.9 negative tolerance is assumed for the link, and an additional 1 db is allowed for detector degradation in both the data channel and the carrier channel. The tabulation is based upon uncoded PCM to allow comparison of the three modulation modes on a common basis. As has been shown earlier, the use of convolutional encoding ( $n = 2$ ), with sequential decoding provides about a 6 db coding gain for the data, which may be used to transmit at four times the uncoded rate with the same probability of bit error.

The tabulation (Table B-1) shows that the PCM/PSK Bi-phase ( $\pm 90^\circ$ ) modulation, applied directly to the carrier results in appreciably better performance at the 5 AU distance considered, than either of the other two modulation modes. In fact, superior performance is obtainable out to about 7.8 AU, at which point the bi-phase detector of the ground receiver begins to threshold. In practice, in the PCM/PM mode, the use of a subcarrier would almost certainly be necessary since the data rate at the 5 AU distance is only 9.3 bits/second, or a little over twice the assumed loop bandwidth of 4 Hz. Even with the increase in symbol rate obtainable through data encoding, the resultant modulation rate is too low for good phase lock loop performance. Resort to the use of a subcarrier further degrades the tabulated performance. Conversely, the PCM/PSK ( $\pm 90^\circ$ ) system can accommodate NRZ type modulation applied directly to the carrier, requires less I.F. bandwidth, and consequently less dynamic range in the phase detector.

TABLE B-1

Relative Performance of the Carrier and Data Channels at Jupiter Mean  
Distance, 5 AU for  $P_t = 10\text{w}$ ,  $G_t = 31.6\text{ db (8')}$ ,  $G_R = 52\text{ db (85')}$ ,  
 $T_s = 55^\circ\text{K}$  (Worst Case; -7.9 db from Nominal)

<u>Received Signal and Noise</u>	<u>PCM/PM</u>	<u>PCM/PSK(NRZ)</u>	<u>PCM/*PSK/PM</u>
1. Signal Power (Nom.)	-155.0	-155.0	-155.0 dbm
2. Noise Density (Nom.)	-184.6	-184.6	-184.6 dbm
3. Signal Power (Worst Case)	-159.5	-159.5	-159.5 dbm
4. Noise Density (Worst Case)	-181.2	-181.2	-181.2 dbm
<u>Data Channel: (Uncoded PCM)</u>			
5. Modulation Loss	- 3.0	-	- 4.1 db
6. Detection Losses	- 1.0	- 1.0	- 1.0 db
7. $S/N_0$ Available	+ 17.7	+ 20.7	+ 16.6 db
8. $ST/N_0$ Required for $P_e^b = 2 \times 10^{-4}$	+ 8.0	+ 8.0	+ 8.0 db
9. Bit Rate Capability	+ 9.3	+ 18.6	+ 7.2 b/s
<u>Carrier Channel</u>			
10. Modulation Loss	- 3.0	-	- 4.6 db
11. Filtering Loss	- 1.0	- 1.0	- 1.0 db
12. Available Loop Signal Power	-163.5	-160.5	-165.1 dbm
13. Loop Noise Power	-175.2	-173.4**	-175.2 dbm
14. $(S/N)$ in Loop ( $B_n = 2B_L = 4\text{ Hz}$ )	+ 11.7	+ 12.9	+ 10.1 db
15. $(S/N)$ Loop Threshold	+ 9.0	+ 9	+ 9.0 db
16. Loop Lock Margin	+ 2.7	+ 3.9	+ 1.1 db

NOTE: \*For the Type III PCM/PSK/PM System (Mariner Mars) only approximately 0.74 of the total power is accounted for in Column III. Of the remaining 0.26 of the received power about 0.1 is employed for the Synchronizing Subcarrier channel; the remaining 0.16 is lost in unusable modulation products. (Reference 8).

\*\*Loop Noise Power is a function of  $2B_L$ , but the function is also affected by a noise product term. (See Equation [2]).

#### A.4 PCM/PSK Detector Performance

The application of PSK bi-phase detection to fully modulated ( $\beta = \pm 90^\circ$ ) PCM (NRZ) telemetry signals cannot be made indiscriminately. In many applications where transmitter power is not subject to strong constraints (near-earth

orbits) the amount of power required for synchronization (i.e. in a power division modulation system) is small, so that the data power is degraded only by 0.5 to 1 db. However, at the extreme distances of the Galactic-Jupiter Probe missions, more and more power is required to keep the phase lock loop (PLL) of the ground receiver in lock. This power can be obtained only at the expense of data rate and/or data quality in a power division system; in the limit, all the available power is required to keep the receiver in lock and no power is left for information (data) transfer. The PSK Biphase technique is not a panacea; but it does appear to offer a minimum of a 3 db gain over its nearest competitor, especially in the area of great interest, the Jupiter intercept phase of the mission, 4 to 5.8 AU from Earth.

#### A.4.1 Significant Features of Bi-Phase Loop

It is well known that a bi-phase loop detector requires more signal power, i.e. has a higher threshold signal level, than the conventional PLL designed to operate on a coherent carrier component; also its threshold is a function of the data (bit or symbol) rate. On the other hand, more signal power is available. The parameter of greatest significance is the variance of the estimate of the phase,  $\sigma_{\phi(t)}^2$  of the VCO signal. An expression for this quantity has been derived by Nichols and Rauch (10) from which the effects of loop bandwidth, data rate capability, I.F. bandwidth and rms phase jitter may be readily calculated. The Nichols and Rauch derivation makes the usual assumption (linearization) that is normally done to simplify the analysis, but then modifies the resultant expression to account for this assumption.

The modified expression is

$$\sigma_{\phi(t)}^2 = \frac{B_n}{2} \left[ \frac{N_0}{S} + \left( \frac{N_0}{S} \right)^2 \frac{n f_b}{2} \right] (\text{rad}^2) \quad (1)$$

$$= 0.126 \text{ (at threshold)}$$

where  $B_n$  is the loop noise bandwidth ( $2B_L$ ) near threshold in Hz  
 $N_0$  is the noise spectral density, single sided, watts/cycle  
 $S$  is the available signal power in watts, and  
 $f_b$  is the PCM bit (or symbol) rate, bits/second. (NRZ).  
 $n$  is the bandwidth expansion factor

The rms phase jitter,  $\phi_e(t)$  is of course the square root of the variance, i.e.,  $\sqrt{\sigma^2} = \sigma = \phi_e(t)$ , and the noise power in the loop (due to the input thermal noise of the system only) is

$$N_{B_n} = B_n N_0 \left[ 1 + \frac{N_0}{S} \frac{nf_b}{2} \right] \text{ (watts)} \quad (2)$$

Equation (2) shows that the noise power in the bi-phase loop exceeds that of the conventional PLL by the term in the bracket. The presence of the term indicates the loop noise power is influenced by the PCM data rate, or more exactly, by the noise power in the bandwidth required by the modulated carrier.

#### A.4.2 Loop Threshold

Various criteria have been proposed and used to define loop threshold. Signal-to-noise ratio (SNR) in the loop noise bandwidth is the most commonly used. But numbers range all the way from 0 db to about 9 db, any of which is equally valid if the statistical nature of the noise and its effects are taken into account. Although a PLL may be said to be in lock "most of the time" or "nearly all the time" at an  $(SNR)_L$  of 4 to 6 db, it has been found in practical (hardware) experience (JPL) (GSFC) that for operational purpose, a  $(SNR)_L$  of 9 db is necessary to allow acquisition of the signal, and the loop will remain in lock without skipping cycles, for extremely long periods.

This SNR (9 db) has been used throughout this study proposal as the value of loop threshold and although a degraded operation somewhat below 9 db may be possible, such a condition is not considered or proposed. The condition for loop threshold is then:

$$S_{\text{threshold}} = B_n N_0 \left[ 1 + \frac{N_0}{S^*} \frac{W}{2} \right] + 9 \text{ db} \quad (3)$$

where  $S^*$  is the available signal power, and

$W$  is the bandwidth in the I.F. which contains the signal spectrum resulting in  $S^*$ .

#### A.4.3 Effects of Data Encoding on Loop Performance

All known PCM data encoding techniques trade bandwidth for coding gain, with a greater or less degree of success, respectively. For example, one biorthogonal,  $N = 5$  (5 bit word) encoding scheme produces a coding gain of about 3 db (at a bit error probability of  $2 \times 10^{-4}$ ) by sending 16 symbols for each 5 bit word; a rate 1/2 convolutional-encode/sequential-decode scheme achieves a coding gain of about 6 db (at the same  $P_e^b$ ) by sending a parity bit interspersed between each "information" bit. The bi-orthogonal coding requires a channel bandwidth of 3.2 times the information rate, while the rate 1/2 convolutional/sequential coding requires a channel bandwidth of only 2 times the information rate. There are of course many types and variations of coding other than those cited on the foregoing. The point of significance, in the application of PSK bi-phase detection, is the bandwidth expansion factor versus the coding gain obtained.

In referring to Equation (3) the second term in the brackets contains  $W$  as defined. Obviously the greater the bandwidth expansion factor becomes, the greater  $W$  must be made to pass essentially all the signal power in the modulated carrier spectrum. As  $W$  is increased, the loop noise power increases and at low signal levels (i.e.,  $N_0/S$  relatively large) the effect is that the loop will threshold sooner as the signal level is reduced.

The end points, ( $\Delta$ ), of the solid curves on Figure A-1 indicate the estimated threshold of the bi-phase loop, using the bandwidths required to pass the indicated data rates. In each case, operation could be extended to a somewhat greater range by accepting a lesser bit rate; that is,  $W$  may be decreased to the point where the SNR in the loop is maintained at 9 db, and the bit rate reduced (by command) to be compatible with the reduced bandwidth. The performance to be expected under this condition is shown by the dashed lines of Figure A-1, and indicates operation at carrier threshold, i.e., 0 db margin. It might be difficult to acquire the signal under this condition.

Table B-2 shows the theoretically expected performance for three degrees of coding – Uncoded PCM; bi-orthogonal encoding, ( $n = 3.2$ ) with word correlation decoding; and convolutional encoding ( $n = 2$ ) with sequential decoding, all for the PSK Bi-phase ( $\pm 90^\circ$ ) detection mode.  $K$  is a constant (above threshold) which includes parameters of allowable bit error rate, coding gain, bandwidth expansion, and losses in the detection process (1 db loss allowed in the cases shown).

Obtainable bit rates (at  $P_e^b = 2 \times 10^{-4}$ ) as a function of distance from earth are plotted in Figure B-1. The data used are based on the worst case condition for the 85 foot antenna with a system temperature of  $55^\circ\text{K}$ . The total negative tolerance, including that for the system temperature, is 7.9 db below nominal.

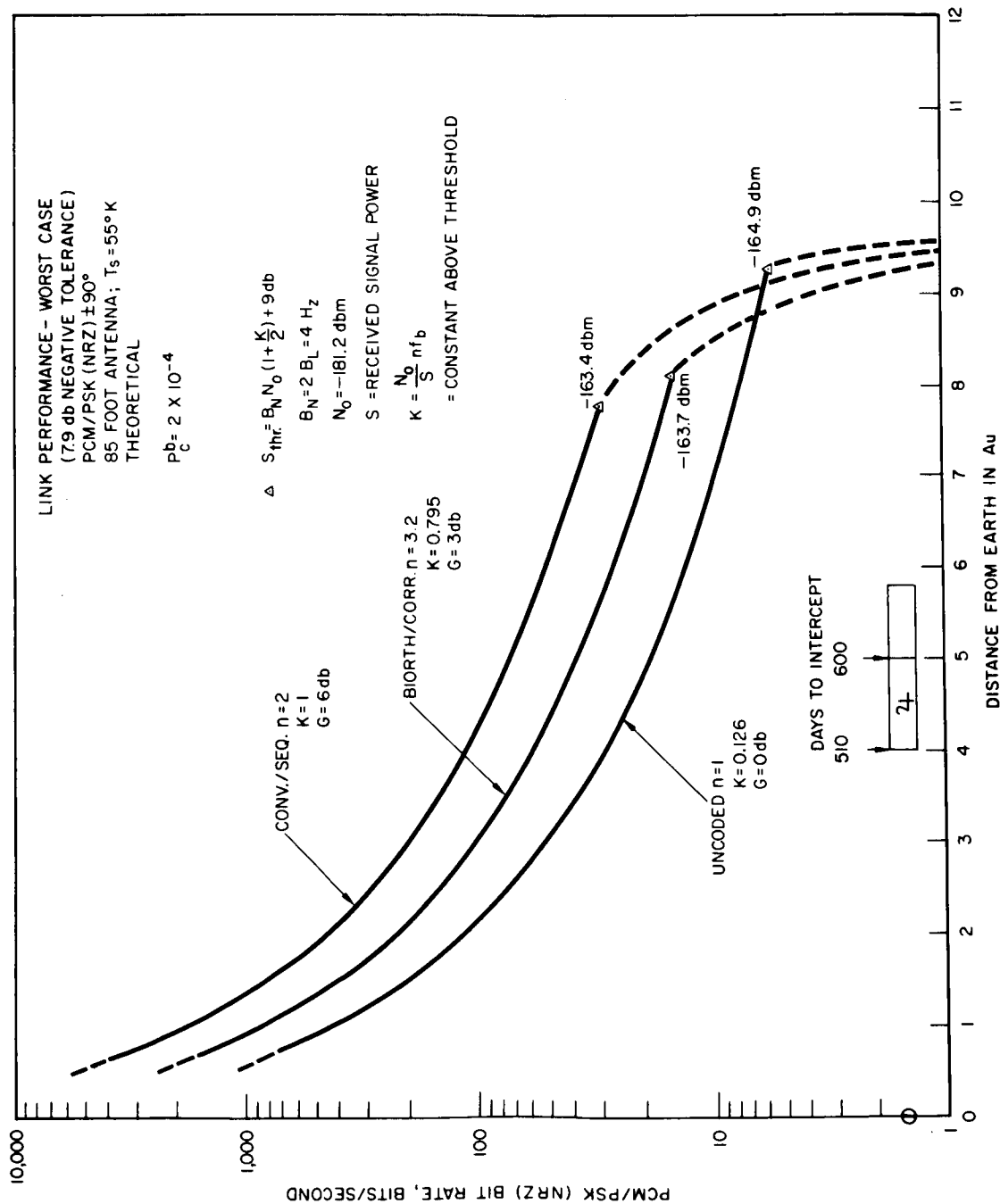


Figure B-1

TABLE B-2  
PSK Bi-Phase Detector Performance with Coded PCM

		Uncoded $\underline{n = 1}$	Bi-orthogonal $\underline{n = 3, 2}$	Conv./Seq. $\underline{n = 2}$	
1. Coding Gain	db	0	3	6	
2. $ST/N_0$ Required	db	8	5	2	$P_e^b = 2 \times 10^{-4}$
3. Filter (Det.) Loss	db	1	1	1	Assumed
4. $ST/N_0$ Input Req.	db	9	6	3	
5. Bandwidth Expansion	db	0	5	3	$n$
6. $(S/N_0 W)_{IF}$ Required	db	9	1	0	
7. K	db	-9	-1	0	$\frac{N_0 W}{S}$
At 5 AU ( $S = -159.5$ dbm; $N_0 = -181.2$ dbm)					
8. W	Hz	12.7	20.7	21.7	$W = nf_b$
	Hz	18.5	117.0	148.0	
9. $f_b$	b/s	18.5	37.0	74.0	$f_b = \frac{K}{n} \frac{S}{N_0}$
At Threshold ( $B_N = 4$ Hz) $(SNR)_L = 9$ db)					
10. $S_{th} = B_N N_0 \left(1 + \frac{K}{2}\right) + 9$ db	dbm	-166.9	-164.7	-164.4	
11. $D_{(threshold)}$	AU	9.3	8.1	7.8	
12. $f_{b(threshold)}$	b/s	5.4	18.0	32.0	

The data points plotted in Figure B-1 were obtained from the following relationships:

$$f_b (D) = \frac{K}{n} \frac{S}{N_0} \text{ (bits/second)}$$

D = Distance from Earth.

$$K = \frac{N_0 n f_b}{S} = \text{a constant (above threshold) for the specific coding type.}$$

n = Bandwidth expansion factor.

S = Received Signal Power (watts)

$N_0$  = Input Noise Spectral Density (watts/Hz)

$$S_{\text{threshold}} = B_N N_0 \left( 1 + \frac{K}{2} \right) + 9 \text{ db}$$

algebraic manipulation from

$$\sigma^2 = \frac{B_n}{2} \left[ \frac{N_0}{S} + \left( \frac{N_0}{S} \right)^2 \frac{n f_b}{2} \right] = 0.126 \text{ (rad}^2\text{)}$$

$$f_{b_{\text{threshold}}} = \frac{K}{n} \frac{B_N N_0 \left( 1 + \frac{K}{2} \right) + 9 \text{ db}}{N_0}$$

For example, for the convolutional/sequential n = 2 code;

$$n = 2, K = 1$$

$$f_b / B_n \cong 6 \text{ (at threshold).}$$

## A.5 Practical Considerations

In practice, an additional 1 db increase in input signal would probably be required in the "carrier" channel to compensate for the loss of power in the tails of the modulated signal spectrum which are excluded in the filtering process, whether the filtering is accomplished at I.F., or after the detector proper. A "matched filter" to recover the signal energy (i.e., to optimize the SNR prior to the multiplication (or squaring circuit) would minimize this loss.

Also, it is obvious that coding types providing the greatest coding-gain to bandwidth-expansion ratio are best suited to PSK bi-phase operation. It is felt that a SNR (in the I.F.) of 0 db is close to the lower limit.

Coding techniques capable of providing gains greater than about 6 db, in general, require a bandwidth expansion of much more than 2. If, for example, the bandwidth required in the I.F. were  $4f_b$  then the SNR (I.F.), for the conditions considered, would be about -5 db. When this noisy signal spectrum is operated upon to regenerate the reference carrier, the  $S \times N$  and  $N^2$  terms result in serious deterioration of the signal-to-noise ratio in the loop, with the consequence that thresholding occurs at a higher signal level (i.e., at a lesser distance from earth).

No experimental verification of the calculated performance has been performed due to the lack of specialized hardware. The thresholding effects in the bi-phase  $\pm 90^\circ$  mode were calculated on the basis of a signal-to-noise ratio in the phase-lock loop of +9 db (i.e., a rms phase jitter of 14.3 degrees).

Again, no experimental data has been acquired. However, JPL used a modified form of the Costas loop detector for Mariner Mars (1954), (Reference 8), and found the  $(SNR)_L$  of +9 db allowed acquisition of the signal, and ability to recover quality data. A bi-phase subcarrier demodulator, using a Costas type loop detector, has been tested by the Space Electronics Branch and the performance was within 1 db of theoretical.

## A.6 Conclusion

The conclusion is that for the conditions considered at the 5 AU nominal Jupiter encounter distance the efficiency is maximized by devoting all the power to the information channel, rather than by dividing it between carrier and information channels. Van Trees (Reference 11) considers the problem of optimum power division, and for the cases he considers, arrives at the same conclusion. It is well known that phase coherent systems must provide synchronization (phase-coherency)

at the receiving end of the link. This is customarily accomplished by choosing the deviation such that a portion of the transmitted power is devoted to a carrier component. However, any point devoted to the carrier, in a power limited system, detracts from the power available for the communication of information. This situation can be circumvented by the application, at the receiving end, of circuitry which can operate on the information power to reconstruct, or to generate, a phase coherent reference carrier. (See Chang (Reference 5), Costas (Reference 4), and Harris (Reference 7).

The PCM/PSK bi-phase modulation/detection mode proposed, with convolutional (rate  $1/2$ ;  $n = 2$ ) coding, and sequential decoding, provides up to 74 bits/second of quality data for the worst case condition ( $-7.9$  db tolerance from nominal), or up to about 470 bits/second for the nominal case, at the 5 AU Jupiter intercept distance for the assumed 600 day mission.

## REFERENCES

1. Telemetry Systems Study Reports (series), Contract NAS 5-1474 - Space General Corporation, 777 Flower St., Glendale 1, California, 1961-1962.
2. Space Telemetry Studies (series), Contract NAS 5-408 New York University, College of Engineering - 1960 - Continuing.
3. Murphy, J. T.; Roche, A. O., et al., Ultra Long-Range Telemetry Study (Contract AF 33 (657)-11462, Dynatronics), Technical Documentary Report No. AL TDR 64-87, April 1964.
4. Costas, J. P., Synchronous Communications, Proc. IRE., Vol. 44, pp. 1713-1718, Dec. 1956.
5. Chang, S.S.L. and Harris, B., An Optimum Self Synchronizing System, First Scientific Report, New York University, College of Engineering, June 8, 1960.
6. Costas, J. P., Synchronous Detection of Amplitude Modulated Signals, National Electronics Conference Proceedings, 1951.
7. Harris, B., Basic Concepts for the Optimum Transmission and Detection of Signals When the Interference is Random Noise, Tech Memo No. 2, N.Y.U., College of Engineering, Dept. of E.E. (Contract NAS 5-408, Aug. 19, 1960).
8. Martin, B. D., The Mariner Planetary Communications System Design, Tech. Report 32-85, Jet Propulsion Laboratory, Pasadena, California, May 15, 1961, (Also JPL Tech. Memo 33-88, May 21, 1962).
9. Martin, B. D., The Pioneer Lunar Probe; A Minimum Power FM/PM System Design, Tech. Report No. 32-215, JPL, C.I.T., March 1962.
10. Nichols, M. H. and Rauch, L. L.
11. Van Trees, H. L., Optimum Power Division in Coherent Communications Systems, MIT Lincoln Laboratory, Tech. Report 301, Feb. 1963.
12. Saunders, R. W., Communication Efficiency Comparison of Several Communications Systems, Proceedings IRE, 1960, pp. 575-588.